From Alarm Propagation to Energy Metabolism:

Mechanisms of Collective Colony Responses

in Seed-harvester Ant Colonies, *Pogonomyrmex Californicus*

by

Xiaohui Guo

A Dissertation Presented in Partial Fulfillment
of the Requirements for the Degree
Doctor of Philosophy

Approved June 2021 by the
Graduate Supervisory Committee:

Jennifer Fewell, Co-Chair
Yun Kang, Co-Chair
Jon Harrison
Jüergen Liebig
Stephen Pratt
Theodore Pavlic

ARIZONA STATE UNIVERSITY

August 2021

ABSTRACT

The flexibility and robustness of social insect colonies, when they cope with challenges as integrated units, raise many questions, such as how hundreds and thousands of individual local responses are coordinated without a central controlling process. Answering such questions requires: 1. Quantifiable collective responses of colonies under specific scenarios; 2. Decomposability of the collective colony-level response into individual responses; and 3. Mechanisms to integrate the colony- and individual-level responses. In the first part of my dissertation, I explore coordinated collective responses of colonies in during the alarm response to an alarmed nestmate (chapter 2&3). I develop a machine-learning approach to quantitatively estimate the collective and individual alarm response (chapter 2). Using this methodology, I demonstrate that colony alarm responses to the introduction of alarmed nestmates can be decomposed into immediately cascading, followed by variable dampening processes. Each of those processes are found to be modulated by variation in individual alarm responsiveness, as measured by alarm response threshold and persistence of alarm behavior. This variation is modulated in turn by environmental context, in particular with task-related social context (chapter 3). In the second part of my dissertation, I examine the mechanisms responsible for colonial changes in metabolic rate during ontogeny. Prior studies have found that larger ant colonies (as for larger organisms) have lower mass-specific metabolic rates, but the mechanisms remain unclear. In a 3.5-year study on 25 colonies, metabolic rates of colonies and colony components were measured during ontogeny (chapter 4). The scaling of metabolic rate during ontogeny was fit better by segmented regression or quadratic regression models than simple linear regression models, showing that colonies do not

follow a universal power-law of metabolism during the ontogenetic development. Furthermore, I showed that the scaling of colonial metabolic rates can be primarily explained by changes in the ratio of brood to adult workers, which nonlinearly affects colonial metabolic rates. At high ratios of brood to workers, colony metabolic rates are low because the metabolic rate of larvae and pupae are much lower than adult workers. However, the high colony metabolic rates were observed in colonies with moderate brood: adult ratios, because higher ratios cause adult workers to be more active and have higher metabolic rates, presumably due to the extra work required to feed more brood.

DEDICATION

For my grandma.

ACKNOWLEDGMENTS

Thank my advisor Jennifer Fewell and Yun Kang for their great support and patient mentorship. Without their encouragement, I would not have decidedly focused on the alarm behavior of ants, which is notoriously difficult to study. I must also thank Jon Harrison, who trained me to measure CO_2 emission rate, and to estimate metabolic rate of colonies. He still encouraged me to continue the metabolic scaling project as I found some results contradicted previous studies. I also thank Jüergen Liebig, Stephen Pratt, and Theodore Pavlic for their help in editing, helpful suggestions, and conversations.

Thank all of my friends and lab-mates Michael Lin, Ioulia Bespalova, Madeleine Ostwald, Kaitlin M. Baudier, Nathan Smith, Colin Lynch, Juliana Calixto, Asma Azizi, Jun Chen, Ti Ericksson, and Benjamin Pyenson for all of your gracious and patient help in experiment design, data analyses, edits and comments of manuscript.

I also thank my undergraduate students Lucas P. Saldyt, Mostafa Ghulam Hazrat, Christopher Sleiman, Taryn O'Boyle, Ciara Syphard, Zach Lebaron, and Kellen Graham Neil Gibson. Without your participation and support, those projects could not have happened.

I am grateful to Arizona State University School of Life Sciences, the National Science Foundation, and DARPA for funding those projects.

TABLE OF CONTENTS

LIST OF TABLES

LIST OF FIGURES

Figure Page

CHAPTER 1

Introduction

Complex adaptive systems

Social insect colonies function as complex adaptive systems (Bonabeau 1998, Fewell 2003), which I can consider as complex systems that respond appropriately to changes in condition or external perturbation (resiliency), and which can maintain their state in the face of environmental variation (robustness). Complex systems can be thought of more generally as having the attribute of decomposability, in that they can be divided into coupled subcomponents (Bechtel & Richardson 1993), but these subcomponents are interconnected rather than fully independent (Simon 1962). Social insect colonies could be considered exemplary complex adaptive systems, in that they are built around numerous heterogeneous subcomponents (workers and tasks). The colony maintains itself and shows characteristic ontogenetic patterns of growth across a variety of environmental conditions. Colonies also respond quickly to changes in environment, whether by recruiting to a valuable new source of food, moving nests when the old one becomes unsuitable, or evaluating and responding defensively to colony attacks.

The organization of the social insect colony contributes to its function as a complex adaptive system. It has been described by Hölldobler and Wilson (1994) as a heterarchy, to emphasize that information and control are not centrally or hierarchically driven, but instead flow from local information exchange and decision making. This distributed system of information exchange and the associated collective decisions it can produce are key to understanding how social insect colonies can function as complex adaptive systems.

Information processing in social insect colonies

Social insect colonies use a rich variety of information, from pheromonal to behavioral, which flexibly moderate their work and social organization. These signals vary in modality from behavioral to chemosensory delivery, and in scope from individual-to-individual communication to blast signaling. Individual chemosensory signals include the cuticular hydrocarbon information used in nestmate recognition, and the nonvolatile chemicals produced by larvae as solicitation signals for brood care and feeding (Cassill & Tschinkel, 1995, 1999; Pankiw *et al.*, 1998). Blast signals, are exemplified by the alarm pheromone release of African honey bees.

Colonies also rely on visual or tactile behavioral signaling for information exchange. A classic example is the dance language of the honey bee, in which patterns of movement indicate direction and distance to resources. In ants, antennal contact behavior is often a key component of information exchange (Waters & Fewell 2012). The pattern of individual communication by antennation rate between foragers in *P. barbatus* and *P. badius* provides inactive foragers information about foraging demands (Greene & Gordon 2007, Pinter-Wollman *et al.* 2013). Direct information can be supplemented by additional contextual information during signaling and information exchange. For example, waiting time for nectar transfer from foragers to receivers in honeybee colonies is a significant information source that downregulates forager waggle dancing, and can shift waggle dancing to tremble dancing, a stop signal for foraging (Seeley & Tovey 1994, Ratnieks & Anderson 1999, Anderson & Ratnieks, 1999). And the same is true for water collection in honey bee colonies: the delay in unloading tells water collectors when to stop collecting water (Kuhnholz & Seeley 1997). Although modality of transmission and context vary, in

most of these examples, a small piece of information is acquired locally by individuals and flows via direct/indirect individual interactions. These allow the colony more broadly to generate collective responses to conditions and needs.

Colony collective response is not generated by signal transmission alone. Individual workers vary in the probability that they will send signals, and in their responses. This individual variation in response is a summation of numerous factors (reviewed in Beshers & Fewell 2001). These include internal factors, such as genetic variation in individual propensity to perform a task, individual age or developmental stage, and associated neurophysiological variation in individual state. As an example of temporal state effects on behavior, less corpulent ants in *T. albipennis* colonies begin foraging faster after several days' food-deprivation because of their lower physiological threshold (Robinson *et al.* 2009). As an example of intrinsic and potentially genetic effects on behavior, honey bee (*A. mellifera*) workers vary in their thresholds to initiate fanning as colony temperatures rise (Oldroyd & Thompson 2006). Intrinsic variation in individual propensity has been shown to be a critical component of flexible colony response to changes in need for specific behaviors, such as fanning (Jones & Oldroyd 2006), and for pollen versus nectar collection (Fewell & Page 1993), and more generally as a critical component of the adaptive regulation of division of labor (Beshers & Fewell 2001, Oldroyd & Fewell 2007).

Task organization and its plasticity

In social insect colonies, those individual activities which contribute to colony maintenance, growth and reproduction can be divided by specific function or purpose; these are called tasks (Hölldobler & Wilson 1990). First proposed by Wilson and Fagen

(1974) and Fagen and Goldman (1977), the categorical analytic method has been used widely in ant colonies to quantitatively evaluate a colony's task behavior repertoire (Wilson 1976, 1978, 1984). According to this method, the relative frequencies of different tasks performed within a colony can be used to assess the structure of task organization. Individual workers may themselves have wide behavioral repertories of tasks as task-generalists (Sharma *et al.* 2004), or narrow behavioral repertories as task-specialists (Charbonneau & Dornhaus 2015).

There are several measures to quantitatively describe task organization (Fewell & Harrison 2016): task allocation, which focuses on the distribution of specific tasks across the whole task repertories; division of labor which is the degree of task specialization across all individual workers; and task activity level, which indicates the intensity and duration of task performance. Those three dimensions of task organization give us a comprehensive view of how social insect colonies, as complex adaptive systems, regulate their task organization. A hallmark of social insect colonies is the ways in which they can continually adjust task organization in order to adapt to changing environmental conditions, via local information exchange and associated feedback loops (Bonabeau 1998).

Flexibility/plasticity of task performance has been taken as one of the indispensable assumptions in many theoretical models to fulfill the functional division of labor in social insect colonies (Beshers & Fewell 2011). Especially in colonies lacking morphological polyethism, task organization is maintained by individuals who are specialized in tasks temporarily while still retaining the behavioral flexibility for task-switching (Anderson & McShea 2001). Many empirical studies have demonstrated that

colonies adaptively adjust labor activities based on changed labor demands via information acquisition and changed physiological status at long and short time scales. For example, in colonies with dramatically changing needs over short periods of time, ant workers could rapidly respond to those changes due to workers' physiological status and probability of being exposed to task stimuli (Gordon 1989, Robinson *et al.* 2009). And in colonies with relatively stable circumstances, the task organization of the colony is mediated mainly by physical changes that are age-induced (Robinson 1987, Mersch *et al.* 2013).

Many studies have investigated the mechanisms by which ant colonies regulate their task organization to adapt to internal and external changes. The principle current model examining proximate mechanisms of adaptive task organization is based on variation in response threshold (Robinson & Page 1989, Bonabeau *et al*. 1996, reviewed by Beshers & Fewell 2001 and Jeanson & Weidenmüller 2014). A number of studies have demonstrated how colonies can adaptively adjust task performance in response to environmental conditions across a diversity of behavioral contexts, including foraging (Fewell and Page 1993, Greene & Gordon 2007), rapid response to changing demand in food intake (Robinson, *et al*., 2009) and thermal homeostasis (O'Donnell & Foster 2001). However, how colonies adaptively respond to changes in some internal factor, e.g. size, and consequently increase their energetic efficiency has not yet been explained satisfactorily. My projects, through metabolic rate measurement during ontogeny of seed harvester ant colonies, would provide frameworks to understand mechanisms of adaptive task organization to changes of colony size.

Adaptive responses at individual and colony level

There are two major layers within these adaptive responses: behavioral decisions and responses at the individual level, and colony level decisions and responses that emerge from individual propensity and decisions. Individual workers may respond to various random events consistently or flexibly (Bonabeau *et al.* 1996, O'Donnell & Foster 2001, Garrison *et al.* 2018), while at the colony level, colonies are able to maintain their homeostatic status under various perturbations (reviewed by Oldroyd & Fewell 2007). The adaptive colony responses raise the central questions of how individuals coordinate with each other to build the emergent collective pattern, and how this coordination may contribute to colony efficiency and/or success.

There have been many research endeavors focusing on collective responses of social insect colonies based on individuals' behavior. It is believed that characteristics of collective responses, e.g. resiliency and robustness, arises from integrative individual decisions, each of which is a product of individual features and interactions, e.g. homeostatic environment maintained by in bumble bee and honey bee colonies (O'Donnell & Foster 2001, Jones *et al.* 2004), and flexible collective defense in *Lasius niger* ant colonies (Sakata & Katayama 2001). In other words, individual features, such as information and behavioral status, could amplify through a network and finally converge to consensus or emergently influence collective pattern at the colony level (reviewed by Feinerman & Korman 2017).

In this dissertation, I propose to examine **how individuals coordinate with each other to achieve adaptive colony responses in two contexts that differ dramatically in time scale: collaborative alarm** elicitation **and colony metabolism during ontogenetic development** (Fig. 2.1). The collaborative alarm elicitation of social insects

associated with individual alarm behavior helps the colony respond immediately and successfully to external threats (Wilson 1958, Matthew *et al*. 1999, Robert *et al.* 1998, Reyes *et al*. 2019, Sasaki *et al*. 2014). Context-dependent alarm signal propagation and dissipation are two regulatory components that determine the accuracy and speed of the colony's alarm response, which stems from success/failure of each individual alarm elicitation. It therefore allows us to ask how the adaptive alarm response of the colony emerges from the individual alarm behaviors. Colony ontogeny is characterized by continual change of colony size, providing us with a system to study how individual task preference and physiological status are affected by colony size, and the associated changes in division of labor and organization of work (Holbrook *et al.* 2011, Karsai & Wenzel 1998, Amador-Vargas *et al.* 2015). Cross-species and cross-colony comparisons suggest that social insects exhibit hypometric scaling of metabolic rates as observed for individual organisms; however, the mechanisms responsible remain unclear. Hypometric scaling of metabolism has been speculated to arise as a function of variation in individual task behaviors, possibly occurring normally during colony ontogeny (Fewell & Harrison 2016). However, no prior studies have examined energetic scaling in social insect colonies during ontogeny. Because collaborative alarm elicitation and adaptive energetic metabolism during ontogeny are processes that occur at such dramatically different time scales, their comparison may provide a more comprehensive understanding about how social insect colonies deal with urgent and prolonged changes in functional demands.

This topic will be addressed by dividing it into the following two component questions:

1.**How do colonies respond to threats via collaborative alarm elicitation**? The purpose of this study is to probe how the adaptive alarm response of a colony emerges from individual alarm behaviors, and how the colony's response is achieved by individual features and interactions.

2.**How do colonies optimize their energy cost/efficiency to respond to their changing colony size during their ontogenetic developments**? The purpose of this study is to determine how individual task activities and possible changes in worker to brood ratio relate to colonial metabolic rate as colonies grow in size over their first year of development.

Figure 1.1 outlines my overall research plan. To answer my first research question (Q1), I performed Study I to develop a method for estimating individual and collective alarm responses in laboratory colonies of *Pogonomyrmex californicus* (**Chapter 2**). Then, I conducted **Study II**, in which I exposed individual ants to distinct social stimuli in order to investigate how social context and individual variation influence individual alarm response and further colony alarm response (**Chapter 3**). To address my second research question (Q2), I conducted **Study III** by using respiratory physiology and activity level estimation to examine how laboratory colonies adapt to their changing colony size and achieve adaptive energetic metabolism during colony ontogeny (**Chapter 4**).

Study species

I studied *Pogonomyrmex californicus*, a seed harvester ant found throughout the Southwestern United States and Northern Mexico. Laboratory colonies of *P. californicus* enable the study of collaborative alarm elicitation because the ants in laboratory nests

move in 2-dimensional space which makes movement-tracking possible. Alarmed ants also show distinct behavior, such as higher movement speeds and more curved movement, which reflect individual inner status and are measurable. This species also enables us to study adaptive energetic metabolism during ontogeny because colony foundation can be initiated in the laboratory, and the growth rate, metabolic rate and mass of colonies are trackable during their development.

Figure 1.1. Flow chart for questions (denoted by Q) consists of three studies.

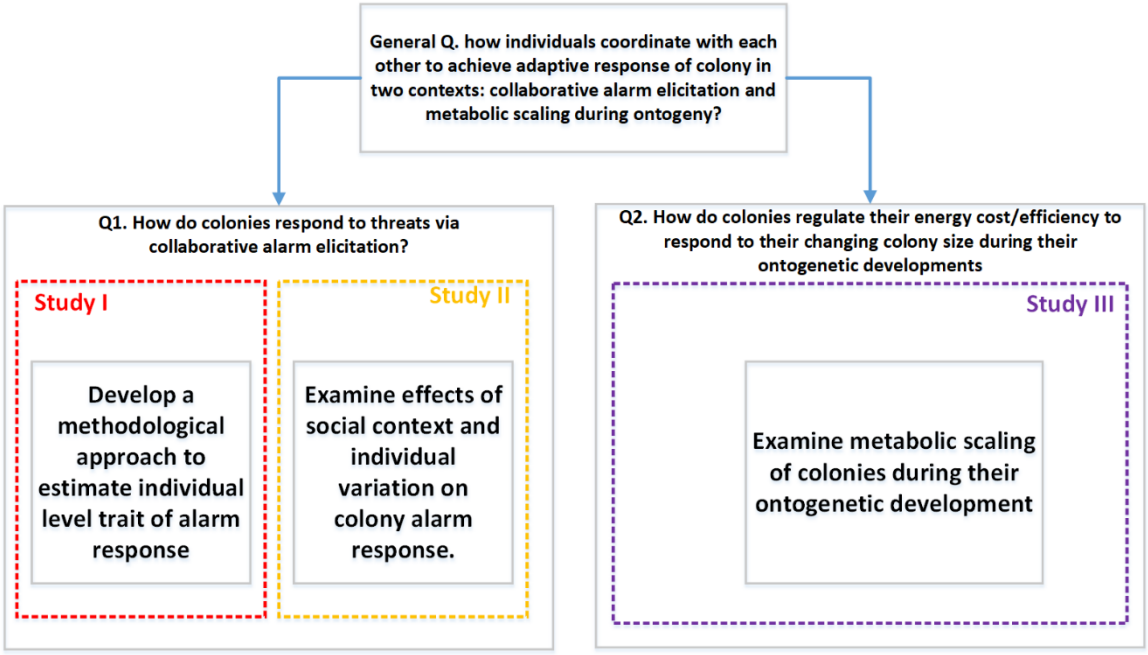

CHAPTER 2

Decoding alarm signal propagation of seed-harvester ants using automated movement tracking and supervised machine

Abstract

Alarm signal propagation through social-insect colonies provides an empirically tractable context for analyzing information flow through a natural system, with useful insights for network dynamics in other social groups, including human social networks. Here, I develop a methodological approach to track alarm spread within the group of harvester ants, *Pogonomyrmex californicus*. I alarmed initial 3 individuals and tracked subsequent signal transmission through the group. Because there was no actual threat, the alarm was false, allowing us to assess amplification and adaptive damping of collective alarm response. I trained a Random-Forest machine learning regression model to quantify alarm behavior of individual workers from multiple movement features associated with alarm behavior in this species. This approach provides reliable continuous assessments of an individual's behavioral state at much finer temporal scales and more consistently than can be achieved visually. I combined the ML alarm state assessments with proximity data from tracking software (ABCTracker) to construct a propagation network of alarm spread. In the group of ants with a right-skewed distribution of individual alarm responsiveness, alarm signals moved a maximal network distance of four degrees away from initiating ants. This short pathway mitigates the issue of false information because it decays quickly (within 2.5 min) absent reinforcement. Alarm was primarily transmitted by contact-mediated interactions and a subset of independent alarm excitations was likely from pheromonal signaling. Using this system, alarm propagation can be manipulated

and assessed to ask and answer a wide range of questions on information and misinformation flow in social networks.

Introduction

Coordination in biological systems often depends on complex, decentralized processes for distributing information among system components (Camazine *et al.* 2003). Within the vertebrate body, detection of a pathogen triggers a cascade of cytokine signaling from individual cells to other individual cells as an appropriate inflammatory response is coordinated (Dimitriou *et al.* 2008). Within a human social network, global awareness of newly discovered information is often accomplished by individuals sharing with a finite number of other individuals (Rogers 2010). These decentralized mechanisms of information distribution are critical to adaptive social function, but they also can be subject to manipulation, and under some conditions, they can fail. Deleterious self-perpetuating "cytokine storms" can lead to multisystem organ failure and death (Nazinitsky & Rosenthal 2010), and misinformation in social networks can continue to spread even long after it has been retracted by its original source (Lewandowsky *et al*. 2012). It is difficult to effectively or ethically manipulate human-domain social networks to understand the mechanisms and functional limits of decentralized information spread. Being able to manipulate and assess biological communication networks in fine detail may unveil strategies converged upon by natural selection with connections to the spread of information and misinformation in other domains. Furthermore, better understanding catastrophic failures of information sharing in one system can lead to new insights into analogous failures in others.

Social insect colonies are ideal model systems for studying natural communication networks. Adaptive responses at the colony level emerge from the collective actions of individuals, each responding to local stimuli from their environment or from other individuals within the colony. As a result, large numbers of individuals can self-organize to regulate diverse aspects of task organization (Gordon 1996, Fewell 2003), including: food distribution (Cassill & Tschinkel, 1999), social defense (Hermann 1984), social immunity (Hart & Ratnieks 2001), collaborative house hunting (Pratt 2005), and foraging (Pinter-Wollman *et al.* 2013). Two elements common to these collective phenomena are an underlying individual-to-individual contact network and a distributed system of information flow over the network. These attributes enable colonies to flexibly and adaptively respond to changing environments and social contexts (Pinter-Wollman *et al.* 2014). Furthermore, the degree of amplification and competition among different sources of information may modulate the shape and intensity of the collective responses (Deneubourg *et al.* 1999).

By tracking individual movement and social interactions, object-tracking techniques have provided useful methodologies to study the dynamic structure of social networks in diverse social groups. In social insect colonies, the technique has been applied to European honeybees (*Apis mellifera*) (Gernat *et al*. 2018), bumblebees (*Bombus ignitus*) (Miranda *et al.* 2012, Azarcoya-Cabiedes 2014), seed-harvester ants (*Pogonomyrmex barbatus*) (Pinter-Wollman *et al.* 2013), *Temnothorax* ants (*Temnothorax rugatulus*) (Blonder & Dornhaus 2011), carpenter ants (*Camponotus fellah*) (Mersch *et al.* 2013), and others. These tracking methodologies do not, by themselves, provide a reliable assessment of individual behavioral state during social

interactions, nor do they assess the reliability of information exchange during encounters between individuals. Researchers have developed more sophisticated statistical and mathematical modelling tools to develop theory about how social insects move information across their communication networks (Sherman 1985, Richardson *et al.* 2017) and how they maintain the dual-functionality of networks to respond to valuable information while ignoring incidental noise or avoiding pathogen spread (Richardson *et al.* 2015, Guo *et al*. 2020, Romano *et al.* 2020). Nevertheless, a gap between empirical and theoretical studies on information movement across the network constrains understanding of how a social-insect colony is organized as a complex adaptive system.

In a functional social network, where behavioral coordination is organized around information, the information flow between individuals should elicit a change in the state of the receiver (Bonnie & Earley 2007). For example, information encoded by the cuticular hydrocarbons on the surface of seed-harvester ants (*P. barbatus*) is used for task recognition and also in decisions on whether to switch to other tasks (Greene & Gordon 2003). Nonvolatile chemicals from ant larvae (either a pheromone or metabolic waste product) have also been suggested as the solicitation signal to motivate brood care and trophallaxis in colonies of fire ants, *Solenopsis invicta* (Cassill & Tschinkel 1995,1999). The queuing delay in nectar transfer from foragers to receivers in honeybee colonies factors significantly into individual decision making related to nectar-foraging recruitment as well as in regulation of signal switching from upregulation to damping of nectar return rates (Ratnieks & Anderson 1999; Anderson & Ratnieks 1999).

In many studies of vertebrate social networks, research has focused on several aspects of information flow, such as: the transmissibility of information, individual

characteristic effects on information flow, and the path of information flow (Ward & Zahavi 1973, Deutsch & Nefdt 1992, Chivers & Smith 1998, Leadbeater & Chittka 2005, Aplin *et al.* 2013, Duboscq *et al.* 2016). In these cases, the focus has been primarily on dyadic relationships, or association networks and how they shape behavior. This is more difficult for the social insects, where individual relationships are usually ephemeral and task based (Fewell 2003), because a colony has numerous informational pathways operating simultaneously around different tasks. These are difficult to disentangle, and the observable behaviors used to make inferences about the impact of information flow are cryptic and difficult to discriminate from baseline behavior. Consequently, tracking and analyzing information dynamics using passive observations of social insect colonies is often prohibitively complex.

Individual-level alarm status in ants can be characterized by observable changes in movement patterns and velocity (Goetsch 1957, Wilson, 1958, Yamagata *et al.* 2010, Mizunami *et al.* 2010), and so information flow within ant alarm networks can be readily observed radiating out from an artificially initiated alarm event. The challenge comes, however, in how to capture the complexities of movement, contact, and response within a social group, especially at the second-to-minute timescales relevant to the amplification and decay of a group-level alarm response.

One way to do this is to employ machine learning (ML) algorithms with complementary modeling techniques to classify behavioral states at a fine-grained level (Dankert *et al.* 2009, Hong *et al.* 2015, Valletta *et al.* 2017). Machine learning approach allows for automatic characterization of behavioral features that normally require labor-intensive observation and by reducing variation in behavioral characterizations that are

due to a lack of intra-rater and inter-rater reliability (Burghardt *et al.* 2012, Kabra *et al.* 2013, Hong *et al.* 2015, Valletta *et al.* 2017). This approach makes it possible to continuously quantify the level of an individual ant's alarm response based on her behavior. Coupled with new tracking methodologies, I can combine ML assessments of behavioral (alarm) state with information on individual contacts, to capture – in real time – the movement of information throughout a social group and assess individual and group-level response to that information. In this study, I combine automated tracking and ML to quantify individual alarm strength based on individual worker movement patterns. I match individual alarm strengths with contact networks to: (a) characterize the spatiotemporal dynamics of alarm spread, (b) identify the relative contribution of different mechanistic pathways (e.g., chemical or physical) to alarm spread, and (c) evaluate varied individual sensitivity to alarm stimuli. My methodology offers a way to more directly assess the influence of information spread on individual behavior and to capture the speed of information transmission and response across a biological social network. Because these networks are also highly manipulable in size, density, social conditions, and the validity of the information being transmitted, this methodology opens a new window into experimental explorations of network information spread as well as the conditions under which misinformation responses can be more effectively damped.

Methods

Animals and Housing.

Experiments were performed on groups of California harvester ant workers, *Pogonomyrmex californicus*, from three laboratory-reared colonies. All three colonies were assessed for colony-level response to alarm stimuli; one colony was additionally

used to develop the ML model for alarm state, and to build the associated alarm propagation network. All colonies were housed in circular plexiglas nests (15 cm diameter), floored with plaster and containing water tubes. Colonies were fed with ad libitum Kentucky bluegrass seeds and provided frozen crickets or mealworms weekly. Colonies and experimental sub-groups were maintained at a consistent temperature of 30 ℃. For test arenas, I used previously unoccupied plexiglas nest chambers, again floored with plaster but with no other contents. The arena was placed on top of a foam pad within an enclosed glass tank to prevent ants from being disturbed by external noise or vibration during experiments. A video camera (Panasonic HC-WXF990) was securely mounted above the glass tank to record all alarm events.

Video capture of alarm events and general methods for ML development.

In order to maintain the similar level of density as in ants' original nests (0.23~0.42 ants/cm^2), we randomly selected 61 workers from each of the 3 colonies and painted them with unique color combinations on the head, thorax, and gaster, using Sharpie oil-based paint markers. Workers of this species are generally monomorphic, and so were selected randomly so as to prevent any bias from location in the original nest. The paint-marked ants were transferred into the test arena and left to acclimate to the new environment overnight prior to testing; no food was provided during acclimation or testing. Prior to stimulating an alarm event, we video recorded two minutes of activity in the arena as a baseline assessment of individual- and group-level movement patterns prior to any manipulation or disturbance. Preliminary experimental results indicated that this time period is sufficiently long to capture the entirety of an alarm event from initiation through decay to baseline activity levels.

After video recording, three ants were randomly selected to serve as initial alarm stimuli. These were carefully removed from the testing arena, using an aspirator to minimize disturbance, and placed into a separate petri-dish. We provided 25 minutes for ants in the testing arena to acclimate after the removal event. The three removed ants were then pinched gently with soft forceps until they displayed visible agitated movement and aggression towards the forceps and dropped into the center of the test arena to initiate the alarm event. The group was video recorded for two minutes immediately after the disturbed ants were added to capture the alarm response.

This protocol was replicated for each of the three colonies to validate its effectiveness of inducing a colony-level alarm response, and to assess whether we could consistently elicit a distinctive pattern of collective alarm response across the three replications. The behavioral responses of all three colonies were assessed by measuring differences in the mean instantaneous speeds of ants during the baseline and alarm events.

We applied my machine learning algorithm to Colony B, the colony showing the strongest alarm response. The methodological protocol, as outlined in Figure 2.1, consisted of video recording the movement patterns of all individuals during baseline and alarm events, then choosing frame sequences in which individuals were visually identified as being alarmed, or not alarmed and with low (calm) or intermediate (alert) movement speeds. We used a frame-by-frame assessment of movement features (a sliding window) to analyze movement features within the selected frame sequences, and to train and test a Random Forest Machine Learning (RFML) Algorithm.

Behavioral characterization of alarm states.

Because we cannot observe the internal state of any ant, we associate the alarm state of an individual ant with observable and consistent behavioral changes linked to the alarm response occurring in the colonies. In my harvester-ant colonies, alarmed individuals move at higher speeds, with more frequent contacts with nestmates. This aligns with the functional expectation of alarm behavior being associated with reacting to a potential threat and communicating that threat to others. To extract this behavioral pattern, we manually applied labels (Alarmed, $\text{Unalarmed}_{\text{alert}}$, and $\text{Unalarmed}_{\text{calm}}$), based on my visual assessments of behavior to a set of video track segments in which the behaviors could be easily differentiated. These were used for ML training and testing.

My raw data (Figure 2.1I) included tracked coordinates, instantaneous speed, and body axis orientation for each ant. The behavior as *Alarmed* presents visually as a distinct increase in movement speed, with a generally circular trajectory and increased encounters with other individuals. This characterization is consistent with ethological descriptions of alarm behavior in other ant species, *P. badius*, *L. emarginatus*, and *C. obscuripes* (Goetsch 1957, Wilson 1958, Mizunami *et al.* 2010). Outside of the context of alarm, ants vary considerably in their speeds and associated movement patterns. Therefore, we also subdivided ants not categorized as *Alarmed* into two sub-categories, including $\textit{Unalarmed}_{\textit{Alert}}$, and $\textit{Unalarmed}_{\textit{calm}}$. Those categorized as $\textit{Unalarmed}_{\textit{calm}}$ were observed moving at moderate speeds and potentially covering significant area in the nest but visually presented lower speeds, less frequent speed changes, and lower levels of contact with other workers. Ants labeled as $\textit{Unalarmed}_{\textit{calm}}$ were stationary or moved at a low

speed; they may have been engaged in social contacts disassociated with alarm, such as allogrooming, such that contact rate with neighbors depended more on task performance than movement.

My algorithm assesses alarm state on a frame-by-frame basis. As with any subjective categorization of animal behavior, the ants that present at intermediate levels of alarm could be labeled in different categories by different observers (i.e., labeling variance due to low inter-rater reliability) or even by the same observer at different times (i.e., labeling variance due to low intra-rater reliability). This lack of labeling reliability motivates my ultimate goal of developing an objective, quantitative approach to assessing alarm state.

Object tracking and feature extraction.

We used the multi-object tracking program, ABCTracker (http://abctracker.org/) (Rice *et al.* 2020), to obtain frame-by-frame movement data for each of workers chosen from three colonies. ABCTracker provides a sequence of time-stamped planar coordinates and body axis orientations for each ant tracked, which allows determination of instantaneous speeds, turning rates, and the number of neighbors.

To detect behavioral transitions at a fine temporal resolution, we developed a sliding time-window method that creates a five-dimensional representation of each individual's movement characteristics and social context at each video frame. For a given ant at frame t, we take a local track window within frames (t, $t+29$) (1 second) and construct a feature vector consisting of 5 metrics computed over this window. These include: the mean frame-wise speed, standard deviation of frame-wise speeds, standard deviation of body axis orientations, convex hull area during the track window and mean

frame-wise number of contacts with neighbors over the window. Sliding the window over a track of length *n* produces (*n-30)* feature vectors.

Supervised machine learning.

To create training and testing datasets, we selectively identified 16 track segments, each visually assessed to contain only one of the three visually identified behavioral states. All feature vectors extracted from a given sub-track were also assigned the same ground truth value as a measure of alarm strength (*AS*) for regression: $AS_{calm} = 0$, $AS_{alert} = 0.5$, or $AS_{alarmed} = 1.0$. Here, the ordinal value (AS) represents a unitless measure of the probability that ants are labeled as alarmed (Malley *et al.* 2012).

Using my data labeled with categorical and ordinal values, we trained a Random-Forest regression model to predict continuous "alarm strength", based on the combined movement features extracted from the tracking data (RandomForest package in R 3.5.0). We then applied the trained model to predict "alarm strength" ($\widehat{AS}$) for unlabeled ant tracks over the entire video.

Results

Validation of experimental procedure.

The movement feature that is most often associated with alarm state in ants is velocity (Goetsch 1957, Wilson 1958, Fujiwara-Tsujii 2006, Mizunami *et al.* 2010). Therefore, we first employed the mean instantaneous speed of ants on each frame to estimate collective alarm responses. We found that mean velocity was significantly higher in the alarm treatment than in the baseline condition (Randomized tests, permutation = 5000, $p \leq 0.00001$) in groups of ants from colony A, B, and C (Fig. 2.2). This result demonstrates that alarm responses of ants were successfully induced via re-

introducing three alarmed ants into the nest. We also observed the decaying collective alarm response of ants over time across all groups of ants.

Feature identifiers of alarm behavior.

By applying the sliding window technique on the raw data of time-stamped planar coordinates and body-axis orientations for ants during the focal alarm event, we extracted 6462 vectors from track segments of 16 focal ants (each vector pairing with manual annotations of categorical alarm status and ordinal alarm strength value includes 5 feature variables: the mean frame-wise speed, standard deviation of frame-wise speeds, standard deviation of body axis orientations, convex hull area of the track window and mean frame-wise number of contacts with neighbors). Pairwise comparisons within each feature variable over the three alarm states supports the validity of using these features to differentiate ant alarm status (Wilcoxon rank-sum test: $p \ll 0.0005$) (Fig. 2.3a). Principal component analysis of the five feature variables indicates that they are effective predictors for classifying ants' alarm status (Fig. 2.3b). Among the 5 principle components, the first two components explained over 80% of variance; PC1 was shown to represent variance in properties of locomotion patterns, and PC2 represents variance in the number of contacts with nestmates (Fig. 2.3c and d). The pairwise comparison and principal component analysis indicate that the 5 selected feature variables are able to describe changes in movement pattern and social context associated with the *Alarmed*, $Unalarmed_{Alert}$, and $Unalarmed_{calm}$ behavioral states. Therefore, we applied those feature vectors to train the Random-Forest regression model (Appendix B).

Alarm strength regression and classification.

A Random-Forest regression model was trained to predict continuous alarm strengths of ants ($\widehat{AS}$), and its accuracy was estimated using the root mean square error (RMSE = 0.0276). The frame-wise mean speed was ranked as the most significant feature variables in predictions followed by the frame-wise standard deviation of speeds, the convex hull area of locomotion, the standard deviation of body axis orientations, and finally the frame-wise mean number of contacts with neighbors. To identify Alarmed ants and estimate their transition from unalarmed to alarmed state, we applied the multiclass Receiver-Operator-Characteristic pairwise analysis to find the best threshold value for differentiating alarmed ants from unalarmed ants (ants in states of $Unalarmed_{calm}$ and $Unalarmed_{alert}$) (Landgrebe & Duin 2007). On an ROC curve for the comparison between Alarmed state and Unalarmed states, a threshold of classification (0.749) was estimated corresponding to the Youden index, *J* (*J* = argmax (TPR(AS_C) – FPR(AS_C))), a metric identifying the maximum potential effectiveness of the classification (64). The area under the ROC curve (AUC) for this comparison was 0.8906. From this, we categorized ants with $\widehat{AS} \geq 0.749$ as alarmed, and those with lower AS as unalarmed.

We also used the Granger causality test to compare the time-series of group average alarm strength $\widehat{AS}_{group}$(t) with the group average speed v_{grop}(t) (Granger 1969) (Fig. 2.4). We transformed the $\widehat{AS}$(t) and v(t) to eliminate a possible autocorrelation. The test with a unit time lag for Average velocity= *f*(Average alarm response) allows us to reject the null hypothesis of non-causality between these two variables (*F*=46.596,

p<.00001), and provides support for the rank of features in Random-Forest regression model that mean velocity contributed the most to the predictability of model.

Spatio-temporal pattern of individual alarm response and recruitment.

Alarm behavior in a social group functions in part to transmit information to others about potential danger (Sherman 1985). To explore the importance of alarm strength ($\widehat{AS}$) predicted from my Random-Forest regression model in alarm transmission, we examined the impact of the presence of alarmed ants that entered the neighboring space of unalarmed ants. Using a 45-pixel as the spatial proximity of ants' physical contact (see Appendix A and C), we identified 20 approaching events between unalarmed ants and their alarmed neighbors. We then measured the standard deviation of alarm strength for the unalarmed ant A^u ($\sigma_{\widehat{AS}(A^u)}$) during the time of approach. Unalarmed ants have an increased tendency to advance in alarm strength as they approach an alarmed ant, with this effect falling off roughly exponentially with distance from the alarmed ant (Fig. 2.5, Eqn. 2.1, α=0.02188, β=0.97166, γ=4.16281E-4, d.f.=3, F=5.16127, p=.01771). This result demonstrates the importance of proximity in the transmission of alarm between ants.

$$\sigma_{\widehat{AS}(A^u)} = \alpha \times \beta^{d_{min}} - \gamma \qquad \text{(Equation 2.1)}$$

It has been found that pheromone-sensitive neurons in an ant's brain exhibit spike activity of 0–4 seconds in response to alarm stimulation (Valentini et al. 2020). In other words, those neuronal activities may be accumulated via consecutive alarm contact-mediated interactions within a historical time window of up to 4 seconds in duration, and then integrated to form motor commands for behavioral responses. However, the alarm response may also associate with memory to reduce the responsiveness out of the 4

seconds' time window due to habituation (Jernigan et al. 2018). Therefore, to estimate temporal pattern of individual alarm transition, we mainly focused on the most recent contact-mediated alarm interactions ($\leq$4 sec) prior to the alarm state transition, and employed this rule to examine the alarm response latency. My results showed 46 ants eventually became alarmed after the introduction of 3 alarmed seed ants. Among those ants, 39 unalarmed ants transitioned to the alarmed state within 1.51 ± 0.1 seconds after contact-mediated alarm stimulations.

Network of alarm signal propagation.

To assess how alarm propagates through the group, we constructed a time-ordered propagation network with weighted and directed pathways (Appendix D). Ants were considered to have transmitted an alarm signal if the behavioral state of contacted unalarmed ants changed within 4 seconds, considered from my rule above to be the maximal latency of ants' alarm state transition. In the time-ordered propagation network, alarm state transitions occurred primarily via contact-mediated interactions (83%), with approximately 17% occurring as independent excitement events. These independent excitations may have been caused by volatile alarm pheromone diffusion from the alarmed ant. Tracing the path of alarm excitation from 3 initially alarmed ants in the time-ordered propagation network indicated that bursty alarm transitions and rapid spreading dynamics happened initially, and the intensity of propagation declines precipitously after the initial events (Fig. 2.6a).

Being assessed as the primary pathway of propagation, the edge with the most weighted on each signal receiver was obtained to construct the time-aggregated network (Appendix D) (Fig. 2.6b). The longest path length from initial signal senders to receivers

was five hops. The number of signal receivers at each network distance showed a significant pattern of linear decline (slope=–5.1, intercept=22.5, p <.025, R^2=0.95).

The time-ordered propagation network allows for quantification of varied individual alarm threshold, which can be captured as the intensities of key sensory cues before a response is elicited (Scheiner *et al.* 2004). Before each alarm state transition, the number of contacts an unalarmed ant made with alarmed neighbors was used as a measure of intensity of alarm stimuli or alarm response threshold. In other words, an unalarmed ant that underwent fewer alarm stimulations prior to becoming alarmed would have a lower threshold. We estimated 46 ants transitioned to the alarmed state after 5.17 ± 1.04 contact-mediated alarm stimulations. In Figure 2.7, a geometric distribution was regressed on the data obtained from the temporal propagation network by using the Lilliefors corrected K-S test, and the expected and observed frequencies were not significantly different (D=0.33, *d.f.*=46, p=0.12). The right-skewed distribution of individual alarm response threshold indicates many sensitive individuals and a few resisters toward alarm stimulations in the group of ants, may function to enhance and prevent spread of false alarms respectively.

Discussion

Alarm behavior in social insect colonies functions to rapidly communicate information about emergent potential threats among individuals both proximal and distal to the threat. It triggers further explorative and scattering behaviors, such as “panic alarm” (Wilson & Regnier 1971), or defensive behaviors, such as mobilizing a collective aggression (Millor *et al.* 1999), or leads to a qualitative re-configuration of the defense system (Sakata & Katayama 2001). In laboratory-reared harvester ant (*P. californicus*)

colonies, alarm behavior can be experimentally induced and observed by introducing alarmed individuals into a quiescent colony, making it a highly tractable system for studying the conditions and mechanisms for adaptive information flow. Colonies showed an immediate increase in alarm behavior after introduction of alarmed ants, and these alarmed colonies gradually decayed back to resting state within 2.5 minutes. This behavioral profile is consistent with other descriptions of alarm behavior (Goetsch 1957, Wilson 1958) and is illustrative of the ability of colonies to respond immediately to potential threats and also to quickly damp alarm response to spurious threat stimuli.

As with many complex social phenomena, it is not trivial to study the rapid sequence of interactions during alarm events using visual assessments or even with motion tracking analyses alone. Using the Random Forest Machine Learning (RFML) model, we were able to consistently quantify changes in individual-level alarm behavior across timeframes of seconds or less from tracking data and categorical/ordinal annotations (Malley *et al.* 2012), which allowed us to identify the significance of individual motion and interaction most critical to alarm spread and decay. We trained my RFML model using large data samples of high-resolution motion data from ants that were each subjectively scored into different levels of alarm. These alarm scores rated by observers' intuition successfully differentiated ants' alarm responsiveness on each dimension of feature variables. In particular, the principle component analysis (PCA) uncovered these feature variables facilitated discernments of RFML approach via the pattern of individuals' movement and their social context, which implies the function of social alarming (Bossert & Wilson 1963, Wilson & Regnier 1971). The resulting trained

RFML model could then serve as a reliable, highly repeatable automatic labeler for alarm state in ants.

My RFML approach allowed for quantifying the contributions different movement behaviors made to alarm behavior. Alarmed ants tended to move at a higher velocity and moved in more circular motion patterns, potentially functioning to explore for additional evidence of threat. Ants that were moving faster but lacking these higher-order motion patterns (e.g., circular or erratic motion) were scored with a lesser degree of alarm. Moving from the individual to the group, we also were able to build a time-ordered network of signal spread as an inroad into understanding how cohesive social groups can quickly transmit and damp signals associated with potential threats.

My findings demonstrate that, unlike the broadcast signals of alarm calls and volatile alarm pheromone, as in the classic responses of ground squirrels and honeybees, the signals in the context of potential within-colony threats for *P. californicus* ants are primarily transmitted individual-to-individual by contact-mediated interactions (Wilson 1958, Sherman 1985, Sledge *et al.* 1999, Reyes *et al.* 2019, Vander Meer *et al.* 2019). In contrast to large-scale defensive signaling via alarm pheromones, individual-to-individual contacts in alarm propagation networks may function to locally scrutinize cryptic potential intruders without generating an immediate and costly full-scale response; this contact-based propagation may help to maintain a moderate collective alarm response and damp quickly when no threat is confirmed. My results also confirm the utility of using proximity-based social networks as proxies for potential information transfer in this in-nest context.

As in the physical interactions to foraging recruitment in the desert ant *Cataglyphis niger* (Razin *et al.* 2013), the alarm signal transmission in my seed-harvester ants was primarily via physical contact. However, harvester ants also use a low-volatile contact pheromone as part of their signaling process (Bossert & Wilson 1963), and my results showed that a small subset of individuals became alarmed independently of physical contact likely via contact with alarm pheromone. Thus, although *P. californicus* primarily spread alarm information through physical contact, there may be a role for non-local signaling. It may be that these ants mix some degree of local and non-local spread, or it may be that the local signaling mechanism is modulated by interactions with non-local signaling. These harvester ants and my methods of analyzing in-nest alarm spread may serve as an insightful model for studying multi-modal communication networks in general (e.g., human social networks where information flow involves various types of social connectivity).

By generating synchronous traces of spreading agents (e.g., food) and transmission events (e.g., trophallaxis), it helps to empirically characterize the spatiotemporal dynamics of agent spread in highly coordinated social groups (Greenwald et al. 2015, 2018). My RFML approach infers alarm transmission events through observation of micro-scale changes in individual behavior, which allows us to characterize information-spread dynamics without having to track a physically instantiated spreading agent. In my alarm signal propagation network, the number of nodes was observed to linearly decay with network distance from the source of alarm signal, which suggests that sustained alarm spread requires updating, which could theoretically differentiate initial perception of threat from sustained information that a

threat is real. In human social networks, the decaying transmissibility of information as a function of network distance has been suggested to limit the spread of information (Wu *et al.* 2004).

The temporal network analysis also offered opportunities to evaluate the success of individual alarm state transition or the sensitivity of alarm response. The geometric distribution of alarm responses in the 61 ants we characterized is right-skewed, which indicates that most individuals will transition to an alarmed state after only a few contacts with other alarmed individuals, while a few individuals are far less sensitive and require many more contacts to become alarmed. The significant variation in alarm sensitivity suggests that further study is needed to study the potential impact of alarm sensitivity and adaptive response of alarm-propagation networks (Sendova-Franks *et al.* 2010, Richardson & Gorochowski 2015, Pinter-Wollman 2015, Crall *et al.* 2018, Guo *et al.* 2020, Valentini *et al.* 2020). My method allows us to bridge varied individual responses and adaptive collective responses to unveil modulatory effects of individual variation on group-level phenomena, such as propagation of important signals (and damping of false signals). These scenarios also provide valuable proxies for understanding effects of superspreading on disease emergence (Lloyd-Smith et al. 2005), how adaptive immune functions are achieved via cellular variations (Wong & Germain, 2018), and how varied social conditions, such as "rumor clustering", mediate reinforcement of information or misinformation in human-domain systems (DiFonzo *et al.* 2013, Shu *et al.* 2017, Grinberg *et al.* 2019, Scheufele & Krause 2019).

Figure 2.1. Stages of the algorithm development from data collection and encoding to estimation of alarm state ($\widehat{AS}$). (I) Object tracking is applied to raw ant videos, producing a set of track matrices, each with size (#frames x 4), representing the (x, y)-position, speed, and orientation data for each frame. (II) A sliding window of length 30 frames is moved across each track. At each frame we extract a multi-dimensional feature vector containing 5 movement metrics computed over the window. (III) We select track segments that are visual exemplars of "$Unalarmed_{calm}$" ($AS = 0$), "$Unalarmed_{alert}$" ($AS = 0.5$), or "Alarmed" ($AS = 1$) behavior and add them to the training and testing datasets with their respective AS numerical labels. (IV) We train a Random Forest model to estimate these regression values from the presented feature vectors.

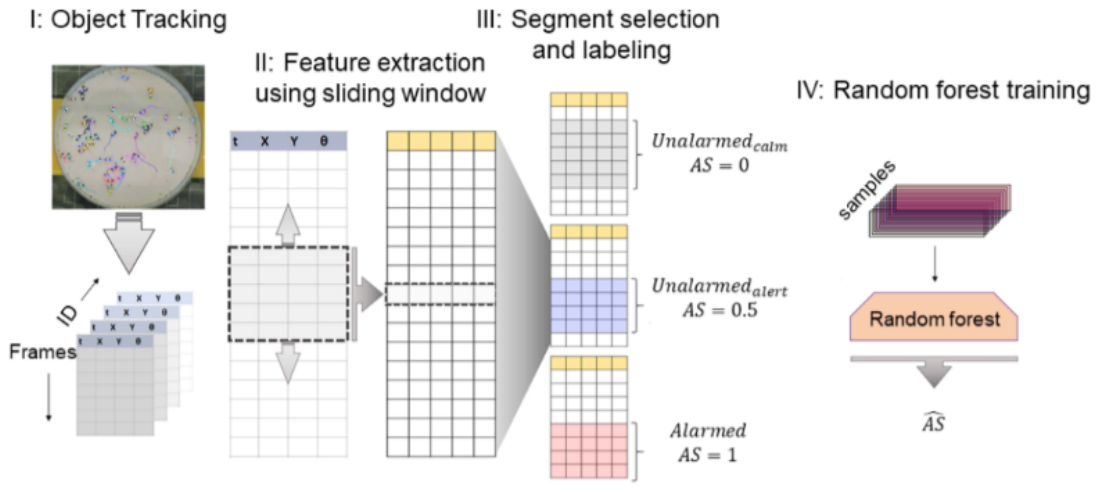

Figure 2.2. Comparison of mean instantaneous speed of ants from three colonies indicates their significant differences between the baseline and alarm event (Randomized test, permutation = 5000, $p \leq 0.00001$) (black: baseline; grey: alarm events).

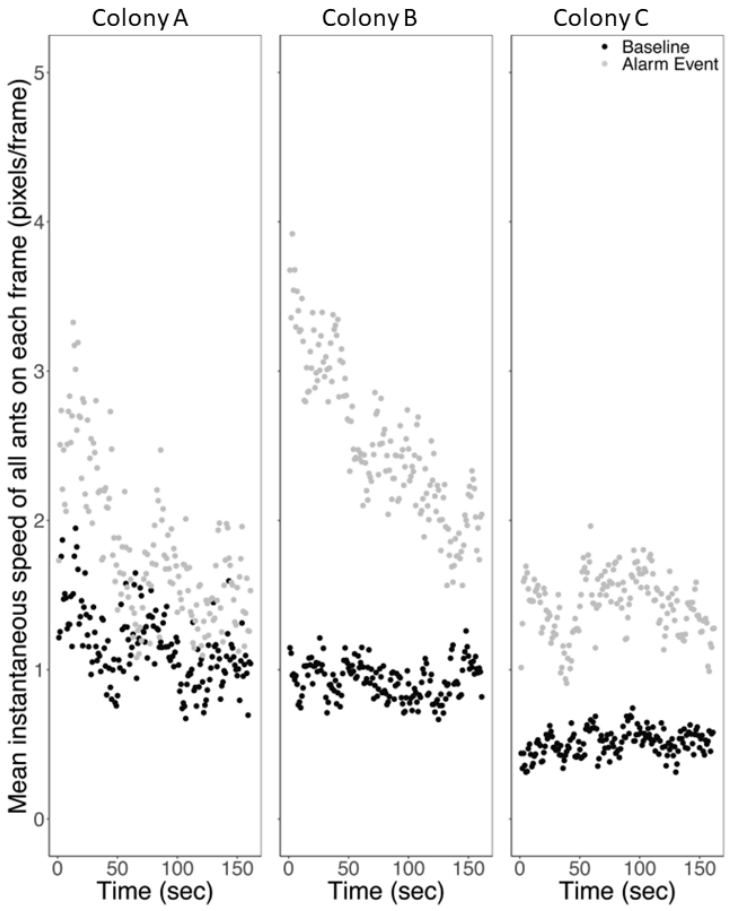

Figure 2.3: Pairwise comparison in Wilcoxon rank-sum test and principal component analysis on five feature variables. (a) Pairwise comparison of each feature variable in Wilcoxon test over three different alarm status, which were visually assessed as $Unalarmed_{calm}$ (grey), $Unalarmed_{alert}$ (light-blue) and *Alarmed* (red). In Wilcoxon test, alarm status is significantly different with each other on five feature variables respectively ($p \ll 0.0005$). (b) The five feature variables in the training data were plotted in the 2D subspace of first two principal components. “grey” represents frames when ants were identified as the $\text{Unalarmed}_{\text{calm}}$, “light-blue” as the $\text{Unalarmed}_{\text{alert}}$, and “red” as the Alarmed. (c&d) PCA weights for the training data. PC1 is a measure of locomotion pattern, and PC2 is a measure of social context.

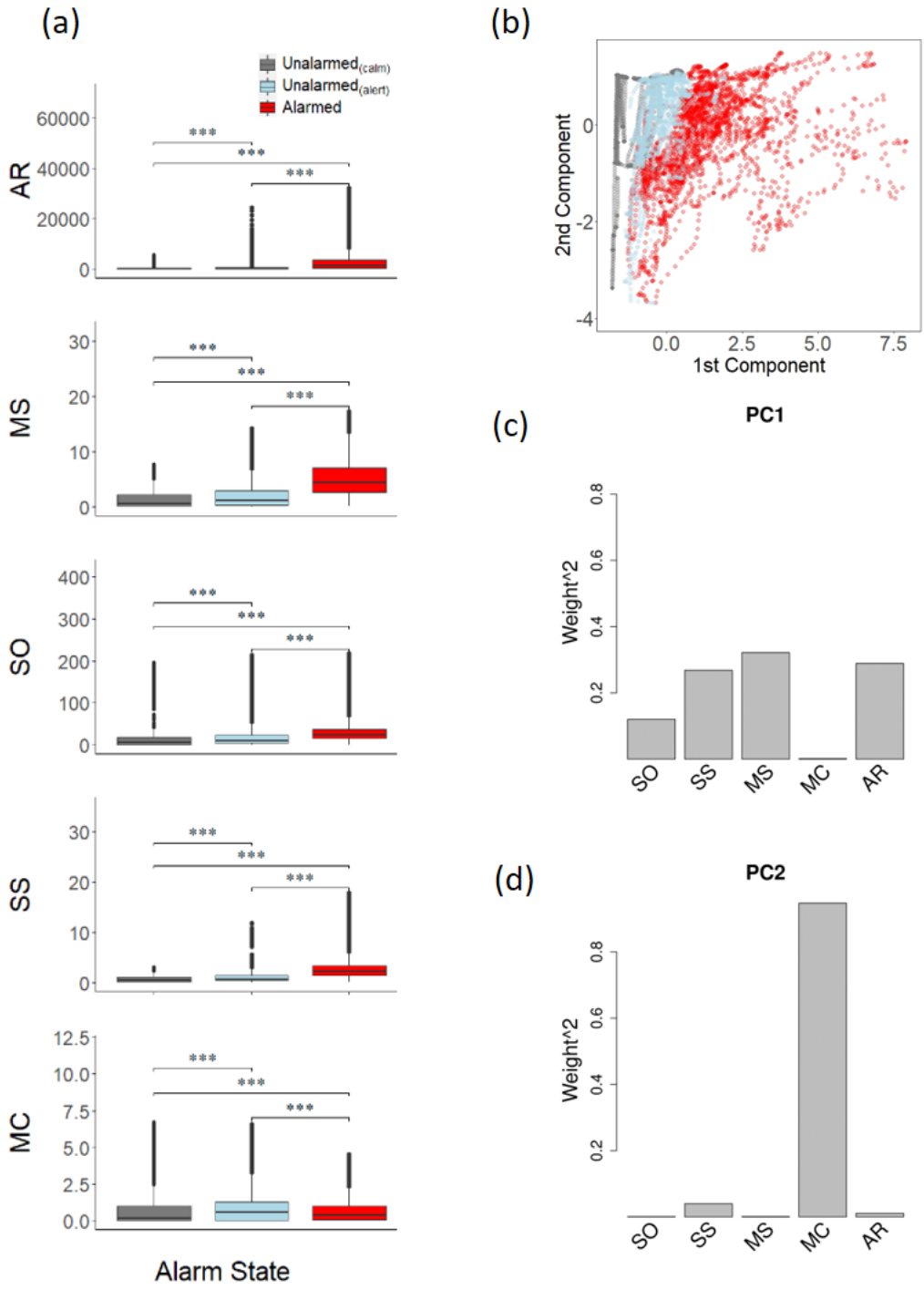
(a)
Unalarmed(calm)
Unalarmed(alert)
Alarmed
AR
MS
SO
SS
MC
***
Alarm State
(b)
2nd Component
1st Component
(c)
PC1
Weight^2
SO
SS
MS
MC
AR
(d)
PC2
Weight^2
SO
SS
MS
MC
AR

Figure 2.4: Comparison average $\widehat{AS}$ predicted by model on each second (grey) and ground truth dataset of average velocity on each second (black) as the visual evaluation indicator.

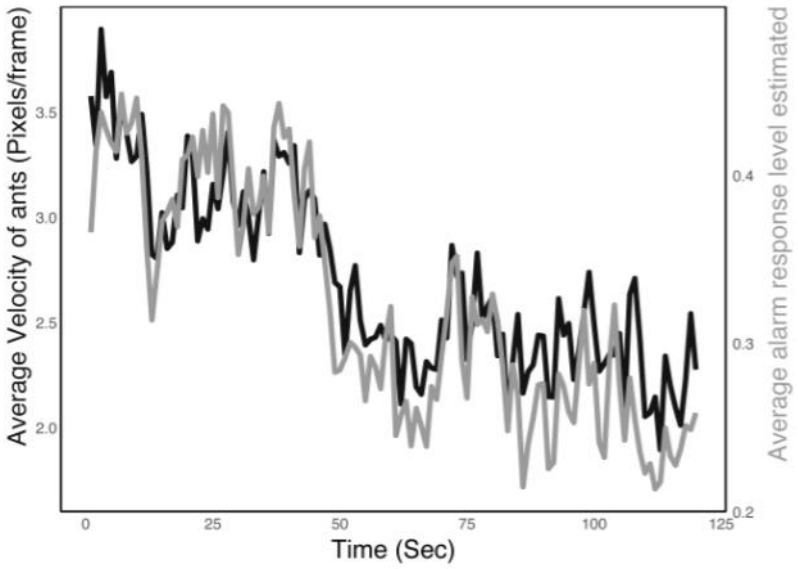

Figure 2.5: Spatial characteristics of alarm recruitment. Variation in unalarmed ants $\widehat{AS}$ during the time of approaching their alarmed neighbors. Each point indicates one unalarmed ant. The y-axis shows the variation in $\widehat{AS}$ during the time the two ants were near each other, and the x-axis shows the minimum distance between the two ants during that time. Unalarmed ants which came closer to alarmed neighbors varied more in their $\widehat{AS}$.

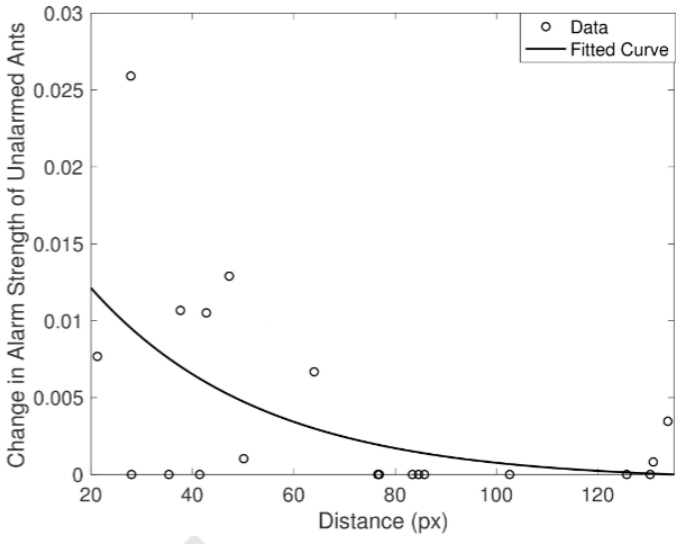

Figure 2.6: The time-aggregated alarm signal propagation network after edge pruning on temporal network of alarm propagation. The low weighted edges were pruned. The edge weighted the most was identified as the primary pathway of alarm signal propagation. “Yellow” represents initially alarmed ants placed into the test arena. “Green” represents ants which become alarmed independently of alarm contact. “Red” represents ants transited to alarmed via alarm contact.

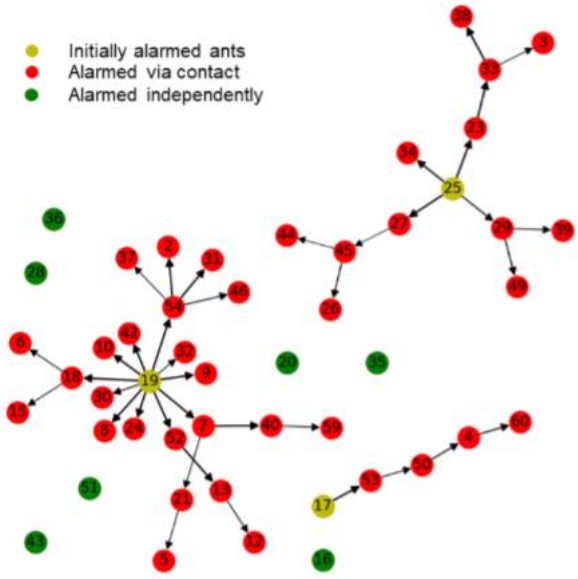

Figure 2.7. A right-skewed distribution of individual alarm response threshold. The Lilliefors corrected K-S test on the alarm response threshold (the number of contact-mediated alarm stimulations prior to alarm transition), indicates observed frequencies are not significantly different from expectations in a geometric distribution (D=0.33, *d.f.*=46, p=0.12). 'Bar' represents observations; 'Curve' represents expectations of a geometric distribution.

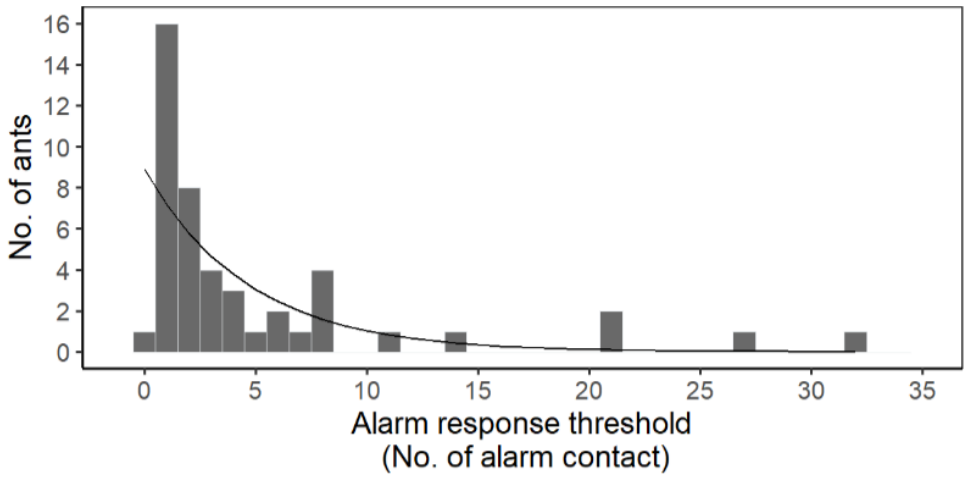

CHAPTER 3

Behind alarm propagation: the roles of individual variation and social task context in modulating alarm spread within harvester ant colonies.

Abstract

Ant colonies face a constant threat of invasion by predators and social parasites, including brood raiding by other ant colonies. Detection of these threats within the colony is therefore critical. However, colonies must balance trade-offs between the energy and disruption costs of rapidly escalating alarm responses to all potential intruders, and the risk of not responding adequately to real threats when they appear. In this study, we ask how the modulation of colony alarm response occurs. We demonstrate that individual worker variation in responsiveness is distributed in a way that allows some workers to maintain higher threat detection sensitivity while mitigating risk to task groups involved in brood care and other colony activities for which alarm response would carry a higher cost. We (1) measured individual variation in alarm responsiveness, and (2) simultaneously manipulated task-contexts (the presence/absence of task-stimuli) to examine the impact of worker task preference on their alarm response behavior. Under conditions with no task-stimuli, individual workers varied in two key behavioral traits relevant to alarm response: the level of stimulus eliciting alarm behavior, and the persistence of alarm behavior once elicited. We demonstrated that this variation is also associated with an ant's task preferences under non-alarm conditions. Specifically, ants more likely to engage in brood care or in allogrooming showed lower alarm responsiveness, while ants engaging in walking/patrolling behavior were more likely to

become and remain alarmed. We also saw significant changes in the traits of alarm sensitivity and persistence when conditions were changed from task-stimuli absence to presence, such that initial sensitivity went up but persistence declined. This context-dependency provides a uniquely empirical and theoretical platform in which to study multiscale decision-making processes. Therefore, we built an agent-based model to investigate how individual traits modulate the collective response. In my simulations, we observed: (1), alarm propagation was stymied by increasing alarm threshold or was promoted by increasing alarm persistence; (2), cascading and dampening effects were modulated by the threshold and persistence respectively. These results suggest that declines of thresholds and persistence might work as an effective information discernment strategy of ants.

Introduction

A social insect colony is a decentralized information system where individuals acquire local information from their nest-mates and the environment, then create new information, in turn, for other individuals as they impose a change on their behavior and environment (Detrain *et al.* 1999). The interdependent relations among individual social insects enable the diverse decisions to converge and finally emerge as a collective behavior pattern, e.g. in organized foraging (Cassill &Tschinkel 1999), food distribution, nest selection (Pratt 2005), and social defense (Hermann 1984). To understand how collective behavioral patterns arise, we must unravel the individual decision-making process rooted in individual traits, and elucidate the mechanism of how individuals interconnect, and share information with one another.

The relation between individual traits and collective behavioral patterns has been studied extensively across species of social insects (Fewell 2013, Mosqueiro *et al*. 2017, Crall *et al.* 2018). One source of emergent collective behavior is group composition of individuals with fixed, but varied individual traits. For example, division of labor promotes efficient task performance in social insect colonies via a composition of individuals with fixed and varied thresholds (Beshers & Fewell 2001, Gordon 1996). Alternatively, individual flexibility of response modulated by social context can also construct emergent collective behavior. Bumblebees in a social setting can dramatically increase their fanning threshold and decrease fanning durations compared to the non-social condition, which facilitated the whole colony to maintain a homeostatic nest temperature with a low investment of thermoregulation efforts (Garrison *et al*. 2018). Although integrative responses as a collective strategy successfully aid colonies to survive in an unpredictable environment regardless of consistent or flexible individual traits, a question still arises: do those two mechanisms coexist to coordinate the activities of the colony's members?

Studying the collective defense strategies of social insects, both in terms of among-individual variability, as well as within-individual flexibility provides insight. However, these topics have mostly been studied separately, leaving the question of how they interplay unaddressed. In the stingless bee *Tetragonisca angustula,* proportion and size of defense-specialized soldiers can be gradually adjusted to suit threats in the local environment (Segers *et al*. 2016), but colonies can also rapidly reassign minors to these defense tasks when soldier forces become abruptly overwhelmed (Baudier *et al*. 2019), enabling the maintenance of consistent defenses. In *Pheidole* ant colonies, the high

proportion of minor workers secures a resilient social defensive response to varied levels of intrusions because minor workers initiate more recruit invitations and have lower thresholds to recruitment than major workers (Detrain & Pasteels 1992). Different from compositional mechanisms, flexible individual alarm responses were found in the ant *Temnothorax rugatulus* (Sasaki *et al*. 2014). This species was either attracted or deterred by alarm pheromone depending on current location (in the nest or at a candidate new nest site). Also, *Lasius niger* workers that surrounded nest-mates and stood were more likely than those walking alone to elicit aggressive behavior (Sakata & Katayama 2001). Nevertheless, studies of among-individual variability and within-individual flexibility on the same colonies are still lacking, probably because methods for quantifying stimulus intensities and the corresponding responses of colony members involved in the collective defensive response are challenging.

Alarm behavior, as a part of defensive behavior, can be characterized by observable changes in movement patterns and velocity (Goetsch 1957, Wilson 1958, Mizunami *et al.* 2010). An appropriate individual alarm response necessitates individual behavioral coordination underlying interactions and social context. These individual processes then further determine a collective performance of defense, e.g. recruiting more ants to engage in aggression, or dampening alarm propagation as appropriate when confronting a non-colony-threatening stimulus (Detrain & Pasteels 1992, Reyes 2019, Maccaro *et al.* 2020). Therefore, it offers opportunities to examine those two potential mechanistic processes rooted in individual traits, and then the relation between individual traits and collective emergence.

Machine-learning approaches combining assessments of behavioral (alarm) state with information on individual contacts enable us to evaluate the intensity of alarm stimuli and corresponding individual alarm responsiveness. In this study, we used machine learning algorithms to estimate individual-level traits of alarm behavior and investigated how groups of ants respond to a non-colony-threatening event (a false alarm) artificially introduced in two experimental conditions (presence/absence of task stimuli). The effects of intrinsic task preferences of ants on their alarm behavioral individual-traits were also examined in a condition free from task stimulus. Finally, we developed an agent-based model to simulate alarm propagation via real-world networks and investigate how individual-level traits contributed to the property of collective alarm response behavior.

Methods

Animals and Housing

Colonies of California harvester ants, *Pogonomyrmex californicus*, were each reared from a newly mated queen collected during July 2016 from Lake Henshaw, CA (lat. 33.2371913, long. 116.7675003). Since August 2016, newly founded colonies had been housed in the laboratory at a temperature of 30 °C in plexiglass containers supplied with ad libitum Kentucky bluegrass seeds and frozen mealworms weekly. Three 3-year-old colonies were haphazardly chosen for experiments. The number of workers in these colonies were 316, 282, and 147. 3 days prior to the alarm inducement experiment, we haphazardly selected 50 ants of the colony to apply color painting. Workers of this species are monomorphic, making size-bias in my worker selections unlikely. Each ant selected was painted with unique color combinations on the head, thorax and gaster, by

using Sharpie oil-based paint markers, and returned back to the original nest after the completion of color labelling (Johnson 2004, Holbrook *et al.* 2011). To prevent ants from being disturbed by external noise or vibration during experiments, the nest or test arena was placed on top of a foam pad within an enclosed glass tank. A video camera (Panasonic HC-WXF990) was securely mounted above the glass tank for video capturing of task behavior and alarm events.

Video capturing and manual recording of task behavior

After painting, we returned ants to their original nests and allowed them to acclimate to their paint markings overnight. The next day we recorded a continuous 6-hmy video to capture task-related behaviors of 50 paint-marked ants in each colony. Each full-length video was clipped into 10 sub-videos (length of each sub-video = 36 minutes). We started at time *t* randomly within each sub-video and followed each individual ant to continuously record her task-related behaviors for 3 minutes. Thirteen task-related behavioral acts were targeted: manipulating brood, carrying brood, antennating brood, manipulating trash, carrying trash, manipulating food, carrying food, allogrooming, grooming, walking, idling, chewing cotton, antennating nestmates. In total, each paint-marked ant was scanned for 30 minutes, and so each colony had 1500 minutes of behavioral scanning across the full-length video.

Test arena design

I took the marked ants and transferred them into different nest environments, circular featured and featureless arenas (circular plexiglass petri-dishes, diameter=15cm), for alarm response testing (diameter=15cm). The featured test arena incorporated task-

related stimuli (brood, food, and trash obtained from their original nest). The featureless test arena was identical except that it did not include the task-stimuli. After transferring 50 paint-marked ants to the test arena, we allowed them to have an overnight acclimation period, then induced alarm in the featured test arena on day 1, and then induced alarm in the featureless test arena on the day 2. Twenty-four hours is a sufficiently long time interval to prevent impacts of repeated exposure to alarm stimulations (Maccaro *et al.* 2020).

To identify effects of task-related stimuli on alarm signal propagation, we used two types of test arenas which were constructed out of previously unoccupied circular plexiglass petri-dishes (diameter=15cm). The featured test arena incorporated task-related stimuli (brood, food, and trash obtained from their original nest). The featureless test arena was identical except that it did not include the task-stimuli. After transferring 50 paint-marked ants to the test arena, we allowed them to have an overnight acclimation period, then induced alarm in the featured test arena on day 1. Next, we transferred them to the featureless test arena, then induced alarm in the featureless test arena on the day 2. Twenty-four hours is a sufficiently long time interval to prevent impacts of repeated exposure to alarm stimulations (Maccaro *et al.* 2020).

Alarm behavior initiation

Prior to stimulating an alarm event, 3 ants were haphazardly selected to serve as initial alarm stimulators. They were carefully removed from the testing arena by using an aspirator to minimize disturbance and placed into a separate petri-dish. After 30 minutes, we then video-recorded ants' activities for 10 minutes. During the video recording, those 3 removed ants were pinched gently with soft forceps until they displayed visible agitated

movement (between 2 and 2.5 minutes). The agitated ants were then dropped into the center of the test arena via a funnel to initiate the alarm events. The full-length video (10 min) was clipped into two 2-minutes long sub-videos: 0~2 minutes for baseline, and t~t+2 minutes for alarm events (t is the time 3 alarmed ants were reintroduced into the test arena). This protocol was replicated for each test arena. Finally, we obtained 4 sub-videos across 2 test arenas for each group of ants.

Tracking and supervised machine learning

We followed the method developed in chapter 2 to estimate each individual ant's frame-by-frame alarm strength: 1. we used the multi-object tracking program, ABCTracker (Rice *et al.* 2020), to generate frame-by-frame trajectorial data of each ant; 2. we created 59 track segments with varied length from 60 to 449 frames and extracted movement features associated with ants' alarm status; 3. we evaluated level of alarm for each ant manually (Table 3.1); 4. we imported features extracted from track segments to train and test the Random Forest Machine Learning (RFML) model; 5. we used the trained RFML model to estimate the alarm status of each ant based on their frame-by-frame movement features for the full video.

Model simulation of collective alarm response

Real-world networks have been extensively used to investigate the mechanism of how individual traits and behavioral rules modulate emergent collective behavior in social insect colonies, or even human societies (Blonder & Dornhaus 2011, Pinter-Wollman *et al.* 2011, Richardson & Gorochowski 2015, Firth *et al*. 2020). The alarm responses were demonstrated to propagate via contact-mediated interactions (Chapter 2).

Hence, we developed an agent-based discrete-time Markov chain model to simulate alarm signal propagation in real-world networks captured from groups of worker ants.

In this model, at any given time t ant worker k is characterized by its attribute $\eta_k(t) = (r_k(t),p_k(t),a_k(t))$, where $r_k(t)$ is the cumulative number of contacts of ant k with alarmed ants by time t, $p_k(t)$ is the amount of time remaining for alarmed state of ant k at time t, and $a_k(t)$ is its alarm status at time t (0 for the *unalarmed*, or 1 for the *alarmed*). We captured real-world networks from 3 groups' alarm events in featureless conditions used as the pre-determined temporal social context. Varied alarm response threshold (R_k) and maximum persistence of alarm behavior (P_k) from geometric distributions are assigned to each ant. The geometric distributions are defined based on the mean value of individual traits estimated empirically in each group. In simulation experiments for each group, three individual agents are randomly chosen as the alarm information seeds to initiate subsequent collective alarm behavior. Each individual had a binary alarm status. Through time, individual agents update their attributes by the process described below (Table 3.2):

1. Every individual ant initiates their alarm states $a_k(0)=0$ except three alarmed seed ants, $a_i(0)=1$;
2. Each alarmed ant updates its alarm duration, $p_k(t)= p_k(t-1)-1$ at each iteration until $p_k(t) = 0$;
3. If an alarmed ant has an unalarmed neighbor j in the real-world network at time t, the unalarmed neighbor j will update its cumulative number of alarm stimulations, $r_k(t)= r_k(t-1)+1$;
4. If the number of alarm stimulations of an unalarmed ant k at time t exceeds its threshold (i.e., $r_k(t) \geq R_k$), its status changes to alarmed, (i.e., $a_k(t)=1$).

5. If an alarmed ant *j* updates its duration of alarm behavior, $p_k(t)=0$, it will transition to the unalarmed status, $a_k(t)=0$, and stay unalarmed for the rest of time.

We assume one time tick in the model is consistent with the time scale of the aggregated real-world social network (Δt = one second). Each simulation is run 120 iterations, and repeated 100 times to incorporate random effects of initial parameters and the information propagation process. Table 3.3 states the parameter definitions and baseline values for the simulation.

We conducted three major simulation experiments on each group to investigate effects of individual alarm response threshold and alarm persistence on the collective alarm responses:

1. Simulations with increasing individual alarm response thresholds by 0%, 50% and 100%, but no changes of persistence.
2. Simulations with increasing individual alarm persistence by 0%, 50% and 100%, but no changes of thresholds.
3. Simulations with increasing individual alarm threshold and persistence by 0%, 50% and 100%, simultaneously.

Results

Validation of collective alarm elicitation

The speed of movement is a widely used indicator to discern the alarm status of ants for human raters (Goetsch 1957, Wilson 1958, Mizunami *et al.* 2010). Here, we employed the mean instantaneous speed of ants to validate my experimental procedures.

We tested the ants' speed difference between the alarm treatment condition and the baseline condition and found statistical significance (Randomized tests, permutation = 5000, $p \leq 0.00001$) in all groups A (Fig. 3.1A&D), B (Fig. 1B&E) and C (Fig. 3.1C&F) across the featured condition (Fig. 3.1D, E&F) and the featureless condition (Fig. 3.1A, B&C). This result demonstrates that alarm responses of ants were successfully induced via three alarmed ants re-introduced into the test arena regardless of experimental conditions and which colonies group of ants coming from.

Alarm status classification

A Random-Forest regression model was trained to estimate continuous alarm strengths of ants, and its accuracy was estimated using the root mean square error (RMSE = 0.065). The frame-wise standard deviation of speed was ranked as the most significant feature variable in predictions followed by the frame-wise mean speed, the convex hull area of locomotion, the standard deviation of body axis orientations and finally the frame-wise mean number of contacts with neighbors. To identify Alarmed ants and estimate their transition from unalarmed to alarmed state, we applied the multiclass Receiver-Operator-Characteristic pairwise analysis to find the best threshold value for differentiating alarmed ants from unalarmed ants (ants in states of *Unalarmed-calm* and *Unalarmed-alert*) (Landgrebe & Duin 2007). On an ROC curve for the comparison between Alarmed state and Unalarmed states, a threshold of classification (0.703) was estimated corresponding to the Youden index, *J*, a metric identifying the maximum potential effectiveness of the classification (Youden 1950). The area under the ROC curve (AUC) for this comparison was 0.9677. From this, we categorized ants with alarm strength above 0.703 as alarmed, and those with lower alarm strength as unalarmed.

Task preference identification

A hierarchical cluster analysis (Euclidian distance and complete-linkage method) consistently classified paint-marked workers of each colony into four separate groups based on the proportion of time spent on each task-related behavior: nurses (7, 7 and 6 ant workers for group A, B and C separately), nest-patrollers (17, 11 and 14 ant workers), idlers (15, 6 and 24 ant workers), and nest-maintainers (7, 14 and 4 ant workers) (Fig. 3.2). Task-related behaviors were also placed into a hierarchical dendrogram (Euclidian distance and complete-linkage method), and consistently clustered into 5 groups (top dendrogram): manipulating brood, walking, idling, chewing cotton and others. In the cluster analyses, those task scores by individual ants reflect the pattern of how ants allocate their time over tasks. A wide repertoire of task-related behaviors indicates the relative importance of one task preferred by ants to other tasks.

Individual-level traits of alarm response behavior

Behavioral response threshold was assessed by the intensities of key sensory cues received before a response is elicited (Scheiner *et al.* 2004). Therefore, before each alarm state transition, we used the number of contacts an unalarmed ant made with alarmed neighbors before becoming alarmed herself as a measure of alarm response threshold. In other words, an unalarmed ant that underwent fewer alarm stimulations prior to becoming alarmed would have a lower threshold. To investigate the effects of task preferences on alarm response, we examined individual alarm response thresholds in the featureless arena (Fig. 3.3). Colony fragments had different numbers of ants transitioning to an alarmed state (29 workers; 18 workers; 30 workers), and their alarm response thresholds were significantly different over their task preferences (Kruskal-Wallis test, $p=0.0028$):

nursing ants had significantly higher alarm response thresholds than nest-maintaining ants (Wilcox test, $p = 0.023$) and nest-patrolling ants (Wilcox test, $p < 0.001$), and idling ants had significantly higher response threshold than nest-patrolling ants (Wilcox test, $p = 0.011$).

A group composed of individuals with varied behavioral persistence has been demonstrated to impact collective behavior (Mosqueiro *et al*. 2017). In the process of alarm response propagation, how long the alarmed ants persisted in their status also impacted their capabilities of alarm recruitment and further the collective alarm response. Therefore, as one of the significant individual-level traits, the persistence of alarm behavior after first-time alarm transition was also examined over tasks in the featureless condition (Fig. 3.4). Individual persistence of alarm behavior was significantly different across tasks (Kruskal-Wallis test, $p<0.01$): nest-patrolling ants had significantly more persistent alarm behaviors than ants preferring the other three tasks (vs brood-care ants: $p<0.001$; vs idling ants: $p<0.01$; vs nest-maintaining ants: $p = 0.018$).

Meanwhile, the relationship between individual alarm persistence (P) and alarm response threshold (R) was examined in an exponential decay model (Fig. 3.5; Eqn.3.1, α=25.2, β=0.75, γ=5.24, *d.f.*=60, F=6.13104, p=.00378). The significant relationship suggests that those two metrics of individual alarm response behavior consistently reflect the hardships in ants' alarm elicitations and performances: individuals demanding more alarm stimulations prior to their alarm transitions tend to perform alarm behavior in shorter durations.

$$\boldsymbol{P} = \alpha \times \beta^{\boldsymbol{R}} + \gamma \qquad \text{(Equation 3.1)}$$

Effects of task context on individual and collective alarm response.

Overall 26 ant workers in three groups became alarmed in both conditions, which enabled us to estimate effects of task-context on alarm responsiveness and their persistence. At the individual level, ant workers significantly dropped both their alarm response threshold (Wilcox test, $p = 0.011$) and persistence of alarm behavior (Wilcox test, $p < 0.01$) in the featured condition (Fig. 3.6), which suggests that task-stimuli modulate alarm response behavior, and cause ant workers to respond more sensitively to perturbations, but to sustain their alarm status for shorter durations.

At the colony level, we evaluated collective alarm response by examining the dynamics of alarmed ant populations and the cumulative number of alarm transitions. Those two metrics showed consistent patterns of alarm activities at the group level, such that alarm response behavior dampened more rapidly, and fewer alarm transitions occurred in the featured condition than in the featureless condition (Fig. 3.7).

Model simulations for collective alarm response rooted in individual-level traits

Comparing all simulations under baseline threshold and persistence conditions, when the threshold alone was increased by 50% and 100%, we observed the percentage of the population cumulatively alarm-recruited dropped from 90% to 84%, and 74% for group A, from 28.6% to 20.4% and 16.3% for group B, and from 74.5% to 56.9% and 45.1% for group C (Fig. 3.8A, D&G). When the persistence alone was increased by 50% and 100%, the percentage increased to 98% and 98% for group A, 55.1% and 73.4% for group B, and 92.2% and 96% for group C (Fig. 3.8B, E&H). In simulations with combined increase of threshold and persistence by 50% and 100%, the percentage increased to 94% and 96% for group A, 38.8% and 38.8% for group B, and 82.4% and

84.3% for group C (Fig. 3.8C, F&I). Those results suggest that high thresholds of ant workers impede alarm propagation, while high persistence facilitates the alarm propagation. Also, persistence was a dominant factor whose increments offset the inhibition effects due to the increase of thresholds, and aid all groups to achieve stronger collective alarm response.

Examining temporal dynamics of alarmed ant populations, we found that all three groups shared common dampening tails after 51, 33, and 73 seconds respectively as threshold alone increased by 50% and 100% (Fig. 3.9B, E&H). Meanwhile, increasing persistence, either alone or in combination with increased threshold, resulted in extended dampening periods (Fig. 3.9A, C, D, F, H&G).

In my simulations, increasing persistence and threshold simultaneously resulted in stronger collective alarm responses and extended dampening periods, which are consistent with the experimental observations (Fig. 3.7). My empirical and theoretical results suggest that task-related stimuli may facilitate ants to achieve information discernment capability by securing strong cascading (low threshold) and rapid dampening (low persistence).

Discussion

In social insect colonies, individual variations in task-independent behavioral traits sometimes relate to task specialization. For example, teams of carpenter ants (*Camponotus fellah*) that are heterogeneous in their mobility could contribute to task specialization by affecting the rate at which individuals encounter different task-related stimuli, and the task specialization, in turn, promotes the individuals' spatial fidelity to develop task stations (Mersch 2013). Carpenter ants (*Camponotus aethiops*) also exhibit

inter-individual differences in responsiveness to sucrose in the dimension of task specialization such as foraging and nursing (Perez 2013). In honey bee colonies, newly emerged workers respond to sucrose concentration differently, which is associated with their later task specialization in pollen or nectar foraging (Page 2013). A spectrum of individual-level traits is examined on the axes of task behaviors, which provides a valuable dimension to investigate where those variations of traits come from and what potential functions they have on the whole colony.

In the featureless condition, my observations of alarm response thresholds and alarm persistence of seed-harvester ants showed variability of alarm response behavior across individuals with different innate task preferences. Nest patrollers had lower thresholds and longer persistence than brood tenders. This result is consistent with a study on social cichlids (*Neolamprologus pulcher*) which found that an individual's tendency to explore a social-context-absent environment made them more likely to defend a communal territory, while less defensive individuals were more likely to maintain the breeding shelter (Bergmüller & Taborsky 2007). The relationship between task-independent behavior and task-related behavior highlights the significance of task behavior syndromes and potential developmental trajectories of task-specialization (Loftus *et al.* 2021).

Among-individual and within-individual behavioral variation are not mutually exclusive (Loftus *et al.* 2021). To some extent, it is evolutionarily adaptive to maintain flexible responses rather than strictly specialize because it maximizes task performance efficiency (Kolmes 1986). For example, individual flexible fanning response in honey bee (*Apis mellifera*) efficiently promotes stable nest thermoregulation (Jones *et al.* 2004),

and arises from individual differences in experience coinciding with relative social influence (Kaspar *et al.* 2018; Cook & Breed 2013). Specifically, individually flexible alarm responses modulated by contexts (presence or absence of task stimuli) also contribute to the resilience of collective alarm response to the non-colony-threatening events we artificially initiated. Simulation results obtained from my agent-based model are consistent with my experimental observations that more sensitive and less persistent individual alarm behavior in the condition of task-stimulus-present causes a rapid dampening collective alarm response, and fewer ants mobilized to alarm. Due to the limited sample size, the impacts of among-individual variability on inter-colony variability was not statistically estimated. However, my model showed that colonies with more variability in persistence also had larger numbers of alarmed ants. Group A with a greater variability of persistence or standard deviation in a geometric distribution (18.94) resulted in more ants alarm-recruited. A wide range of persistence distribution ensures the presence of some individuals with high persistence who may cause super-spreading events. However, individuals with low persistence may mitigate the alarm propagation simultaneously. Therefore, to maintain an average low threshold and persistence of individuals may be sufficient for colonies to capture potential threatening events and to discern the real-threats from environmental perturbations.

In social insect colonies, environment as a part of information background deeply involves parallel individual information processing and decision making, and is considered to contribute to the robustness of the whole system. “Common stomach” theory believes materials stored in the internal/external storage area, e.g. the comb where individuals can deposit or acquire materials, may be an “information center” that

efficiently coordinates individual decision making for task allocation (Schmickl & Karsai 2016). Meanwhile, task-related stimulus pairing with individual spatial fidelities may up-/down-regulate the spatial distribution of individuals and encountering rate at which individuals transmit valuable information, but avoid information noisy (Guo *et al*. 2020). Even the residuals of spreading agents persisting in the environment, e.g. chemical road-signs in *C. fellah* ants' nest (Heyman *et al*. 2017), may also allow colonies to achieve dual-functionalities of networks to enhance or inhibit the spreading of different types of agent (Richardson & Gorochowski 2015). However, those theoretical research endeavors are still lacking sufficient empirical evidence. Here, we combined machine learning and automated tracking to empirically demonstrate the rapid dampening of collective alarm response when task stimuli are present, which implies the modulation effects of task stimulus in individual alarm information processing, and further in alarm responses at group level.

Due to the high metabolic cost of alarm behavior in social insects (Moritz *et al*. 1985), an appropriate level of collective alarm response was needed for seed-harvester ants to mitigate signal propagation in the nest when a non-colony-threatening event was initiated by re-introducing agitated ants instead of real threats. The trade-off between high metabolic cost and discerning every potential threat necessitates negative feedbacks to down-regulate the collective response of group-living animals, but the proximate mechanisms mediating this down-regulation are still not clearly understood. We speculate direct brood interactions or indirect brood pheromone interactions may primarily modulate the individual plasticity of alarm response and behavior persistence. There is evidence of strong brood influence on other collective adult behaviors in a

variety of social hymenopterans. Cyclical changes in emigration and raid frequency are primarily driven by worker-sensed larval hunger in many army ants and clonal raider ants ("The Brood Stimulation Hypothesis," reviewed by Baudier 2021; Schneirla 1950; Ulrich *et al.* 2016). Nonvolatile chemicals produced by larvae work as solicitation signals for brood care and feeding in fire ants and honey bees (Cassill & Tschinkel 1995, 1999, Pankiw *et al*. 1998). Also, adult honey bees adaptively shut off their circadian rhythms in behavior or clock gene expression in the presence of brood or brood pheromone (Shemesh *et al.* 2010). Otherwise, nest waste or processed food particles carrying the chemical signature of the original nest also possibly triggered ants to recognize the test arena as their nest, and led them to behave differently. Future studies analyzing effects of single task-related stimuli will provide insight into the details of these dampening processes.

Overall, my empirical results highlight the coexistence of among-individual and within-individual variability in alarm response behavior. My simulation experiments show that varied collective alarm responses originate from two flexible individual-level traits, alarm behavior thresholds and persistence. The consistent patterns found in the simulation and empirical results suggest socially mediated behavioral flexibility plays an important role in the resilience of alarm behavior elicitation.

Table 3.1: Training data from 59 track segments.

No. of Video Sources	Number of ants	Alarm Strength	Alarm Status	Frames
3	16	0	*Unalarmed-calm*	2917
4	21	0.5	*Unalarmed-alert*	3908
6	22	1	*Alarmed*	3755

Table 3.2: Value of parameters and variables updated per iteration.

Algorithm1: The mechanism of the model within a time unit, Δt .

```
1  for k ∈ A(t) = {l : a_l(t) = 1} do
2      if p_k(t) = −1 then
3          p_k(t + Δt) = P_k;
4      Else if p_k(t) > 0 then
5          p_k(t + Δt) = p_k(t) − 1;
6      for j as contact of k do
7          if j ∈ U(t) = {l : a_l(t) = 0} then
8              r_j(t + Δt) = r_j(t) + |{m : a_m(t) = 1
                   and ant m had contact with j at time t ;          }
9          if r_j(t + Δt) > R_j then
10             p_j(t + Δt) = −1;
11     end
12 end
```

Table 3.3: Value of parameters and variables updated per iteration.

	Notation Definition	Baseline Value (Colony A, B and C)	Source
$\boldsymbol{N}$	Number of agents.	49, 50, 51	Estimated from each group
$\boldsymbol{A(t)}$	Set of alarmed ants at time *t*.		
$\boldsymbol{U(t)}$	Set of unalarmed ants at time *t*.		
$\boldsymbol{r_k(t)}$	Cumulative number of contact of ant *k* with alarmed ants at time *t*.		
$\boldsymbol{R_k}$	Initial alarm response threshold of ant *k* from a geometric distribution with the mean (α)	$grn(\alpha)$; $(\alpha = 5.45, 7.94, 6.67)$	Estimated from each group
$\boldsymbol{p_k(t)}$	Persistence of alarm behavior of ant *k* at time *t*.		
$\boldsymbol{P_k}$	Maximum persistence of alarm behavior of ant *k* from a geometric distribution with the mean (β)	$grn(\beta)$; $(\beta = 19.45, 9.89, 15.67)$	Estimated from each group
$\boldsymbol{a_k(t)}$	Alarm status of ant *k* at time *t*.	0/1	

Figure 3.1: Comparison of mean instantaneous speed of ants. In all groups of ants, there are significant differences between the baseline and alarm event (Randomized test, permutation = 5000, $p \leq 0.00001$) in two experimental conditions (black: baseline; grey: alarm events; 1st row: featureless condition; 2nd row: featured condition).

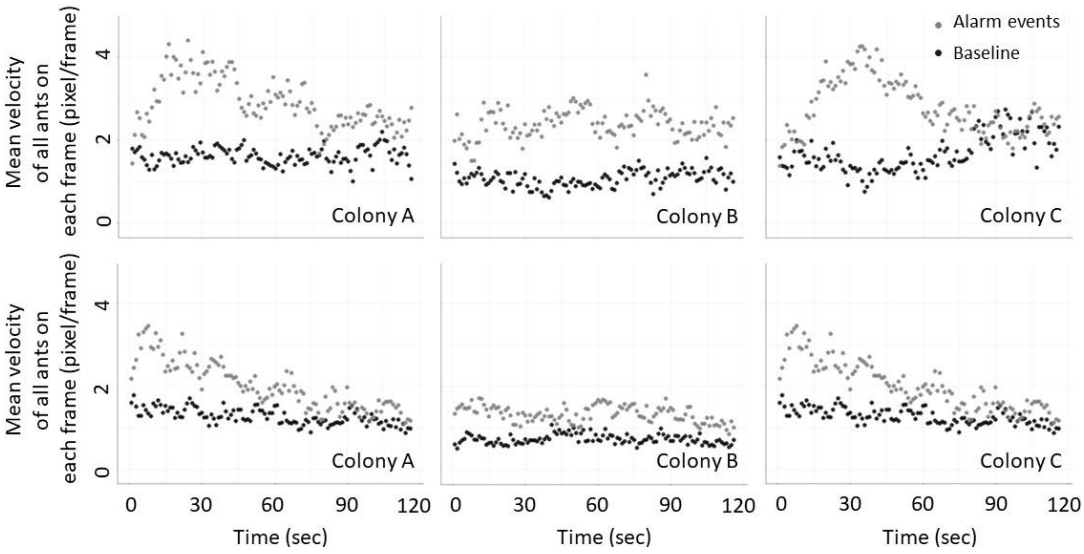

Figure 3.2: Hierarchical cluster analysis (Euclidian distance, Complete-linkage method) of workers according to time spent on tasks (left dendrogram) shows that workers are separated into four major tasks groups (brood-carer, walker, idler and constructor). Clustering of tasks shows a similar pattern (top dendrogram) where five task-related behaviors were identified, e.g. nursing (manipulating brood), wandering (walking), inactivity (idling), constructing (chewing-cotton) and other tasks (self-grooming, manipulating trash, antenating brood, carrying brood, carrying trash, carrying food, manipulating food, grooming nestmates, and antenating nestmates). Z-scores indicate whether individual workers (represented by thin colored cells in the central graph) spend more time (maximum value of z score — red), less time (minimum value of z score — blue) than the mean amount of time spent on that tasks for all workers.

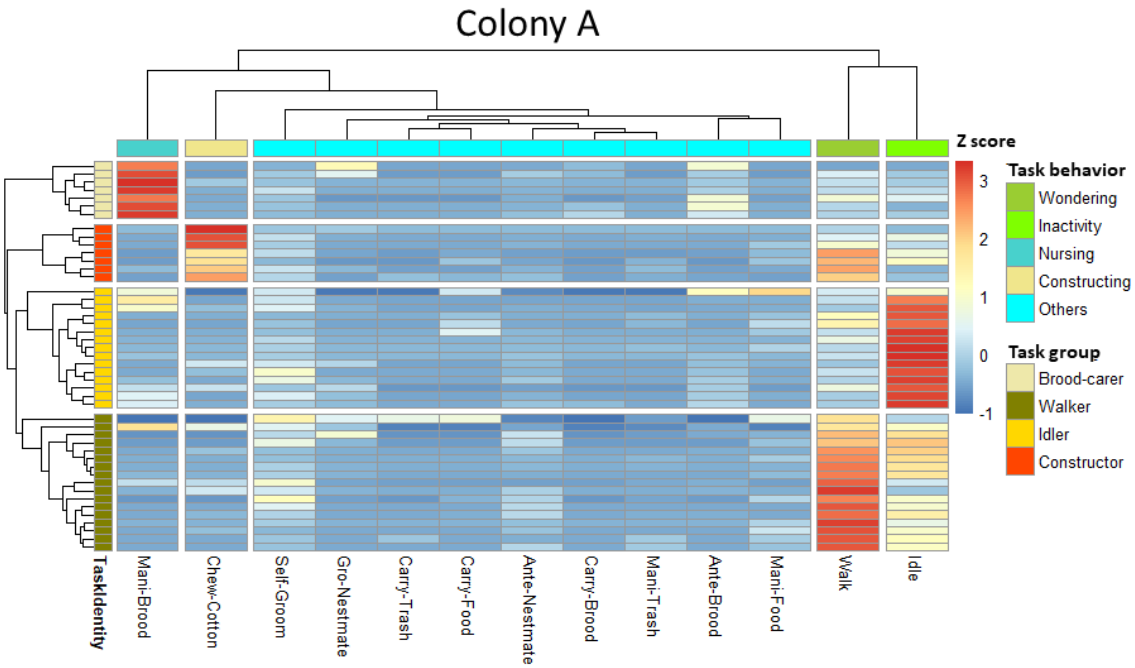

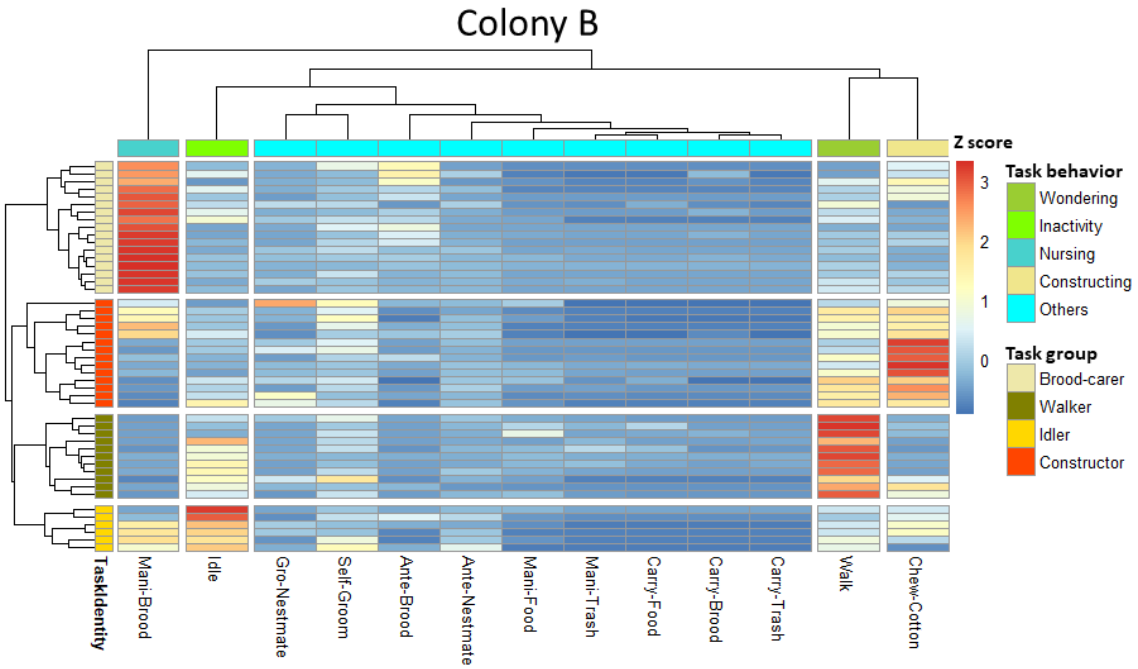
Colony B
Z score
3
2
1
0
Task behavior
Wondering
Inactivity
Nursing
Constructing
Others
Task group
Brood-carer
Walker
Idler
Constructor
TaskIdentity
Mani-Brood
Idle
Gro-Nestmate
Self-Groom
Ante-Brood
Ante-Nestmate
Mani-Food
Mani-Trash
Carry-Food
Carry-Brood
Carry-Trash
Walk
Chew-Cotton

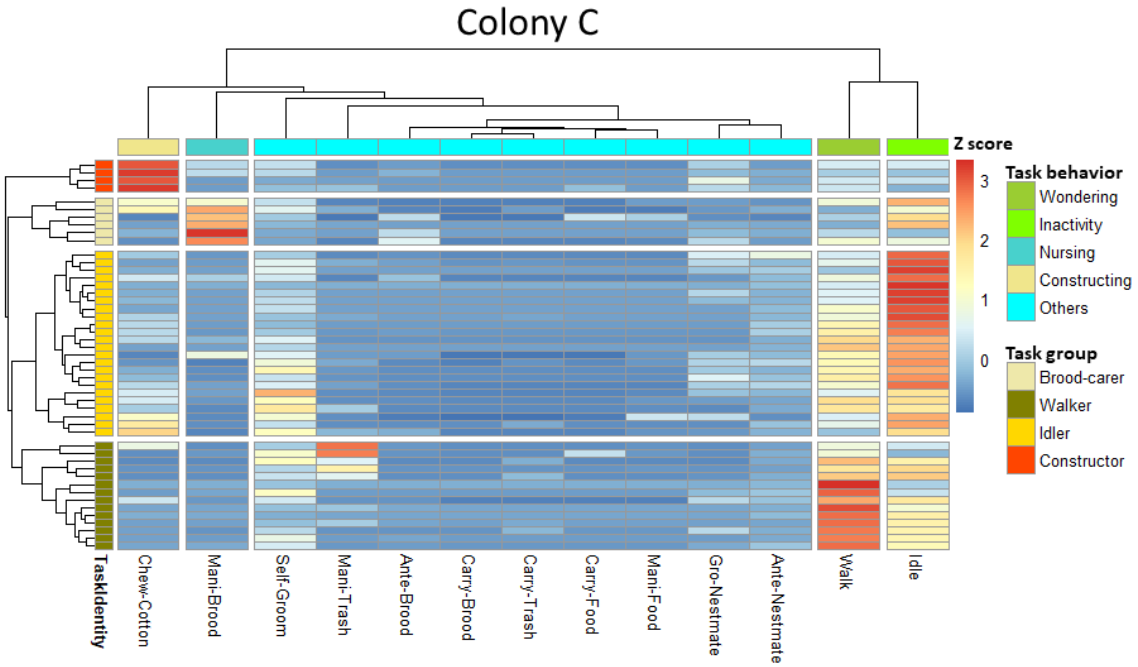
Colony C
Z score
3
2
1
0
Task behavior
Wondering
Inactivity
Nursing
Constructing
Others
Task group
Brood-carer
Walker
Idler
Constructor
TaskIdentity
Chew-Cotton
Mani-Brood
Self-Groom
Mani-Trash
Ante-Brood
Carry-Brood
Carry-Trash
Carry-Food
Mani-Food
Gro-Nestmate
Ante-Nestmate
Walk
Idle

Figure 3.3. Comparison of individual alarm response thresholds over task-preferences in the featureless condition. It shows that task-preference is a significant factor in ants' alarm response thresholds (Kruskal-Wallis test, p = 0.0028). Pairwise comparisons of thresholds demonstrate that brood-tenders had significantly more alarm stimulations prior to the alarm transition than nest maintainers (Wilcoxon test, p = 0.023) and nest patrollers (Wilcoxon test, p <0.001). Also, Idlers had significantly more alarm stimulations prior to their alarm transitions than nest-maintainers (Wilcoxon test, p = 0.011).

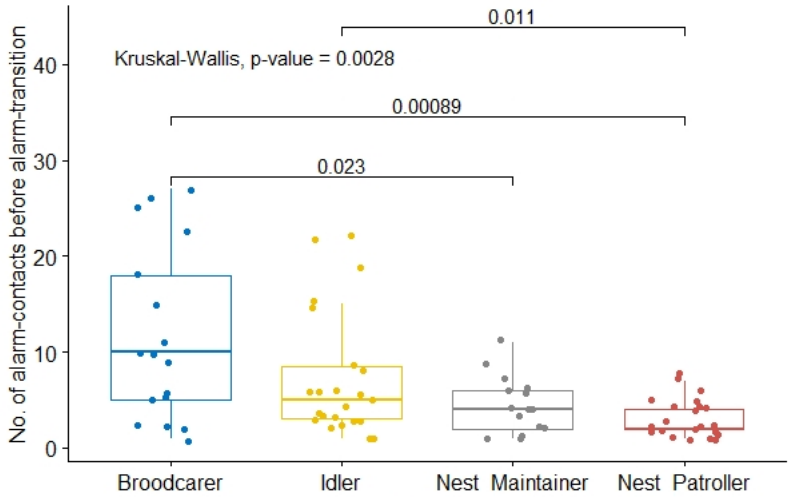

Figure 3.4: Comparison of individual alarm behavioral persistence over task-preferences in the featureless condition. It shows that the task-preference is a significant factor in differing ants' alarm behavioral persistence (Kruskal-Wallis test, p = 0.0012). Pairwise comparisons of thresholds demonstrate that nest-patrollers had significantly more persistent alarm behavior than nest maintainers (Wilcoxon test, p = 0.018), idlers (Wilcoxon test, p <0.01) and brood-tenders (Wilcoxon test, p <0.001).

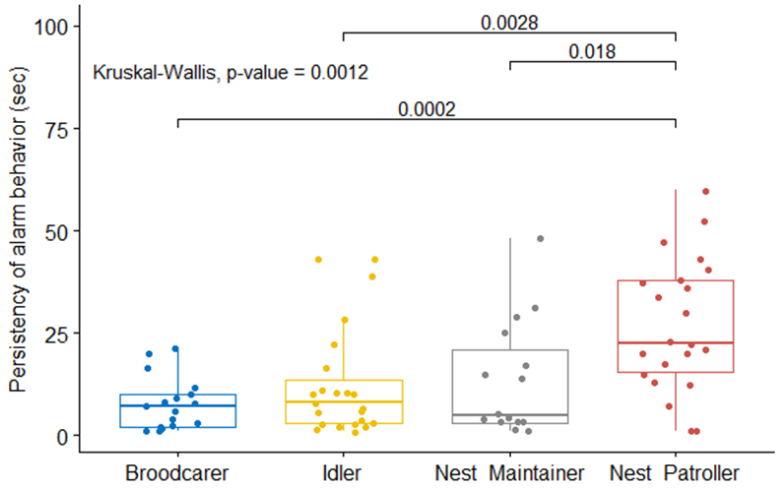

Figure 3.5: Relation between alarm response threshold and alarm behavioral persistence. The significant nonlinear correlation between alarm response threshold (R) and alarm behavioral persistence (P) was estimated in the exponential decay model (red curve). It indicates that ants' alarm behavioral persistence exponentially decays as alarm thresholds increase (F=6.13104, *d.f.* = 60; p=.00378).

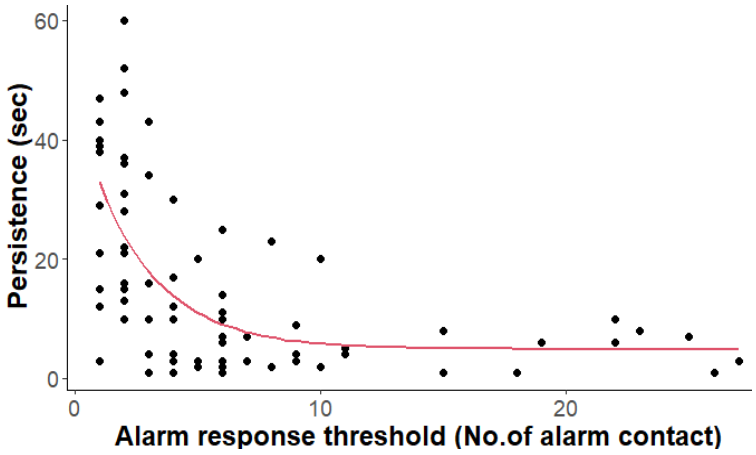

Figure 3.6: Pairwise comparison of alarm response thresholds and alarm behavioral persistence. For 26 ants who transitioned into the alarm status in both of conditions (featured & featureless), there are significantly lowered alarm thresholds (Wilcoxon test, $p = 0.011$) and persistence (Wilcoxon test, $p < 0.01$) in the featured condition.

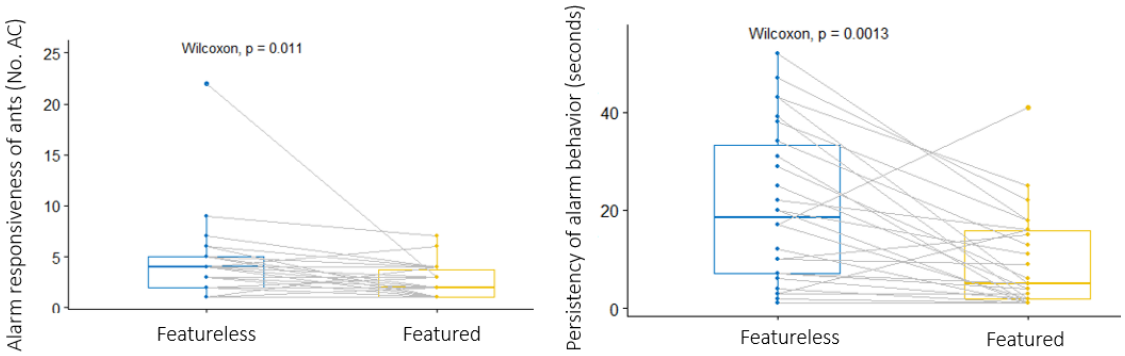

Figure 3.7: Comparison of collective alarm response behavior in three groups. It was observed that cumulative number of alarm transition events by time *t* consistently dropped in featured condition (blue shade area) than in featureless condition (blue shade area), and alarmed ants' population at time *t* in featured condition (blue shade area), consistently dampened more rapidly than in the featureless condition (green shade area).

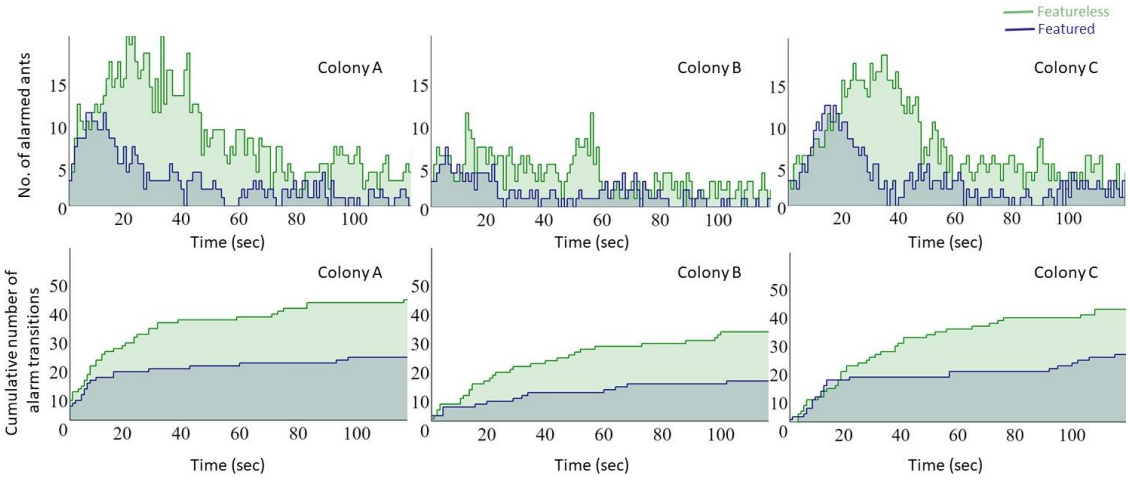

Figure 3.8: Model predictions of alarm propagation for the cumulative number of alarm transition events. Simulation experiments were run in scenarios to: (1), increase persistence alone by 50% and 100% (A, D&G); (2), increase threshold alone by 50% and 100% (B, E&H); (3), increase threshold combined with persistence by 50% and 100% (C, F&I). Solid lines and shaded areas represent the mean value and 5%~95% confidence interval boundaries, respectively, after 100 repeated simulations.

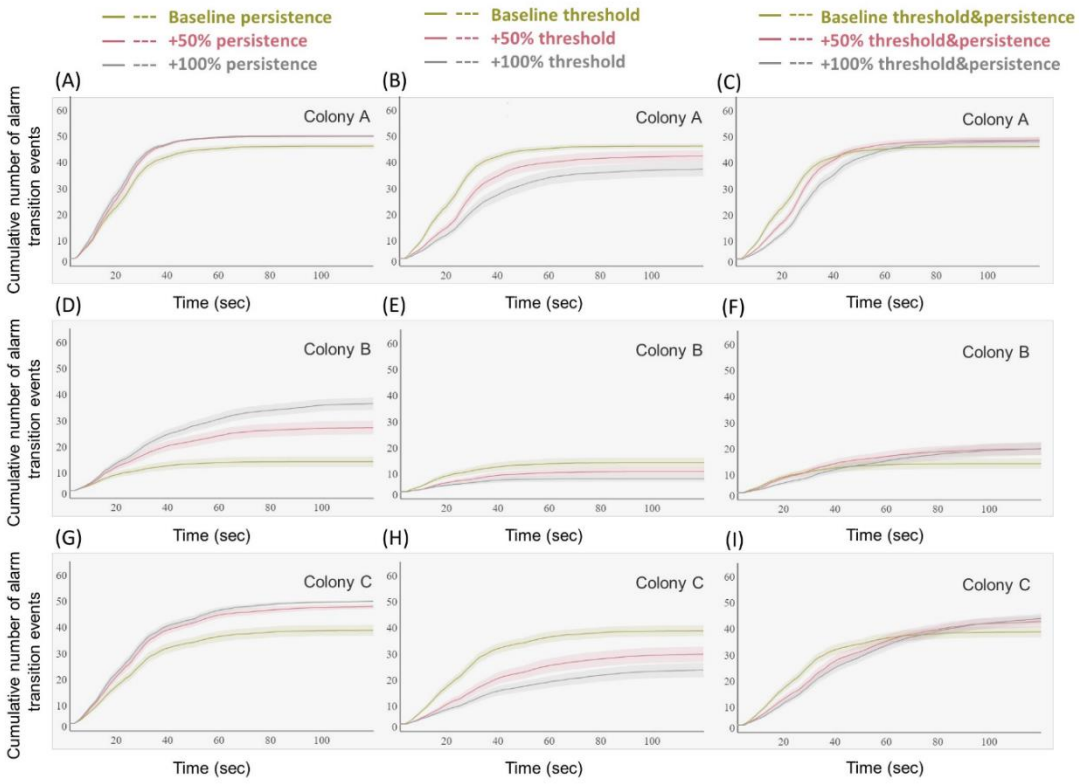

Figure 3.9: Model predictions of alarm propagation for the dynamics of alarm ants' population. Simulation experiments were run in scenarios to: (1), increase persistence alone by 50% and 100% (A, D&G); (2), increase persistence alone by 50% and 100% (B, E&H); (3), increase threshold combined with persistence by 50% and 100% (C, F&I). Solid lines and shaded areas represent the mean value and 5%~95% confidence interval boundaries, respectively, after 100 repeated simulations.

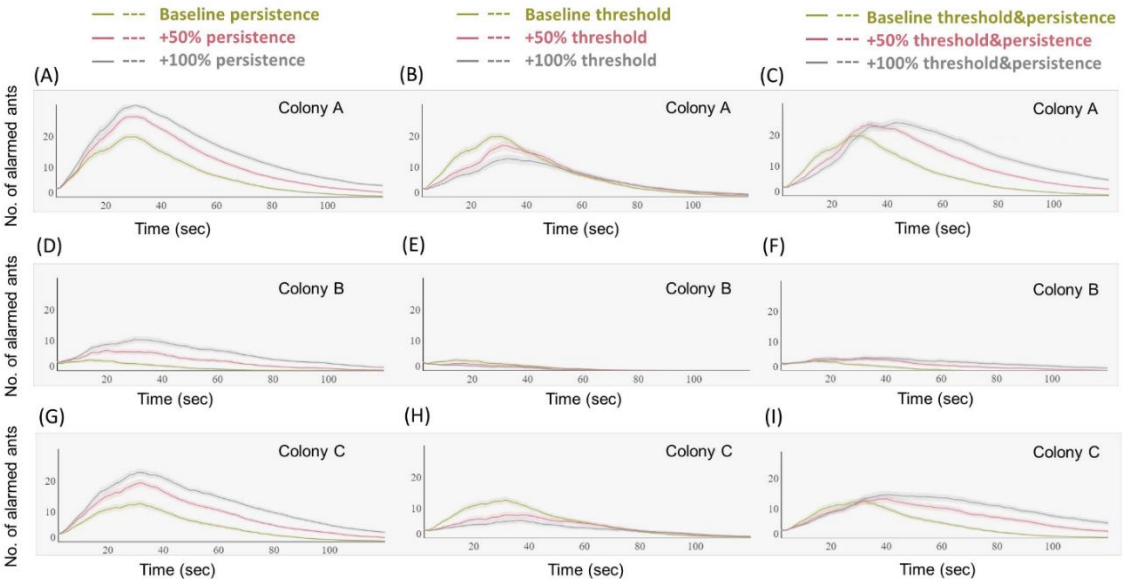

CHAPTER 4

Brood:worker ratios determine metabolic scaling of seed harvester ant colonies during ontogeny

Abstract

The negative allometric scaling of metabolic rate with mass has been demonstrated in many species of social insects, but the proximate mechanisms remain unclear. System composition theory suggests that that variation in heterogeneous metabolic components can contribute to the allometric scaling of metabolism in organisms and social insect colonies, but how system composition affects the metabolism of social insect colonies remains unclear. To understand how social insect colonies achieve hypometric scaling of metabolism, we repeatedly measured the metabolic rate and mass of 25 seed-harvester ant colonies and their sub-components (brood and mature ants) during ontogenetic growth over 3.5 years. Metabolic did not scale with a universal power-law, but rather was better explained by the segmented regression model, with isometric scaling (b=1) below the break point (0.31g colony mass), and hypometric scaling (b=0.9) in larger colonies. Brood have much lower metabolic rates than adults, and colonies with higher ratios of brood:workers had higher metabolic rates and activity of workers, presumably due to the increased effort of rearing brood. Changing brood:worker ratios explain changing scaling of metabolic rate of colonies during ontogeny, and provide at least a partial explanation of hypometric scaling of metabolism in *P. californicus* colonies.

Introduction

Social insect colonies show many characteristics of complex adaptive systems, as they are able to successfully defend themselves (Hermann 1984), regulate nest

temperature (Garrison *et al.*, 2018), regulate their sex-ratio (Chapuisat *et al.* 1997), reallocate the task performances of workers (Gordon & Mehdiabadi 1999), and eliminate infections (Cremer *et al.* 2007). Like populations of individual animals (reviewed in Glazier, 2010), social insect colonies exhibit hypometric metabolic scaling, suggestive of highly integrative function (reviewed by Fewell & Harrison 2016; Chown *et al.* 2007, Hou *et al.* 2010, Cao & Dornhaus 2013, Shik *et al*. 2014, Waters *et al,* 2010, Waters *et al.* 2017). Most, but not all animal species also exhibit hypometric scaling of metabolic rate during ontogenetic growth; however, metabolic scaling patterns during ontogeny tend to be more variable, and even biphasic or multiphasic (Holliday *et al.* 1967, Post & Lee 1996, Bochdansky & Leggett 2001). As for individual organisms, the mechanisms responsible for hypometric metabolic scaling within populations or during ontogeny remain controversial and unclear (White & Kearney 2011, Harrison 2018). No prior studies have examined the metabolic scaling of social insect colonies during development. Here we examine metabolic scaling during ontogeny of colonies of the harvester ant, *Pogonomyrmex californicus*, and test a systems composition model explanation for patterns of metabolic scaling.

Most of the theoretical models explaining metabolic scaling can be categorized into four major types: surface area theory, resource transport theory, system composition theory and resource demand theory (reviewed in Glazier 2014). Declining surface area to volume seems unlikely to explain hypometric scaling in ant colonies because the lab colonies that have been studied have high and stable supplies of food and oxygen and structures that seem unlikely to require declining surface:volume ratios with colony size (Shik *et al.* 2014, Waters *et al.* 2013, Waters *et al.* 2017). Resource transport theory

suggests that transport of materials within the next might become limited as colonies grow, but, again, the flexible structure of colonies and the lack of food-limitation in lab colonies makes this seem unlikely. However, there is some support for system composition theory in explaining hypometric scaling in social insect colonies, if this is viewed from the perspective of changes in the type or activity of colony members (Shik 2010, Cao & Dornhaus 2013, Waters *et al.* 2013, Waters *et al.* 2017). Models suggest that the ratio of work:workforce declines with colony size (Jeanson *et al.* 2007), leading to increased division of labor (Holbrook 2011, 2013) and reduced activity of workers (Charbonneau & Dornhaus 2015; Waters *et al.* 2017). However, these changes in worker activity have not provided a full explanation of metabolic scaling of ant colonies (Fewell & Harrison 2016; Waters *et al*. 2017).

The amount of brood, or the ratio of brood to adult workers, has the potential to be an important parameter affecting colony metabolic rate. Brood actively or passively modulate processes of colonial food intake (Wheeler 1918, Markin 1970, Went *et al*. 1972, Cassill & Tschinkel 1999, Dussutmy & Simpson 2009), and task allocation (Le conte *et al.* 1990, Pankiw 2007). Their begging behavior (Creemers *et al.* 2003) or chemical signals (Cassill & Tschinkel 1995, Le conte *et al.* 2001, Pankiw 2007) can initiate more feeding or brood-tending behavior of workers in ants and honeybee colonies. Since the metabolic rates of ants (and other animals) increases with activity (Lighton *et al*. 1993), it is plausible that variation in the amount of brood (a proxy of task demand for adult workers, who care for the brood) and the ratio of brood:adult workers (a proxy of the ratio of work to workers) may be important factors affecting colonial metabolic rates.

Here we evaluate the metabolic rates of whole colonies, adult ants, and brood, as well as, colony composition, of 25 seed-harvester ant colonies (*P. californicus*) during their development. First, we test whether there are multiple phases of metabolic scaling. Second, we test whether changes in colony composition, specifically the mass ratio of brood to the whole colony, can explain patterns of colonial metabolic scaling during ontogeny of this ant.

Methods

Animals and nests: Fifty newly mated *P. californicus* foundresses were collected in July 2017 in Pine Valley, San Diego county, California (32°490 2000 N, 116°310 4300 W, 1,136 m elevation). Because queens of this population are pleometrotic, 25 colonies were initiated with 2 queens for each to maximize survivability of colonies for a long-term study. Colonies were reared at 29-31°C in plexiglass containers supplied with *ad libitum* Kentucky bluegrass seeds, frozen mealworms, and fruit flies (*Drosophila melanogaster*) weekly. At the start of the experiment (9/2017), colonies were two months old and contained 7~83 monomorphic workers each. Initially, each nest provided a total surface area of 70.9 cm^2 and was partitioned into a brood chamber and foraging arena. We increased nest surface area to 242 cm^2 to prevent crowding during the last period of the study (4/5/2019~12/19/2020).

Respirometry methods: CO_2 emission rates from each colony was measured 9/17/2017~11/14/2017 for the session one, 11/17/2017~1/23/2018 for the session two, 1/3/2018~3/1/2018 for the session three, 4/2/2018~5/28/2018 for the session four, 4/5/2019~5/23/2019 for the session five, and 10/16/2020~12/19/2020 for the session six. For each colony, CO_2 emission rates from whole colonies, the brood, and the adult

workers were measured with flow through respirometry (Fig. 4.1). Metabolic rate chambers were a 0.74-L airtight aluminum respirometry chamber for sessions 1~4, and 1.0-L airtight acrylic respirometry chamber for sessions five and six (4/5/2019~12/19/2020). Dry, CO_2-free air from a compressed air tank flowed through the chamber (125 mL min for the small chamber or 250 mL min for the large one), regulated by Tylan mass flow valves and controller. We used an infrared CO_2&H_2O analyzer (LI-7000, LI-COR, Lincoln, NE) to measure the carbon dioxide concentration of excurrent air. Room temperature was also measured simultaneously. Analog data were digitized (UI2, Sable Systems International (SSI), Las Vegas, NV) and recorded on a PC (ExpeData, ver. 1.2.6, SSI) at 1-Hz sampling frequency.

Twelve-hours prior to CO_2 measurement, colony enclosures were placed into the respirometry chamber with a loose lid for over-night acclimation. During the daytime, the respirometry chamber was enclosed, and the CO_2 from the whole colony was measured for approximately 2 hours after 1~2 hours' washout. Simultaneously, we video-recorded the colonies for two hours, with these data used to assess ant activity levels. After completion of whole-colony CO_2 emission rates, we gently transferred mature ants (ant workers + queens) out of the nest, and counted and weighed them. Next, we measured the CO_2 emission rate from the nest including brood for 2 hours, first waiting for 1~2 hours to permit washout of CO_2 introduced into the nest when it was opened. To estimate metabolic rate of brood (eggs, larvae and pupae), I used two different procedures:

1) For sessions two - four, I separately measured to CO_2 emission rates of pupae and larvae+eggs. To do so, after measurement of whole-colony CO_2 emission rate, I transferred pupae out of the nest, and weighed them. Next the CO_2 emission rates from

the nest, including larvae, eggs, food and debris, were measured for 2 hours after a 2~3 hours' washout period. Pupal mass-specific CO_2 emission rates were calculated from the difference between whole-colony CO_2 emission rate and the CO_2 emission rate of the nest without pupae, and mass of pupae in the nest. Next, larvae and eggs were transferred out of the chamber, and weighed. Then, the CO_2 emission rate from the nest, including only food and debris, were measured for 2 hours, after 3~4 hours' washout. Larval+egg mass-specific CO_2 emission rates were calculated from the difference between the CO_2 emission rates of nests with and without larvae+eggs and the mass of larvae+eggs.

2) For the session one, five and six, I only measured the CO_2 emission rates of all the brood together (eggs, larvae, pupae). After measuring whole-colony CO_2 emission rates, I transferred all brood out of the chamber, and weighed them. Next, the CO_2 emission rates from the nest lacking brood were measured for 2 hours, after a 2~4 hours' washout period. Brood mass-specific CO_2 emission rates were calculated from the difference between the CO_2 emission rates of nests with and without brood and the mass of brood in the nest.

After the respirometry measurements, adult ants and brood were returned to the nest. The entire experiment was approximately 12 hours in duration. We assumed a respiratory quotient of 0.80 (Lighton & Bartholomew 1988), and standardized the metabolic rate to the temperature of 25 °C, assuming a Q_{10} of 2.0. The regression analyses were performed with "lmer4" and "lmertest" packages of R 3.6.0.

Activity levels: Activity levels of ant workers were estimated in Swarmsight (Birgiolas *et al.* 2017). This program quantifies the number of pixel changes between frames of a video, and is therefore sensitive to background vs foreground differences.

Ideally, objects in the foreground (such as ants) contrast heavily with a light, consistent background. However, my colonies were fed *ad libitum* with Kentucky bluegrass seeds, so background color varied between videos. To control for this effect, we measured the number of pixels seed piles took up in a randomly-selected video frame and divided this by the total number of pixels present in the nest and foraging arena. The seeds were darker than the background which made it more difficult to detect movement. Therefore, the seed proportion had a significant negative effect on activity per capita rate (linear regression, $y = -33.095 \cdot x + 23.463$; $F_{(1,36)} = 11.951$, p=0.001523). To correct for this, we subtracted the effect of seed proportion from my activity per capita rate. Expressed mathematically, corrected activity per capita = activity per capita - (-33.095)·seed proportion (pixel/frame).

As each video was 6 hours in length, we could not analyze entire videos without experiencing lag or other technical difficulties. An optimization study on *P. californicus* showed that dividing the video into eight 11-min segments optimally traded-off behavioral metrics which are auto-correlated in time with metrics which are independent of the time they are sampled (Lynch *et al.* in prep). As the ants of this study are the same species and were raised under the same conditions, we opted to analyze only 8 randomly-selected subsections of the video. Finally, we analyzed colonies present in sessions 1 and 6, as these colonies alone provided the full range of brood ratios (0.35 ± 0.15) and mass specific metabolic rate of mature ants ($2529.61 \pm 741.78\ uw/gram$).

Results

Effects of ontogeny on colony demography

For these 25 colonies, over the 6 experimental sessions, the number of workers increased on average by 6%, 31%, 142%, 406%, and 1639%, while the mass of brood increased by -41%, 20%, 28%, 182%, and 1212% (Table 4.1). Eleven colonies survived to the end of the experiment, and had colonial growth rates that varied more than 3x (Table 4.2). In the linear mixed model including colony as a random factor (Fig. 4.2), we found the ratio of broods' biomass to the number of ant workers declined over time (y= -7.084e-07$\cdot x$+1.899e-03; $F_{(1,104)} = 4.2077$, p=0.043),

Changes in the metabolic scaling pattern during ontogeny

To test for consistency in metabolic scaling during ontogeny, we assessed the relationship between colonial metabolic rate and colony mass during 2-3 months (sessions 1-2), 3-10 months (sessions 3-4), and 20-40 months (sessions 5-6) (Fig. 4.3). During the first 3 months of colony growth, colonial metabolic rates scaled hypermetrically (slope = 1.1$\pm$0.1, statistically greater than 1.0, t=-2.23, p=0.03). During the next 8 months of ontogeny, colonial metabolic rates scaled isometrically, with a slope (1.08$\pm$0.08) not significantly different from 1 (t=-1.53, p=0.14). During 20-40 months of ontogeny, colonial metabolic rate scaled hypometrically (slope =0.94$\pm$0.03), statistically less than 1.0 (t= 3.55, p <0.001).

To examine metabolic scaling patterns during their entire development, we compared three linear mixed models: a linear model, a segmented model, and quadratic model. The linear model yielded isometric scaling, with a metabolic scaling exponent of 0.99 with a confidence interval from 0.93 to 1 (Fig. 4.4A). The segmented model (Post

and Lee 1996) found a scaling exponent of 1 (C.I.=0.96-1.04) below the break point (colony mass = 0.31 g), and an exponent of 0.9 (C.I. = 0.85-0.95) above the break point (Fig. 4.4B). The quadratic model (Fig. 4.4C&D) found that the scaling exponent continually declined as the colony grew. The F-statistic showed that the 5-parameter segmented model and quadratic regression model were significantly improved over the 4-parameter linear regression model (Table 4.3), and the segmented model was the most informative model based on AIC and BIC criteria.

Metabolism of mature ants and brood

The mass-specific metabolic rate (*MSMR*) of larvae and pupae were not significantly different from each other (Wilcoxon test, W = 643, p=0.42), which allowed us to aggregate larvae and pupae together for further comparison. Brood had significantly lower *MSMR* than mature ants (Wilcoxon test, W = 285, p<0.0001, Fig. 4.5). The *MSMR* of mature ants (workers + queens, $MSMR_{mature}$) was higher in colonies that had a higher ratio of brood to whole colony mass, r; ($MSMR_{mature} = 1788.17 + 2016.04 \cdot r$; $F_{(1, 96.5)} = 44.6$, p <0.000001, with a linear mixed model including colony as a random factor, Fig. 4.5).

The corrected activity level per capita of mature ants estimated in the "SwarmSight" related to the mass ratio of brood with an LMM ($y = 13.74 + 27.58 \cdot r$; $F_{(1, 27.5)} = 11.359$, p = 0.0027) (Fig. 4.6). In this model, colony ID was again encoded as a random effect, and brood ratio had a significant positive relationship with activity. Combining the correlation between $MSMR_{mature}$and mass ratio of brood, we can provide an integrative picture of how mature ants respond to the brood in my colonies: a higher mass ratio of broods can

stimulate mature ants' activity level, and consequently increase their mass specific metabolic rate.

A composition-model for metabolic scaling during ontogeny

I developed a composition model (equation 4.4) based on equations 4.1, 4.2 and 4.3 to investigate the mechanism of metabolic scaling patterns during the ontogeny, to test whether the mass ratio of brood to the whole colony can determined the work effort of mature ants and generate the hypermetric scaling during early growth and hypometric scaling later.

$$MSMR_{colony} = r \cdot MSMR_{brood} + (1 - r) \cdot MSMR_{mature} \quad \text{equation 4.1}$$

$$MSMR_{mature} = \alpha \cdot r + Q \quad \text{equation 4.2}$$

$$r = {Mass_{brood}}/{Mass_{colony}} \quad \text{equation 4.3}$$

$$MSMR_{colony} = r \cdot (MSMR_{brood} + \alpha - Q) - \alpha \cdot r^2 + Q \quad \text{equation 4.4}$$

In the composition model, $MSMR_{colony}$ is the mass-specific metabolic rate of whole colony, $MSMR_{brood}$ is the mass-specific metabolic rate of brood, r is the ratio of brood to whole colony mass, α is the coefficient of correlation between $MSMR_{mature}$ and mass ratio of brood (r), and Q is the basic $MSMR$ of mature ants without reinforcement effects of broods on their metabolic rate. In this model, $MSMR_{colony}$ is a function of independent variable r (0.04 - 0.56), a known value of parameter $MSMR_{brood}$ (1032 uw/gram) and α and Q. To study a long-term dynamic mass ratio of brood to the whole colony, we chose the 11 colonies that survived and fit my model to the data (*d.f.* = 61, RMSE = 351.21). I also estimated the value of parameter Q (3349.3 uw/gram, C.I. = (1512.934-5185.709)), and α (4615.6 uw/gram, C.I. = (1678.863~7552.435)) in the

composition model and compared them to the independent estimates in the simple linear mixed model ($MSMR_{mature} = Q + \alpha \cdot r$; Q =1890.27 uw/gram; α = 2133.58 uw/gram, $F_{(1,58.2)}$=21.924, p <0.0001). Both Q and α estimated in the simple LMM are located in the confidence intervals estimated in the composition model. A maximum value of $MSMR_{colony}$ was estimated at the ratio of broods ($r^* = (MSMR_{brood} + \alpha - Q)/(2 \cdot \alpha) = 0.25$). Thus the composition model predicts that the relationship between brood mass ratio and colonial metabolic rate will have two phases: and increasing phase (ratio< 0.25) in which increasing brood ratio indirectly causes a rise in colonial metabolic rate by increasing worker activity, and a decreasing-phase (ratio ≥0.25) when an increasing brood ratio directly causes a decline in colonial metabolic rate because the brood have a much lower metabolic rate than the workers.

The composition model qualitatively describes how ontogenetic development of colony affects their metabolic scaling relation, and it predicts colonies can have a lower (hypometric) scaling exponent via pathway 1 (as brood ratio declines below 0.25, pathway 1) or pathway 3 (as brood ratio increases from 0.25 to 0.6, pathway 3), and a hypermetric scaling exponent via pathway 2 (as brood ratio declines from 0.6 to 0.25, pathway 2) or pathway 4 (as brood ratio increases from 0.25 to 0.6, pathway 4 (Fig. 4.7), or an iso-metric scaling exponent if brood ratio is constant or changing equally above and below 0.25. Especially, as the ratio of brood to the whole colony declines over the full range of 0.6 to 0.1, the response can be biphasic: above 0.25, colonial *MSMR* rises as brood ratio declines because colonies have a higher proportion of energetically expensive individuals (mature ants) (Fig. 4.5). At lower values of this parameter (<0.25), colonial

MSMR falls due to the fact that workers can exert less effort to care for the brood (Fig. 4.6).

The temporal dynamics of the ratio of brood mass to ant worker or mass ratio of broods to the whole colony were complex (Fig. 4.8). Therefore, to examine predictions of my model within each individual colony, we applied the stratified random sampling technique on the data of 11 survived colonies to simulate the demographic changes of individual colonies by following rules as below:

1. Randomly select 5 colonies from all colonies with $r < 0.25$, and store them if the larger colony has a lower brood mass ratio;
2. Estimate the scaling exponent in the linear regression model on those 5 samples;
3. Repeated step one and two for 100 iterations.
4. Repeated step one to three for the colonies with $r \geq 0.25$.

We then estimated the average scaling exponent of random samples for pathway 1 ($r < 0.25$) was 0.86 ± 0.09, which was significantly lower than the scaling exponent estimated for pathway 2 ($r \geq 0.25$), 0.96 ± 0.12 (Wilcoxon test, W= 7869, p<0.00001) (Fig. 4.9). It suggests a shift of scaling exponent from iso- or hypermetric to hypometric if the dynamic ratio of broods declines through the phase ($r \geq 0.25$) and then the phase ($r < 0.25$).

Discussion

We found that metabolic rate of *P. californicus* colonies did not scale with a simple power law, but instead that the pattern of scaling changed during ontogeny from

hypermetric toward hypometric scaling. We also showed that brood have much lower metabolic rates than adults, and that workers increase their activity and metabolic rates as they have more brood to care for. Finally, though the temporal dynamics of brood mass ratio were complex, my systems composition model predicted a multiphasic pattern of colony metabolic rate, as brood mass ratio varied over time. Switches in metabolic scaling pattern from hyper or isometric to hypometric arise from the changes both the absolute value and direction of changes in the brood mass ratio because: 1) brood are metabolically cheaper than mature ants; and 2) brood can stimulate task activities and metabolic rate of mature ants.

Brood mass ratio likely influences whole colony metabolism by up-/down-regulating the brood tending or feeding activities of ant workers. Cassill and Tschinkel (1999) estimated that each individual brood is contacted 700 times by caregiver ants per hmy in a fire ant colony (*S. invicta*). Meanwhile, Cassill and Tschinkel (1995) observed that fire ant workers (*S. invicta*) increased their trophallaxis rate if brood were deprived of food, which suggests that brood actively solicit feeding from ant workers. Other task activities are likely also affected by the amount of brood. For example, in the clonal raider ant colony (*Cerapachys biroi*), a higher proportion of brood was observed to stimulate ant workers to increase their foraging activity (Ulrich *et al.* 2016). Similarly, the presence of brood in leaf-cutting ant colonies (*Acromyrmex lundi*) stimulates workers to excavate and enlarge the nest (Römer & Roces 2014). Therefore, an increased brood mass ratio likely causes each adult worker to have to work harder by increasing the amount of time they spend performing brood care, or increasing the intensity with which they perform other

tasks such as foraging (Fig. 4.6), consequently increases the mass-specific metabolic rate of mature ants (Fig. 4.5)

The observation that immature holometabolous insects have mass-specific metabolic rates approximately half that of adults has been shown before for diverse species (Lighton and Lovegrove 1990, Vogt and Appel 1999, Petz *et al.* 2004, Klok *et al.* 2010), and cannot be explained by simple allometric scaling and the fact that adults are slightly smaller than late-instar larvae or pupae (Waters & Harrison 2012). This may be due to the fact that in holometabolous insects, adults are much more mobile that larvae and skeletal muscle has a high maintenance and use cost (Reinhold 1999). While we did not find a difference in metabolic rates between eggs+larvae and pupae, we did not investigate this in detail, and it likely that more complex patterns occur.

Comparing to the metabolic scaling exponents (b=0.75 and b=0.79) of seed-harvester ant colonies (*P. californicus*) in two recent studies (Waters *et al.* 2013, 2017), we did not find scaling exponent as hypometric (for a simple linear model: b=0.96, C.I. = 0.93-1.0) (Fig. 4.4A). However, we had a wider range of colonial mass (0.0417~8.1912 g vs 0.32~3.16 g or 0.316 ~1.78 g, respectively, in the Waters *et al.* studies). We re-examined the metabolic scaling relation in LMM model after adopting a similar mass range as the Waters *et al* studies, and found the hypometric scaling exponents of 0.89 (C.I.=0.83~0.95) and 0.89 (C.I.=0.83~0.96) respectively. The smallest colonies in those two studies were similar in size to the break point estimated in my segmented model (0.31 gram) (Fig. 4.4B). Below the break point, my colonies showed an isometric metabolic scaling exponent of 1.0 (C.I.= 0.96~1.04) that was found in the human and fish during their early developments (Holliday *et al*. 1967, Post & Lee 1996, Bochdansky & Leggett 2001).

In the general perspective of system composition theory, divergent scaling patterns may arise from the heterogeneous metabolic rates of system components when the masses of these components change disproportionately with increasing body size (Glazier 2014). Because ant workers of *P. californicus* are generally monomorphic, we proposed a new criterion in my composition model to divide a whole colony into segments: immature ants and mature ants. Not like the traditional decomposition method, e.g. dividing heterogeneous metabolic components by ants' caste types, task performances, and activity levels (Shik *et al.* 2010, Waters *et al*. 2017, Cao & Dornhaus 2013), my approach provides a fundamental and reliable criterion for differentiation between metabolic segments, and helps us investigate metabolic scaling quantitatively. Moreover, a metabolic rate of colony in my composition model is not simply determined by the proportion of each metabolic component as in a traditional system composition model (Glazier 2014). The complex relation between different metabolic compartments of the colony brings the theoretical model closer to the real system, where every decomposed metabolic segments should coordinate with each other to emerge as a system with collective properties.

The disproportionate growth of brood vs mature ants has been found in *T. rugatulus* and *P. badius* ant colonies (Cao & Dornhaus 2013, Tschinkel 1999). For example, in Florida harvester ants (*P. badius*) colonies, the colony-level brood: worker ratio declined from an average of 1.4 in incipient colonies to 0.33 in colonies of 6,000 workers (Tschinkel 1999). Among my 25 colonies, the ratio of broods to ant workers (gram/worker) was found to significantly decline over days in the LMM model. However, within each individual colony, changes in brood mass ratio were complex and did not show a simple linear change over time. Therefore, we applied a simulation-based approach. In my stratified random

sampling simulations within the range of $r < 0.25$, as brood mass ratio declined, hypometric scaling of metabolic rate (b<1) was observed due to the less active mature ants. In contrast, simulations of declining brood mass ratio when brood mass ratios were ≥ 0.25 had a significantly higher exponent (isometric or even hypermetric scaling exponent) due because in this range, brood are being replaced by mature ants that have a much higher mass-specific metabolic rate. Those simulations also suggest that a biphasic scaling pattern can be attained as the ratio declines through the phase ($r \geq 0.25$) and then the phase ($r < 0.25$) during the colony growth.

While my results support a strong role for brood mass ratio in determining the pattern of metabolic scaling during ontogeny of ant colonies, there are likely other important effects of colony size. When the colony size of seed-harvester ant colonies (*P. californicus*) was reduced by 50%, while keeping the same brood mass ratio ($17.25\% \pm 16.24\%$), hypometric scaling was observed (Waters *et al.* 2017), which partially supports the composition model's prediction: bigger colonies with lower ratio of broods will have the hypometric scaling of metabolic rate because colonies with low brood ratios tend to be less active on average. However, my composition model cannot explain why colonies with the same ratio of broods have different mass-specific metabolic rate of colony between pre-reducing and post-reducing because the composition model doesn't explicitly address the relation between r and $Mass_{colony}$. We believe incorporating this relation into the composition model will enable us to predict the value of metabolic scaling exponents, and to quantitatively analyze how varied scaling exponents arises from the disproportionate growth of brood:workers.

Table 4.1. Demography of colonies over six experimental sessions.

Experimental session	Days	Sample size	Number of ant workers	Mass of brood (grams)
1	0~58	25	44.1±24.7	0.092±0.069
2	61~128	25	46.7±25.8	0.054±0.051
3	108~165	20	57.6±24.4	0.11±0.065
4	197~253	15	106.6±37.5	0.118±0.05
5	565~613	14	223.2±108	0.259±0.158
6	1125~1189	11	767±379.6	1.207±1.03

Table 4.2. Parameters estimated in the exponential growth model (The number of ant workers as the dependent variable, and the number of days on growth as the independent variable).

Colony ID	Growth rate	P-value	Intercept	P-value
17-10	0.001279	0.03655	4.237285014	4.66E-05
17-11	0.001868	0.000837	3.943690673	4.07E-06
17-12	0.002911	0.00318	3.822795996	0.000269
17-15	0.001676	0.000368	3.850468907	4.95E-06
17-19	0.002686	0.000181	4.06065861	2.91E-06
17-21	0.003873	0.002327	3.082310558	0.0005
17-22	0.001832	2.38E-06	4.083301605	8.63E-09
17-23	0.003016	0.005058	2.967798	0.001178
17-26	0.002803	0.001573	3.80957114	3.99E-05
17-8	0.002723	0.000329	4.091178832	5.40E-06
17-9	0.002016	0.004538	4.14841575	2.50E-05

Table 4.3: Comparison of regression models for fitting data. All of models include colony ID as the random effect.

Model description	Function	Number of parameters	Adjusted R-squared	Chisq-test	AIC	BIC
Linear regression	log MR = 3.29 +0.96·log Mass; CI_{slope} = (0.93 – 1.00)	4	0.964		-235.62	-224.82
Segmented regression	log MR = 3.31 +1·log Mass - 0.1·(log Mass<-0.504)·(log Mass >=-0.504; CI_{slope1} = (0.96 –1.04); CI_{slope2} = (0.85 – 0.95)	5	0.970	χ^2= 10.955, *d.f.* = 1, p < 0.0001	-244.58	-231.08
Quadratic	log MR = 3.33 + 0.94·log Mass - 0.062·$(\log Mass)^2$; CI_{slope1} = (0.90 – 0.98); CI_{slope2} = (-0.11 – -0.01)	5	0.969	χ^2= 5.42, *d.f.* = 1, p = 0.01988	-239.05	-225.55

Figure 4.1. System design schematic and respirometry chamber. (A) Compressed air is dried and CO_2 removed, and then divided into identical flows through the reference channel of the CO_2 analyzer, and through the colony and then the measuring channel of the CO_2 analyzer. The difference of in CO_2 level between those two channels is multiplied by flow rate to calculate CO_2 emission rate. (B) A circular airtight aluminum respirometry chamber was used for sessions 1~3. (C) A rectangular airtight acrylic plastic respirometry chamber was used for sessions 4~6.

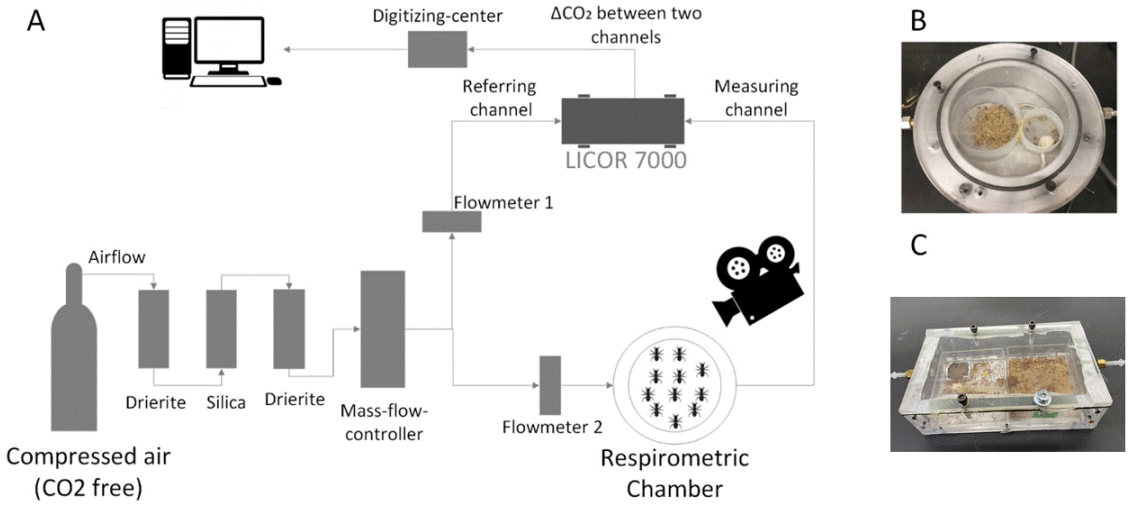

Figure 4.2: Growth of ant workers and brood over experimental sessions, corresponding to 3.5 years of colonial growth. Left: mass of brood; Middle: the population of workers. Right: Ratio of brood mass to worker number (gram/worker) over time; LMM model including colony as a random factor; y= -7.084e-07· x+1.899e-03; $F_{(1,104)}$ = 4.2077, p=0.043).

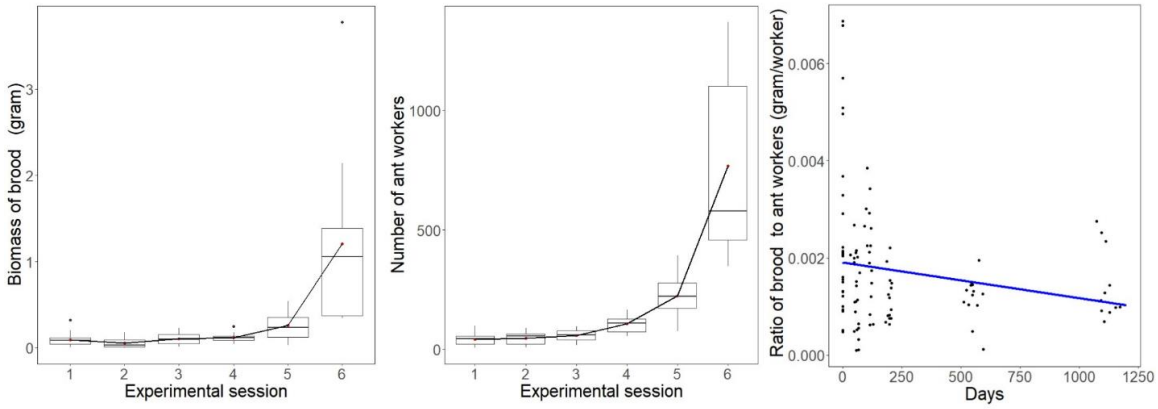

Figure 4.3: Logarithmic biomass of colonies and their metabolic rate allometry on double-log axes within each time-aggregated period. (A) Colonies grew in mass (stars indicate significant differences in colony mass, Wilcoxon tests, $p < 0.001$). (B) During the first three months, colonial metabolic rates scaled hypermetrically (slope statistically greater than 1.0), while for colonies older than 20 months, colonial metabolic rates scaled hypometrically (statistically less than from 1.0).

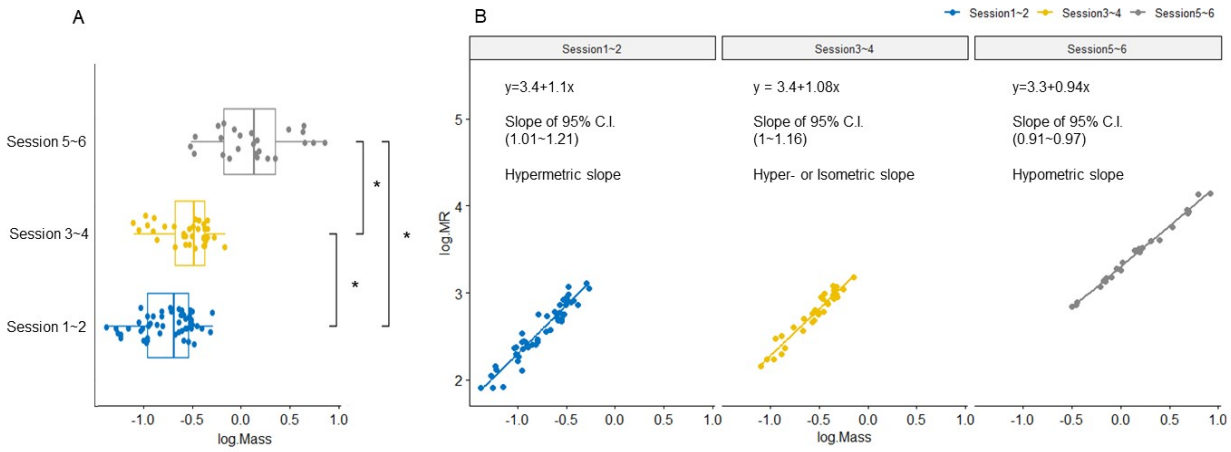

Figure 4.4. Metabolic scaling of seed-harvester ant colonies during 3.5 years of ontogeny as assessed by four different regression models. (A) Linear model; (B) Segmented model; (C) Quadratic model. See Table 4.3 for description of each model and of fit. (D) The 1st order derivative of the quadratic regression ($y = 0.94 - 0.124 \cdot x$) to illustrate the decreasing metabolic scaling exponent as colonies grow.

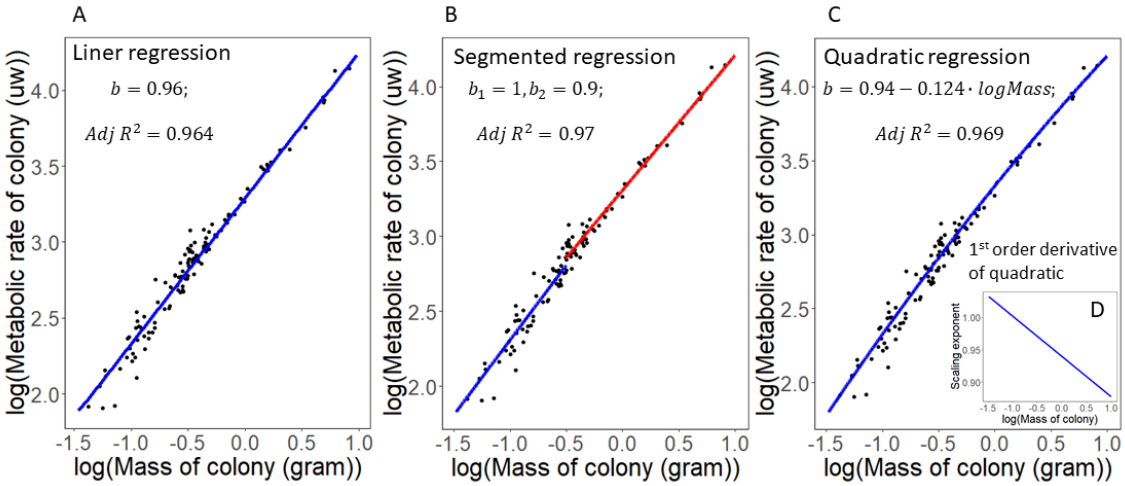

Figure 4.5. Mass-specific metabolic rate of colony components and correlation between mass ratio of brood and mass-specific metabolic rate of mature ants. Left: Mass-specific metabolic rate of colony components. The mass-specific metabolic rates of pupae and larvae did not significantly differ (Wilcoxon test, W= 643, p = 0.42). Brood (pupae + larvae) had significantly lower mass-specific metabolic rate than mature ants (adult ant workers + queens) (Wilcoxon test, W = 285, p <0.0001). Right: The mass-specific metabolic rate of mature ants (queens + ant workers) increased with the proportion of colony mass that was brood (LMM model including colony as a random factor: $y = 1788.17 + 2076.04 \cdot x$; $F_{(1, 96.5)}$= 44.6, p <0.000001).

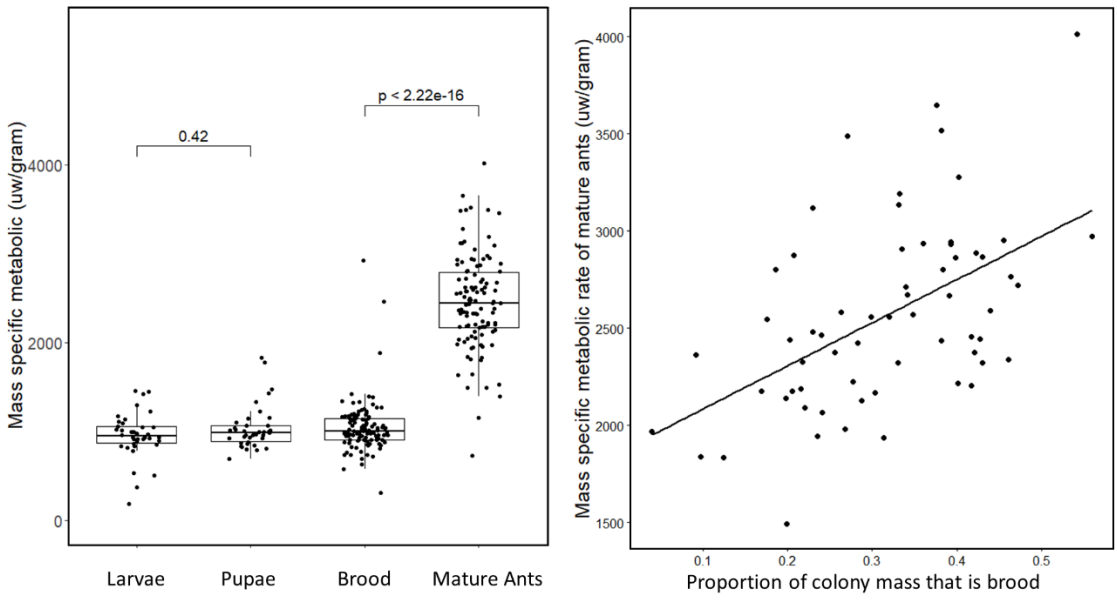

Figure 4.6. The activity level per capita of mature ants increased with the proportion of colony mass that is brood (LMM: $y = 13.74 + 27.58 \cdot r$; $F_{(1, 27.5)} = 11.359$, $p = 0.0027$).

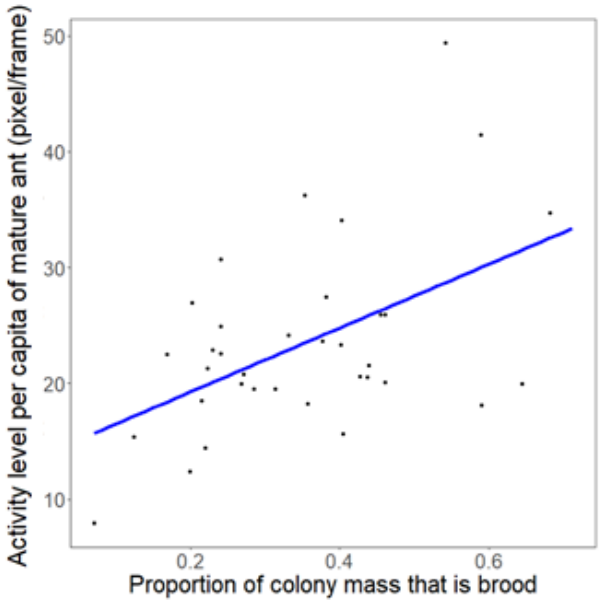

Figure 4.7: Composition model fitting to the data obtained from 11 survived colonies over 6 experimental sessions and its predictions. Left: Colonial mass specific metabolic rate as a function of the proportion of the colony mass that is brood. Points indicate mass-specific metabolic rates for brood mass ratios of 11 colonies over 6 sessions. The hump-shaped line shows the prediction for my systems composition model (Eqn. 4.3). Right: and potential pathways we predicted to achieve different metabolic scaling processes as the growth of colony size. In the pathway 1, colonies start with high ratios of broods, and gradually decrease the ratio through the phase ($r \geq 0.25$) for metabolic hypermetry because an increased proportion of metabolically expensive individuals (mature workers) emerge in the nest. Then, the ratio decreases through the phase ($r < 0.25$) for metabolic hypometry due to the less active mature ants.

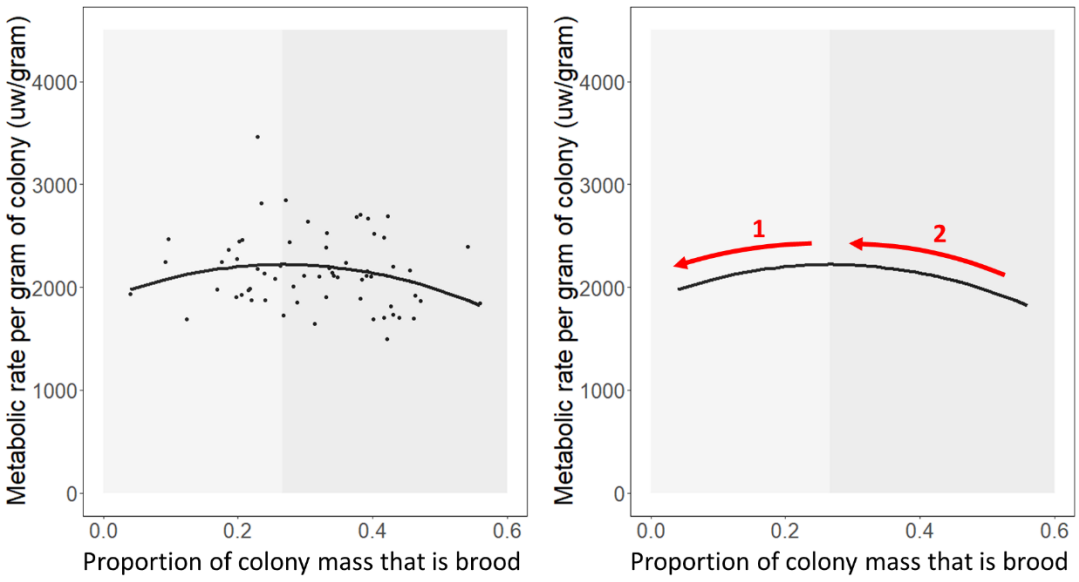

Figure 4.8. Demography of 11 colonies survived to the end of experiment. Temporal dynamics of ratio of brood to ant workers (mg/#ant workers) (left) and ratio of brood mass to whole colony mass (right) for the 11 colonies that survived to the end of the experiment. The grey areas indicate the six experimental sessions.

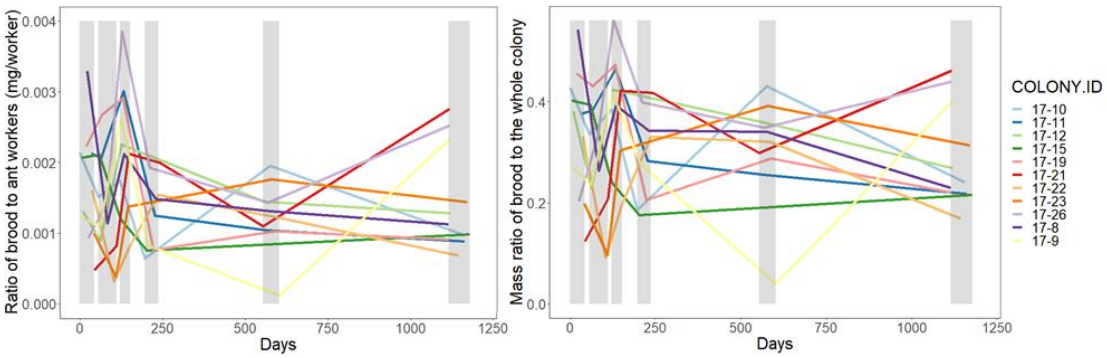

REFERENCES

Amador-Vargas, S., Gronenberg, W., Wcislo, W. T., & Mueller, U. (2015). Specialization and group size: brain and behavioural correlates of colony size in ants lacking morphological castes. *Proc. R. Soc. B*, *282*(1801), 20142502.

Anderson, C., & Ratnieks, F. L. (1999). Task partitioning in foraging: general principles, efficiency and information reliability of queueing delays. In Information processing in social insects (pp. 31-50). Birkhäuser, Basel.

Anderson, C., & McShea, D. W. (2001). Individual versus social complexity, with particular reference to ant colonies. *Biological reviews*, *76*(2), 211-237.

Aplin, L. M., Farine, D. R., Morand-Ferron, J., Cole, E. F., Cockburn, A., & Sheldon, B. C. (2013). Individual personalities predict social behavimy in wild networks of great tits (Parus major). Ecology letters, 16(11), 1365-1372.

Azarcoya-Cabiedes, W., Vera-Alfaro, P., Torres-Ruiz, A., & Salas-Rodríguez, J. (2014). Automatic detection of bumblebees using video analysis. Dyna, 81(187), 81-84.

Baudier, K. M., Ostwald, M. M., Grüter, C., Segers, F. H., Roubik, D. W., Pavlic, T. P., Pratt, S. C., & Fewell, J. H. (2019). Changing of the guard: mixed specialization and flexibility in nest defense (*Tetragonisca angustula*). Behavioral Ecology, 30(4), 1041-1049.

Baudier, K.M. (2019) Brood Stimulation Hypothesis. In *Encyclopedia of Social Insects* (ed. C.K. Starr). Switzerland, Springer International.

Bechtel, W., & Richardson, R. C. (1993). 2010. Discovering Complexity: Decomposition and Localization as Strategies in Scientific Research. Repr

Bergmüller, R., & Taborsky, M. (2007). Adaptive behavioural syndromes due to strategic niche specialization. BMC ecology, 7(1), 1-7.

Beshers, S. N., & Fewell, J. H. (2001). Models of division of labor in social insects. *Annual review of entomology*, 46(1), 413-440.

Birgiolas, J., Jernigan, C. M., Smith, B. H., & Crook, S. M. (2017). SwarmSight: Measuring the temporal progression of animal group activity levels from natural-scene and laboratory videos. Behavior research methods, 49(2), 576-587.

Blonder, B., & Dornhaus, A. (2011). Time-ordered networks reveal limitations to information flow in ant colonies. PloS one, 6(5), e20298.

Bonabeau, E., Theraulaz, G., & Deneubourg, J. L. (1996). Quantitative study of the fixed threshold model for the regulation of division of labmy in insect societies. Proceedings of the Royal Society of London. Series B: Biological Sciences, 263(1376), 1565-1569.

Bochdansky, A. B., & Leggett, W. C. (2001). Winberg revisited: convergence of routine metabolism in larval and juvenile fish. Canadian Journal of Fisheries and Aquatic Sciences, 58(1), 220-230.

Bonabeau, E. (1998). Social insect colonies as complex adaptive systems. *Ecosystems*, *1*(5), 437-443.

Bonnie, K. E., & Earley, R. L. (2007). Expanding the scope for social information use. Animal Behaviour, 74(2), 171-181.

Bossert, W. H., & Wilson, E. O. (1963). The analysis of olfactory communication among animals. *Journal of theoretical biology*, *5*(3), 443-469.

Burghardt, G. M., Bartmess-LeVasseur, J. N., Browning, S. A., Morrison, K. E., Stec, C. L., Zachau, C. E., & Freeberg, T. M. (2012). Perspectives–minimizing observer bias in behavioral studies: a review and recommendations. *Ethology*, *118*(6), 511-517.

Camazine, S., Deneubourg, J. L., Franks, N. R., Sneyd, J., Bonabeau, E., & Theraula, G. (2003). Self-organization in biological systems. Princeton university press.

Cao, T. T., & Dornhaus, A. (2013). Larger laboratory colonies consume proportionally less energy and have lower per capita brood production in Temnothorax ants. Insectes sociaux, 60(1), 1-5.

Cassill, D. L., & Tschinkel, W. R. (1995). Allocation of liquid food to larvae via trophallaxis in colonies of the fire ant, Solenopsis invicta. *Animal Behaviour*, *50*(3), 801-813.

Cassill, D. L., & Tschinkel, W. R. (1999). Information flow during social feeding in ant societies. In *Information processing in social insects* (pp. 69-81). Birkhäuser, Basel.

Cassill, D. L., & Tschinkel, W. R. (1999). Regulation of diet in the fire ant, Solenopsis invicta. Journal of Insect Behavior, 12(3), 307-328.

Charbonneau, D., & Dornhaus, A. (2015). Workers 'specialized' on inactivity: behavioral consistency of inactive workers and their role in task allocation. *Behavioral ecology and sociobiology*, *69*(9), 1459-1472.

Chapuisat, M., Liselotte, S., & Keller, L. (1997). Sex–ratio regulation: the economics of fratricide in ants. Proceedings of the Royal Society of London. Series B: Biological Sciences, 264(1385), 1255-1260.

Chivers, D. P., & Smith, R. J. F. (1998). Chemical alarm signalling in aquatic predator-prey systems: a review and prospectus. Ecoscience, 5(3), 338-352.

Chown, S. L., Marais, E., Terblanche, J. S., Klok, C. J., Lighton, J. R. B., & Blackburn, T. M. (2007). Scaling of insect metabolic rate is inconsistent with the nutrient supply network model. Functional Ecology, 21(2), 282-290.

Cook, C. N., & Breed, M. D. (2013). Social context influences the initiation and threshold of thermoregulatory behavimy in honeybees. *Animal Behaviour*, *86*(2), 323-329.

Crall, J. D., Gravish, N., Mountcastle, A. M., Kocher, S. D., Oppenheimer, R. L., Pierce, N. E., & Combes, S. A. (2018). Spatial fidelity of workers predicts collective response to disturbance in a social insect. Nature communications, 9(1), 1-13.

Creemers, B., Billen, J., & Gobin, B. (2003). Larval begging behavimy in the ant Myrmica rubra. Ethology Ecology & Evolution, 15(3), 261-272.

Cremer, S., Armitage, S. A., & Schmid-Hempel, P. (2007). Social immunity. Current biology, 17(16), R693-R702.

Dankert, H., Wang, L., Hoopfer, E. D., Anderson, D. J., & Perona, P. (2009). Automated monitoring and analysis of social behavior in Drosophila. *Nature methods*, *6*(4), 297-303.

Deutsch, J. C., & Nefdt, R. J. (1992). Olfactory cues influence female choice in two lek-breeding antelopes. Nature, 356(6370), 596-598.

Deneubourg, J. L., Camazine, S., & Detrain, C. (1999). Self-organization or individual complexity: a false dilemma or a true complementarity?. In Information processing in social insects(pp. 401-407). Birkhäuser, Basel.

Detrain, C., & Pasteels, J. M. (1992). Caste polyethism and collective defense in the ant, *Pheidole pallidula*: the outcome of quantitative differences in recruitment. *Behavioral Ecology and Sociobiology*, *29*(6), 405-412.

Detrain, C., Deneubourg, J. L., Pasteels, J. M., & Pasteels, J. M. (Eds.). (1999). Information processing in social insects. Springer Science & Business Media.

Dimitriou, I. D., Clemenza, L., Scotter, A. J., Chen, G., Guerra, F. M., & Rottapel, R. (2008). Putting out the fire: coordinated suppression of the innate and adaptive

immune systems by SOCS1 and SOCS3 proteins. Immunological reviews, 224(1), 265-283.

DiFonzo, N., Bourgeois, M. J., Suls, J., Homan, C., Stupak, N., Brooks, B. P., ... & Bordia, P. (2013). Rumor clustering, consensus, and polarization: Dynamic social impact and self-organization of hearsay. Journal of Experimental Social Psychology, 49(3), 378-399.

Duboscq, J., Romano, V., MacIntosh, A., & Sueur, C. (2016). Social information transmission in animals: lessons from studies of diffusion. Frontiers in psychology, 7, 1147.

Dussutour, A., & Simpson, S. J. (2009). Communal nutrition in ants. Current Biology, 19(9), 740-744.

Fagen, R. M., & Goldman, R. N. (1977). Behavioural catalogue analysis methods. *Animal Behaviour*, *25*, 261-274.

Feinerman, O., & Korman, A. (2017). Individual versus collective cognition in social insects. *Journal of Experimental Biology*, *220*(1), 73-82.

Fewell, J. H., & Page, R. E. (1993). Genotypic variation in foraging responses to environmental stimuli by honey bees, Apis mellifera. *Experientia*, *49*(12), 1106-1112.

Fewell, J. H. (2003). Social insect networks. *Science*, *301*(5641), 1867-1870.

Fewell, J. H., & Harrison, J. F. (2016). Scaling of work and energy use in social insect colonies. *Behavioral ecology and sociobiology*, *70*(7), 1047-1061.

Finn, R. N., Rønnestad, I., van der Meeren, T., & Fyhn, H. J. (2002). Fuel and metabolic scaling during the early life stages of Atlantic cod Gadus morhua. Marine Ecology Progress Series, 243, 217-234.

Firth, J. A., Hellewell, J., Klepac, P., Kissler, S., Kucharski, A. J., & Spurgin, L. G. (2020). Using a real-world network to model localized COVID-19 control strategies. Nature medicine, 26(10), 1616-1622.

Fujiwara-Tsujii, N., Yamagata, N., Takeda, T., Mizunami, M., & Yamaoka, R. (2006). Behavioral responses to the alarm pheromone of the ant Camponotus obscuripes (Hymenoptera: Formicidae). Zoological science, 23(4), 353-358.

Garrison, L. K., Kleineidam, C. J., & Weidenmüller, A. (2018). Behavioral flexibility promotes collective consistency in a social insect. Scientific reports, 8(1), 15836.

Gernat, T., Rao, V. D., Middendorf, M., Dankowicz, H., Goldenfeld, N., & Robinson, G. E. (2018). Automated monitoring of behavior reveals bursty interaction patterns and rapid spreading dynamics in honeybee social networks. *Proceedings of the National Academy of Sciences*, *115*(7), 1433-1438.

Glazier, D. S. (2010). A unifying explanation for diverse metabolic scaling in animals and plants. Biological Reviews, 85(1), 111-138.

Granger, C. W. (1969). Investigating causal relations by econometric models and cross-spectral methods. Econometrica: journal of the Econometric Society, 424-438.

Goetsch, W. (1957). The ants. Ann Arbor, Michigan: University of Michigan Press.

Gordon, D. M. (1989). Dynamics of task switching in harvester ants. *Animal Behaviour*, *38*(2), 194-204.

Gordon, D. M. (1996). The organization of work in social insect colonies. Nature, 380(6570), 121-124.

Gordon, D. M., & Mehdiabadi, N. J. (1999). Encounter rate and task allocation in harvester ants. Behavioral Ecology and Sociobiology, 45(5), 370-377.

Greene, M. J., & Gordon, D. M. (2003). Cuticular hydrocarbons inform task decisions. Nature, 423(6935), 32-32.

Greene, M. J., & Gordon, D. M. (2007). Interaction rate informs harvester ant task decisions. *Behavioral Ecology*, *18*(2), 451-455.

Greenwald, E., Segre, E., & Feinerman, O. (2015). Ant trophallactic networks: simultaneous measurement of interaction patterns and food dissemination. Scientific reports, 5, 12496.
Greenwald, E. E., Baltiansky, L., & Feinerman, O. (2018). Individual crop loads provide local control for collective food intake in ant colonies. Elife, 7, e31730.

Grinberg, N., Joseph, K., Friedland, L., Swire-Thompson, B., & Lazer, D. (2019). Fake news on Twitter during the 2016 US presidential election. Science, 363(6425), 374-378.

Guo, X., Chen, J., Azizi, A., Fewell, J., & Kang, Y. (2020). Dynamics of social interactions, in the flow of information and disease spreading in social insects colonies: Effects of environmental events and spatial heterogeneity. Journal of Theoretical Biology, 492, 110191.

Harrison, J. F. (2018). Approaches for testing hypotheses for the hypometric scaling of aerobic metabolic rate in animals. *American Journal of Physiology-Regulatory, Integrative and Comparative Physiology*, *315*(5), R879-R894.

Hart, A. G., & Ratnieks, F. L. (2001). Task partitioning, division of labmy and nest compartmentalisation collectively isolate hazardous waste in the leafcutting ant Atta cephalotes. Behavioral Ecology and Sociobiology, 49(5), 387-392.

Herbert, S. (1962). The architecture of complexity. Proceedings of the American Philosophical Society, 106(6), 467-482.

Hermann, H. R. (Ed.). (1984). Defensive mechanisms in social insects. Greenwood.

Heyman, Y., Shental, N., Brandis, A., Hefetz, A., & Feinerman, O. (2017). Ants regulate colony spatial organization using multiple chemical road-signs. Nature Communications, 8(1), 1-11.

Holbrook, C. T., Barden, P. M., & Fewell, J. H. (2011). Division of labor increases with colony size in the harvester ant Pogonomyrmex californicus. *Behavioral Ecology*, *22*(5), 960-966.

Holbrook, C. T., Eriksson, T. H., Overson, R. P., Gadau, J., & Fewell, J. H. (2013). Colony-size effects on task organization in the harvester ant Pogonomyrmex californicus. *Insectes sociaux*, *60*(2), 191-201.

Hölldobler, B., & Wilson, E. O. (1990). *The ants*. Harvard University Press.

Hölldobler, B., & Wilson, E. O. (1994). *Journey to the ants: a story of scientific exploration*. Belknap Press of Harvard University Press.

Holliday, M. A., Potter, D., Jarrah, A., & Bearg, S. (1967). The relation of metabolic rate to body weight and organ size. Pediatric Research, 1(3), 185-195.

Hong, W., Kennedy, A., Burgos-Artizzu, X. P., Zelikowsky, M., Navonne, S. G., Perona, P., & Anderson, D. J. (2015). Automated measurement of mouse social behaviors using depth sensing, video tracking, and machine learning. *Proceedings of the National Academy of Sciences*, *112*(38), E5351-E5360.

Hou, C., Kaspari, M., Vander Zanden, H. B., & Gillooly, J. F. (2010). Energetic basis of colonial living in social insects. Proceedings of the National Academy of Sciences, 107(8), 3634-3638.

Jones, J. C., Myerscough, M. R., Graham, S., & Oldroyd, B. P. (2004). Honey bee nest thermoregulation: diversity promotes stability. Science, 305(5682), 402-404.

Jeanson, R., Fewell, J. H., Gorelick, R., & Bertram, S. M. (2007). Emergence of increased division of labor as a function of group size. *Behavioral Ecology and Sociobiology*, *62*(2), 289-298.

Jeanson, R., & Weidenmüller, A. (2014). Interindividual variability in social insects–proximate causes and ultimate consequences. *Biological Reviews*, *89*(3), 671-687.

Jernigan, C. M., Birgiolas, J., McHugh, C., Roubik, D. W., Wcislo, W. T., & Smith, B. H. (2018). Colony-level non-associative plasticity of alarm responses in the stingless honey bee, Tetragonisca angustula. Behavioral ecology and sociobiology, 72(3), 58.

Johnson, R. A. (2004). Colony founding by pleometrosis in the semiclaustral seed-harvester ant *Pogonomyrmex californicus* (Hymenoptera: Formicidae). Animal Behaviour, 68(5), 1189-1200.

Jones, J. C., Myerscough, M. R., Graham, S., & Oldroyd, B. P. (2004). Honey bee nest thermoregulation: diversity promotes stability. *Science*, *305*(5682), 402-404.

Jones, J. C., & Oldroyd, B. P. (2006). Nest thermoregulation in social insects. *Advances in insect Physiology*, *33*, 153-191.

Kabra, M., Robie, A. A., Rivera-Alba, M., Branson, S., & Branson, K. (2013). JAABA: interactive machine learning for automatic annotation of animal behavior. *Nature methods*, *10*(1), 64.

Karsai, I., & Wenzel, J. W. (1998). Productivity, individual-level and colony-level flexibility, and organization of work as consequences of colony size. *Proceedings of the National Academy of Sciences*, *95*(15), 8665-8669.

Kaspar, R. E., Cook, C. N., & Breed, M. D. (2018). Experienced individuals influence the thermoregulatory fanning behavimy in honey bee colonies. *Animal Behaviour*, *142*, 69-76.

Klok, C. J., Kaiser, A., Lighton, J. R., & Harrison, J. F. (2010). Critical oxygen partial pressures and maximal tracheal conductances for Drosophila melanogaster reared for multiple generations in hypoxia or hyperoxia. *Journal of Insect Physiology*, *56*(5), 461-469.

Kolmes, S. A. (1986). Have hymenopteran societies evolved to be ergonomically efficient? Journal of the New York Entomological Society, 447-457.

Kuhnholz, S., & Seeley, T. D. (1997). The control of water collection in honey bee colonies. Behav Ecol Sociobiol, 41(6), 407–422.

Landgrebe, T. C., & Duin, R. P. (2007). Approximating the multiclass ROC by pairwise analysis. *Pattern recognition letters*, *28*(13), 1747-1758.

Le Conte, Y., Arnold, G., Trouiller, J., Masson, C., & Chappe, B. (1990). Identification of a brood pheromone in honeybees. Naturwissenschaften, 77(7), 334-336.

Le Conte, Y., Mohammedi, A., & Robinson, G. E. (2001). Primer effects of a brood pheromone on honeybee behavioural development. Proceedings of the Royal Society of London. Series B: Biological Sciences, 268(1463), 163-168.

Leadbeater, E., & Chittka, L. (2005). A new mode of information transfer in foraging bumblebees?. Current Biology, 15(12), R447-R448

Lewandowsky, S., Ecker, U. K., Seifert, C. M., Schwarz, N., & Cook, J. (2012). Misinformation and its correction: Continued influence and successful debiasing. Psychological science in the public interest, 13(3), 106-131.

Lighton, J. R. B., & Bartholomew, G. A. (1988). Standard energy metabolism of a desert harvester ant, Pogonomyrmex rugosus: effects of temperature, body mass, group size, and humidity. Proceedings of the National Academy of Sciences, 85(13), 4765-4769.

Lighton, J. R. and B. G. Lovegrove (1990 A temperature-induced switch from diffusive to convecttve ventilation in the honeybee. *Journal of Experimental Biology*, *154*(1), 509-516.

Lighton, J. R., Weier, J. A., & Feener, D. H. (1993). The energetics of locomotion and load carriage in the desert harvester ant Pogonomyrmex rugosus. Journal of Experimental.

Lloyd-Smith, J. O., Schreiber, S. J., Kopp, P. E., & Getz, W. M. (2005). Superspreading and the effect of individual variation on disease emergence. *Nature*, *438*(7066), 355-359.

Loftus, J. C., Perez, A. A., & Sih, A. (2021). Task syndromes: linking personality and task allocation in social animal groups. Behavioral Ecology, 32(1), 1-17.

Lovegrove, B. G. (2000). The zoogeography of mammalian basal metabolic rate. The American Naturalist, 156(2), 201-219.

Maccaro, J. J., Whyte, B. A., & Tsutsui, N. D. (2020). The Ant Who Cried Wolf? Short-Term Repeated Exposure to Alarm Pheromone Reduces Behavioral Response in Argentine Ants. *Insects*, *11*(12), 871.

Malley, J. D., Kruppa, J., Dasgupta, A., Malley, K. G., & Ziegler, A. (2012). Probability machines: consistent probability estimation using nonparametric learning machines. *Methods of information in medicine*, *51*(1), 74.

Maino, J. L., & Kearney, M. R. (2014). Ontogenetic and interspecific metabolic scaling in insects. The American Naturalist, 184(6), 695-701.

Markin, G. P. (1970). Food distribution within laboratory colonies of the argentine ant, *Tridomyrmex humilis* (Mayr). Insectes Sociaux, 17(2), 127-157.

Matthew F Sledge, FR Dani, A Fortunato, U Maschwitz, SR Clarke, E Francescato, R Hashim, ED Morgan, GR Jones, and S Turillazzi. Venom induces alarm behavimy in the social wasp polybioides raphigastra (hymenoptera: Vespidae): an investigation of alarm behaviour, venom volatiles and sting autotomy. Physiological entomology, 24(3):234–239, 1999.

Mersch, D. P., Crespi, A., & Keller, L. (2013). Tracking individuals shows spatial fidelity is a key regulator of ant social organization. *Science*, *340*(6136), 1090-1093.

Millor, J., Pham-Delegue, M., Deneubourg, J. L., & Camazine, S. (1999). Self-organized defensive behavior in honeybees. Proceedings of the National Academy of Sciences, 96(22), 12611-12615.

Miranda, B., Salas, J., & Vera, P. (2012). Bumblebees detection and tracking. In Workshop Vis. Observation Anal. Anim. Insect Behav. ICPR (pp. 1-4).

Mizunami, M., Yamagata, N., & Nishino, H. (2010). Alarm pheromone processing in the ant brain: an evolutionary perspective. Frontiers in Behavioral Neuroscience, 4, 28.

Moritz, R. F., Southwick, E. E., & Breh, M. (1985). A metabolic test for the quantitative analysis of alarm behavior of honeybees (*Apis mellifera* L.). Journal of Experimental Zoology, 235(1), 1-5.

Mosqueiro, T., Cook, C., Huerta, R., Gadau, J., Smith, B., & Pinter-Wollman, N. (2017). Task allocation and site fidelity jointly influence foraging regulation in honeybee colonies. Royal Society open science, 4(8), 170344.

Nazinitsky, A., & Rosenthal, K. S. (2010). Cytokine storms: systemic disasters of infectious diseases. Infectious Diseases in Clinical Practice, 18(3), 188-192.

O'Donnell, S. & Foster, R. L. Thresholds of response in nest thermoregulation by worker bumble bees, Bombus bifarius nearcticus (Hymenoptera: Apidae). Ethology 107, 387–399 (2001).

Oldroyd, B. P., & Thompson, G. J. (2006). Behavioural genetics of the honey bee Apis mellifera. *Advances in insect physiology*, *33*, 1-49.

Oldroyd, B. P., & Fewell, J. H. (2007). Genetic diversity promotes homeostasis in insect colonies. *Trends in ecology & evolution*, *22*(8), 408-413.

Page Jr RE. 2013. The spirit of the hive. Cambridge (MA): Harvard University Press.

Pankiw, T., Page Jr, R. E., & Fondrk, M. K. (1998). Brood pheromone stimulates pollen foraging in honey bees (Apis mellifera). *Behavioral ecology and sociobiology*, *44*(3), 193-198.

Pankiw, T. (2007). Brood pheromone modulation of pollen forager turnaround time in the honey bee (Apis mellifera L.). Journal of insect behavior, 20(2), 173.

Perez, M., Rolland, U., Giurfa, M., & d'Ettorre, P. (2013). Sucrose responsiveness, learning success, and task specialization in ants. *Learning & Memory*, *20*(8), 417-420.

Petz, M., Stabentheiner, A., & Crailsheim, K. (2004). Respiration of individual honeybee larvae in relation to age and ambient temperature. *Journal of Comparative Physiology B*, *174*(7), 511-518.

Pinter-Wollman, N., Wollman, R., Guetz, A., Holmes, S., & Gordon, D. M. (2011). The effect of individual variation on the structure and function of interaction networks in harvester ants. Journal of the Royal Society Interface, 8(64), 1562-1573.

Pinter-Wollman, N., Bala, A., Merrell, A., Queirolo, J., Stumpe, M. C., Holmes, S., & Gordon, D. M. (2013). Harvester ants use interactions to regulate forager activation and availability. *Animal behaviour*, *86*(1), 197-207.

Pinter-Wollman, N., Hobson, E. A., Smith, J. E., Edelman, A. J., Shizuka, D., De Silva, S., ... & McDonald, D. B. (2014). The dynamics of animal social networks: analytical, conceptual, and theoretical advances. Behavioral Ecology, 25(2), 242-255.

Post, J. R., & Lee, J. A. (1996). Metabolic ontogeny of teleost fishes. Canadian Journal of Fisheries and Aquatic Sciences, 53(4), 910-923.

Pratt, S. C. (2005). Quorum sensing by encounter rates in the ant Temnothorax albipennis. Behavioral Ecology, 16(2), 488-496.

Ratnieks, F. L., & Anderson, C. (1999). Task partitioning in insect societies. II. Use of queueing delay information in recruitment. *The American Naturalist*, *154*(5), 536-548.

Razin, N., Eckmann, J. P., & Feinerman, O. (2013). Desert ants achieve reliable recruitment across noisy interactions. *Journal of the Royal Society Interface*, *10*(82), 20130079.

Reinhold, K. (1999). Energetically costly behavimy and the evolution of resting metabolic rate in insects. *Functional Ecology*, *13*(2), 217-224.

Reyes, A., Curbelo, M., Tejera, F., Rivera, A., Simon, G., Ramos, O., ... & Altshuler, E. (2019). Transmission of danger information past physical barriers by ants. *arXiv preprint arXiv:1904.03236*.

Rice, L., Tate, S., Farynyk, D., Sun, J., Chism, G., Charbonneau, D., ... & Shin, M. C. (2020). ABCTracker: an easy-to-use, cloud-based application for tracking multiple objects. arXiv preprint arXiv:2001.10072.

Richardson, T. O., & Gorochowski, T. E. (2015). Beyond contact-based transmission networks: the role of spatial coincidence. Journal of The Royal Society Interface, 12(111), 20150705.

Richardson, T. O., Liechti, J. I., Stroeymeyt, N., Bonhoeffer, S., & Keller, L. (2017). Short-term activity cycles impede information transmission in ant colonies. PLoS computational biology, 13(5), e1005527.

Robert K Vander Meer, Michael D Breed, Karl E Espelie, and Mark L Winston. Pheromone communication in social insects. Ants, wasps, bees and termites. Westview, Boulder, CO, 162, 1998.

Robinson, G. E. (1987). Regulation of honey bee age polyethism by juvenile hormone. *Behavioral Ecology and Sociobiology*, *20*(5), 329-338.

Robinson GE, Page REJ. 1989. Genetic basis for division of labor in an insect society. In The Genetics of Social Evolution, ed. MD Breed, REJ Page, pp. 61– 80. Boulder, CO: Westview

Robinson, E. J., Feinerman, O., & Franks, N. R. (2009). Flexible task allocation and the organization of work in ants. Proceedings of the Royal Society B: Biological Sciences, 276(1677), 4373-4380.

Rogers, E. M. (2010). Diffusion of innovations. Simon and Schuster.

Romano, V., MacIntosh, A. J. J., and Sueur, C.. (2020). Stemming the flow: Information, infection, and social evolution. Trends in ecology & evolution, DOI:https://doi.org/10.1016/j.tree.2020.07.004

Römer, D., & Roces, F. (2014). Nest enlargement in leaf-cutting ants: relocated brood and fungus trigger the excavation of new chambers. PLoS One, 9(5), e97872.

Sakata, H., & Katayama, N. (2001). Ant defence system: a mechanism organizing individual responses into efficient collective behavior. *Ecological Research*, *16*(3), 395-403.

Sasaki, T., Hölldobler, B., Millar, J. G., & Pratt, S. C. (2014). A context-dependent alarm signal in the ant Temnothorax rugatulus. *Journal of Experimental Biology*, 217(18), 3229-3236.

Scheiner, R., Page, R. E., & Erber, J. (2004). Sucrose responsiveness and behavioral plasticity in honey bees (Apis mellifera). Apidologie, 35(2), 133-142.

Shemesh, Y., Eban-Rothschild, A., Cohen, M., & Bloch, G. (2010). Molecular dynamics and social regulation of context-dependent plasticity in the circadian clockwork of the honey bee. Journal of Neuroscience, 30(37), 12517-12525.

Scheufele, D. A., & Krause, N. M. (2019). Science audiences, misinformation, and fake news. Proceedings of the National Academy of Sciences, 116(16), 7662-7669.

Schmickl, T., & Karsai, I. (2016). How regulation based on a common stomach leads to economic optimization of honeybee foraging. Journal of theoretical biology, 389, 274-286.

Schmidt-Nielsen, K., & Knut, S. N. (1984). Scaling: why is animal size so important?. Cambridge university press.

Schneirla, T. C. (1950). The relationship between observation and experimentation in the field study of behavior. Annals of the New York Academy of Sciences, 51(6), 1022-1044.

Seeley, T. D., & Tovey, C. A. (1994). Why search time to find a food-storer bee accurately indicates the relative rates of nectar collecting and nectar processing in honey bee colonies. *Animal Behaviour*, *47*(2), 311-316.

Segers, F. H., von Zuben, L., & Grüter, C. (2016). Local differences in parasitism and competition shape defensive investment in a polymorphic eusocial bee. Ecology, 97(2), 417-426.

Sendova-Franks, A. B., Hayward, R. K., Wulf, B., Klimek, T., James, R., Planqué, R., ... & Franks, N. R. (2010). Emergency networking: famine relief in ant colonies. Animal Behaviour, 79(2), 473-485.

Sherman, P. W. (1985). Alarm calls of Belding's ground squirrels to aerial predators: nepotism or self-preservation?. Behavioral Ecology and Sociobiology, 17(4), 313-323.

Sharma, V. K., Lone, S. R., Goel, A., & Chandrashekaran, M. K. (2004). Circadian consequences of social organization in the ant species Camponotus compressus. *Naturwissenschaften*, *91*(8), 386-390.

Shik, J. Z. (2010). The metabolic costs of building ant colonies from variably sized subunits. Behavioral Ecology and Sociobiology, 64(12), 1981-1990.

Shik, J. Z., Santos, J. C., Seal, J. N., Kay, A., Mueller, U. G., & Kaspari, M. (2014). Metabolism and the rise of fungus cultivation by ants. The American Naturalist, 184(3), 364-373.

Shu, K., Sliva, A., Wang, S., Tang, J., & Liu, H. (2017). Fake news detection on social media: A data mining perspective. ACM SIGKDD explorations newsletter, 19(1), 22-36.

Sledge, M. F., Dani, F. R., Fortunato, A., Maschwitz, U., Clarke, S. R., Francescato, E., ... & Turillazzi, S. (1999). Venom induces alarm behavimy in the social wasp Polybioides raphigastra (Hymenoptera: Vespidae): an investigation of alarm behaviour, venom volatiles and sting autotomy. *Physiological entomology*, *24*(3), 234-239.

Somero, G. N. (2002). Thermal physiology and vertical zonation of intertidal animals: optima, limits, and costs of living. Integrative and comparative biology, 42(4), 780-789.

Tschinkel, W. R. (1999). Sociometry and sociogenesis of colony-level attributes of the Florida harvester ant (Hymenoptera: Formicidae). Annals of the Entomological Society of America, 92(1), 80-89.

Ulrich, Y., Burns, D., Libbrecht, R., & Kronauer, D. J. (2016). Ant larvae regulate worker foraging behavior and ovarian activity in a dose-dependent manner. Behavioral ecology and sociobiology, 70(7), 1011-1018.

Valletta, J. J., Torney, C., Kings, M., Thornton, A., & Madden, J. (2017). Applications of machine learning in animal behavimy studies. *Animal Behaviour*, *124*, 203-220.

Valentini, G., Masuda, N., Shaffer, Z., Hanson, J. R., Sasaki, T., Walker, S. I., ... & Pratt, S. C. (2020). Division of labmy promotes the spread of information in colony emigrations by the ant Temnothorax rugatulus. Proceedings of the Royal Society B, 287(1924), 20192950.

Vander Meer, R. K., Breed, M. D., Winston, M., & Espelie, K. E. (2019). *Pheromone communication in social insects: ants, wasps, bees, and termites*. CRC Press.

Vogt, J. T., & Appel, A. G. (1999). Standard metabolic rate of the fire ant, Solenopsis invicta Buren: effects of temperature, mass, and caste. Journal of insect physiology, 45(7), 655-666.

Von Herbing, I. H., Gallager, S. M., & Halteman, W. (2001). Metabolic costs of pursuit and attack in early larval Atlantic cod. Marine Ecology Progress Series, 216, 201-212.

Ward, P., & Zahavi, A. (1973). The importance of certain assemblages of birds as "information-centres" for food-finding. Ibis, 115(4), 517-534.

Warburton, S. J., Burggren, W. W., & Pelster, B. (Eds.). (2006). *Comparative developmental physiology: contributions, tools, and trends*. Oxford University Press.

Waters, J. S., Holbrook, C. T., Fewell, J. H., & Harrison, J. F. (2010). Allometric scaling of metabolism, growth, and activity in whole colonies of the seed-harvester ant Pogonomyrmex californicus. The American Naturalist, 176(4), 501-510.

Waters, J. S., & Fewell, J. H. (2012). Information processing in social insect networks. PloS one, 7(7), e40337.

Waters, J. S. and J. F. Harrison (2012). Insect metabolic rates. Metabolic Ecology: A Scaling Approach. J. Brown, R. Sibly and A. Brown. New York, John Wiley and Sons.

Waters, J. S., Ochs, A., Fewell, J. H., & Harrison, J. F. (2017). Differentiating causality and correlation in allometric scaling: ant colony size drives metabolic hypometry. Proceedings of the Royal Society B: Biological Sciences, 284(1849), 20162582.

Went, F. W., Wheeler, J., & Wheeler, G. C. (1972). Feeding and digestion in some ants (Veromessor and Manica). BioScience, 22(2), 82-88.

Wheeler, W. M. (1918). A study of some ant larvae, with a consideration of the origin and meaning of the social habit among insects. Proceedings of the American Philosophical Society, 293-343.

White, C. R., & Kearney, M. R. (2011). Metabolic scaling in animals: methods, empirical results, and theoretical explanations. *Comprehensive Physiology*, *4*(1), 231-256.

Wieser, W., & Forstner, H. (1986). Effects of temperature and size on the routine rate of oxygen consumption and on the relative scope for activity in larval cyprinids. Journal of Comparative Physiology B, 156(6), 791-796.

Wilson, E. O. (1958). A chemical releaser of alarm and digging behavior in the ant *Pogonomyrmex badius* (*Latreille*). *Psyche: A Journal of Entomology*, *65*(2-3), 41-51.

Wilson, E. O., & Regnier Jr, F. E. (1971). The evolution of the alarm-defense system in the formicine ants. The American Naturalist, 105(943), 279-289.

Wilson, E. O., & Fagen, R. M. (1974). On the estimation of total behavioral repertories in ants. *Journal of the New York Entomological Society*, 106-112.

Wilson, E. O. (1976). Behavioral discretization and the number of castes in an ant species. *Behavioral Ecology and Sociobiology*, *1*(2), 141-154.

Wilson, E. O. (1978). Division of labor in fire ants based on physical castes (Hymenoptera: Formicidae: Solenopsis). *Journal of the Kansas Entomological Society*, 615-636.

Wong, H. S., & Germain, R. N. (2018, April). Robust control of the adaptive immune system. In Seminars in immunology (Vol. 36, pp. 17-27). Academic Press.

Wu, F., Huberman, B. A., Adamic, L. A., & Tyler, J. R. (2004). Information flow in social groups. Physica A: Statistical Mechanics and its Applications, 337(1-2), 327-335

Yamagata, N., Nishino, H., & Mizunami, M. (2007). Neural pathways for the processing of alarm pheromone in the ant brain. Journal of Comparative Neurology, 505(4), 424-442.

APENDIX A

SPATIAL PROXIMITY FOR PHYSICAL CONTACT

We followed seven pairs of ants that made physical contact, and measured the minimum Euclidean distance between each pair during contact (d_1 = 37 pix; d_2 = 44 pix; d_3 = 39 pix; d_4 = 37 pix; d_5 = 43 pix; d_6 = 44 pix; d_7 = 45 pix), (Fig. A1). The maximum of those distance was used as my spatial proximity criterion for physical contacts ($d_{contact}$ = 45 pix).

Figure A1: Snapshots for 7 samples of physical contact in spatial proximity estimation.

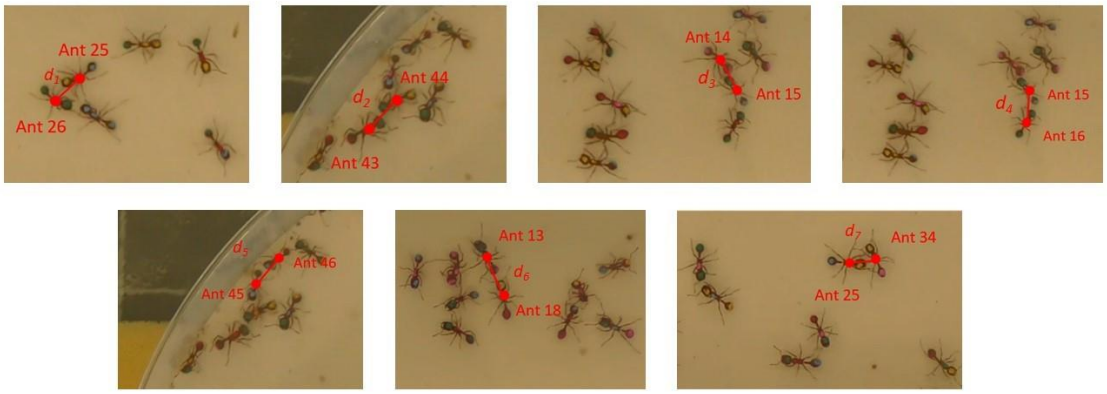

APPENDIX B

TRAINING AND TESTING DATA

To create the training and testing datasets, we identified 16 track segments from different ants, which varied in length from 100-900 frames, with each containing a consistent movement pattern that was visually assessed to fall into only one of the three alarm states throughout the segment: Alarmed, $\text{Unalarmed}_{\text{alert}}$ or $\text{Unalarmed}_{\text{calm}}$ (Table B1).

We then applied sliding window technique to segments, producing 6462 feature vectors in total. Each feature vector includes 5 variables: the mean frame-wise speed, standard deviation of frame-wise speeds, standard deviation of body axis orientations, convex hall area of locomotion and mean frame-wise number of contact with neighbors over the sliding window (Fig. B1). All feature vectors within a given segment were randomly assigned to either the training or the testing set. Training data consisted of 3412 feature vectors and testing data contained 3050 feature vectors (Table B2).

Table B1: Details of the 16 track segments:

Ant ID	Tracking source	Alarm Status	Alarm Level	Frame Start	Frame End
50	Baseline	Calm	0	3001	3300
1	Baseline	Calm	0	1	600
3	Baseline	Calm	0	1	900
2	Baseline	Calm	0	1	600
26	Alarm event	Alert	0.5	1	500
28	Alarm event	Alert	0.5	1	400
4	Alarm event	Alert	0.5	1	200
2*	Alarm event	Alert	0.5	120	300
32	Alarm event	Alert	0.5	1	420
27	Alarm event	Alarmed	1	101	1000
54	Alarm event	Alarmed	1	1	900
10	Alarm event	Alarmed	1	60	200
19	Alarm event	Alarmed	1	1	300
25	Alarm event	Alarmed	1	1	300
7	Alarm event	Alarmed	1	61	240
42	Alarm event	Alarmed	1	91	210

*: Ant (id = 2) in the video of alarm event is different from the ant (id = 2) in the video of the alarm event.

Table B2: Amount of data used to train the machine learning model.

	Alarmed (1.0)	Alert (0.5)	Calm (0.0)	Total
$N_{training}$	1251	151	2010	3412
$N_{testing}$	1380	1400	270	3050
Total	2631	2951	2280	6462

Figure B1: Features extracted from the segmental tracks. Three ants with different alarm status were given as examples (grey: calm ant; blue: alert ant; red: alarmed ant). The calm ant was assigned to have an alarm strength value (AS =0) from frame 1 to 600. The alert ant has AS = 0.5 from the frame 1 to 150. The alarmed ant has AS = 1 from frame 1 to 300. Five feature variables over the session were highlighted for training data set on three ants which were labeled with "$Unalarmed_{calm}$", "$Unalarmed_{alert}$" and "Alarmed".

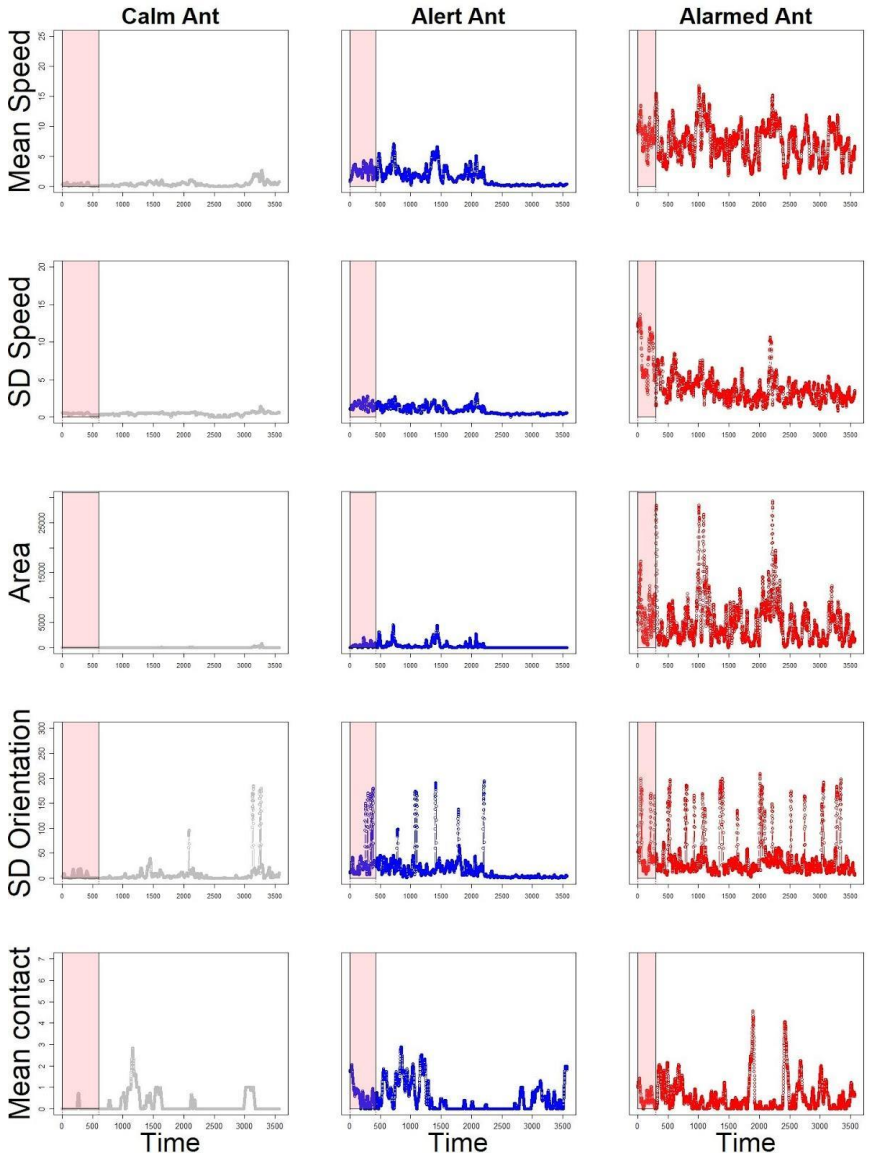

APPENDIX C

DISTANCE-DEPENDENT EFFICACY OF ALARM SIGNAL PROPAGATION

Immediately after the introduction of the three alarmed ants (t=0 sec), 5 additional ants transitioned into the alarmed state, because they came in immediate contact with initially seeded ants. We identified those 8 ants as the initially alarmed, and analyzed their impacts on nearby ants in unalarmed states. For ant with id i and alarm status $s \in$ {a(*alarmed*), u(*unalarmed*)}, A^s_i, set of neighboring ants is defined as

$$N(A_i^s) = \{A_j^{s'} : A_j^{s'} \in Cl(A_i^s), r)\},$$

where $l(A^s_i)$ is the location of ant and r = 135 pixel (3x45pix) is neighborhood radius, and $C(l(A^s_i),r)$ is the circle with center $l(A^s_i)$ and radius r. Following an alarmed ant A^a_i, we find an unalarmed ant $A^n_j \in N(A^a_i)$ that meets the following criteria:

1. $\widehat{AS}(A^u_j) \leq 10\%$, that is, A^u_j is in a calm state.
2. $N(A^u_j) \subseteq \{A^a_i\}$, that is, the only potential ant in the neighborhood of A^u_j is A^a_i.
3. A^u_j has an integrated process of entering and exiting from the spatial range of a seed A^a_i, (Fig. C1).

After filtering out the target alarmed and unalarmed ants, we calculate the dependent variable standard deviation of A^u_j's alarm strength ($\sigma_{\widehat{AS}(A^u_j)}$) across a time window at which she comes toward and moves away from A^a_i. The minimal distance of A^u_j away from A^a_i, d_{min}, across this time window was assigned as the independent variable.

Figure C1: An illustration of movement of unalarmed ant A_j^u toward and away from alarmed neighbor A_j^a as time goes. In order to investigate the correlation between distance d and the change in alarm strength of unalarmed ant A_j^u (measured by standard deviation σ_{AS}), we keep track of their distance at time t, d_t, and alarm strength of unalarmed ant $\widehat{AS}(A_j^u)$.

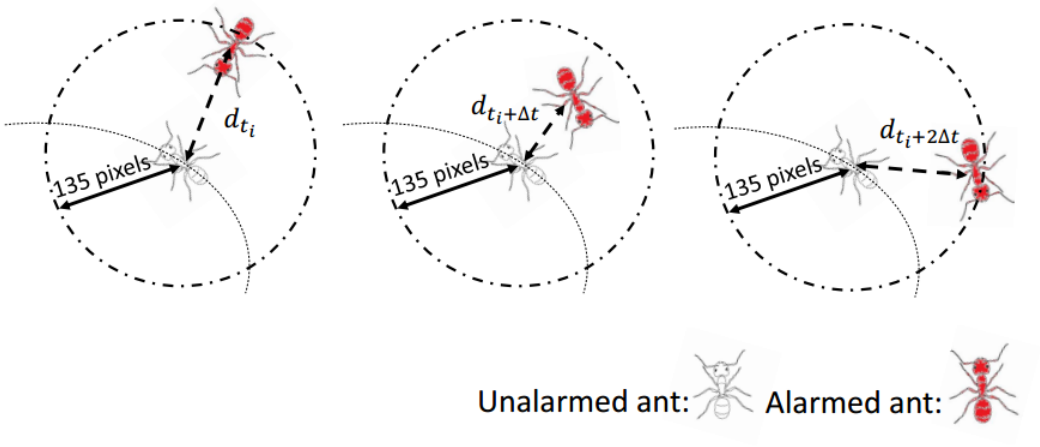

APPENDIX D

PATHWAY OF ALARM SIGNAL PROPAGATION

Ants' alarm strength predicted from the Random Forest regression model ($\widehat{AS}$), coupled with tracking data on inter-individual distance, allowed us to identify the network pathways of alarm signal propagation indirectly by overlapping two layers of events: individual average alarm response level every second (30 frames) and its seconds-stamped contact networks. We simultaneously mapped the change in alarm state of ants engaged in contact events, based on the rule that unalarmed ants are allowed to respond to alarm recruitment with a maximum of 4 seconds' latency (Fig. D1).

The time-ordered and time-aggregated alarm-signal propagation networks were built by using packages of ndtv, tsna (in R 3.5.0.), networkx and teneto (in Python 3.8.3.). Physical contacts were recorded as potential pathways of alarm signal propagation whenever two ants' distance went within $D_{contacting}$ = 45 pixels. Specifically, if an unalarmed ant becomes alarmed without a latency (case 1) or with a latency within 4 seconds (case 2) after alarm contact, a directional tie between the pair of ants undergoing alarm contact will be included from alarmed ant to unalarmed ant as the potential pathway of alarm propagation (Fig. D2a). These contacts were defined as events in which previously unalarmed ants cumulatively increased their alarm strength above the threshold (0.749) for the first time and within 4 seconds' time window after contacting any alarmed ant. The weights of edges were obtained by assessing the standard deviation of $\widehat{AS}$ on unalarmed ants within a unit of time (1 second) as their contact with alarmed neighbors, which indicates the varied effectiveness of alarm contacts on alarm state transition (Fig. D2b). If an ant became alarmed without alarm contact, we labelled this node as an independent alarm transition. The weighted highest edge to an unalarmed ant was identified as the primary pathway of alarm propagation. After pruning other low

weighted edges, the static propagation network was formulated by aggregating the time-ordered propagation events (Fig. D2c).

Figure D1: Networking rules of alarm-signal propagation for three cases. In cases 1 and 2, alarm propagation relies on physical contact without a latency (case 1) or with a latency within 4 seconds (case 2) after contacting an alarmed neighbor. In case 3, alarm signal propagation is achieved independently of physical contact.

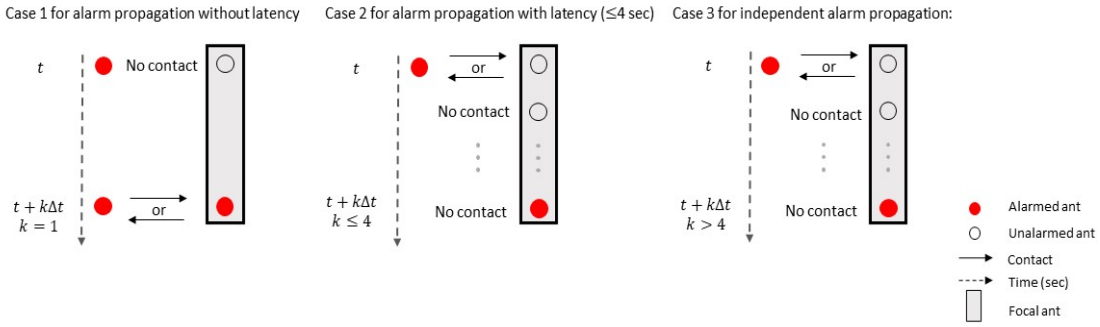

Figure D2: Alarm signal propagation networks. (a) The time-ordered network of alarm propagation. In the network layout, y-axis indicates the id number of ants, and x-axis indicates the time in seconds. Each colored node represents an ant with the unique id number. Each weighted edge represents the varied effectiveness of an alarm contact on alarm state transition of unalarmed ant. (b)The time-ordered network of alarm propagation at first 10 seconds with all weighted edges. Red arrows indicated the primary pathways of alarm propagation by identifying the weighted highest edge on each unalarmed signal receiver. (c) Time-aggregated network at first 10 seconds obtained from assessing primary pathways of alarm propagation. “Yellow” represents initially alarmed ants placed into the test arena. “Green” represents ants which become alarmed independently of alarm contact. “Red” represents ants transited to alarmed via alarm contact.

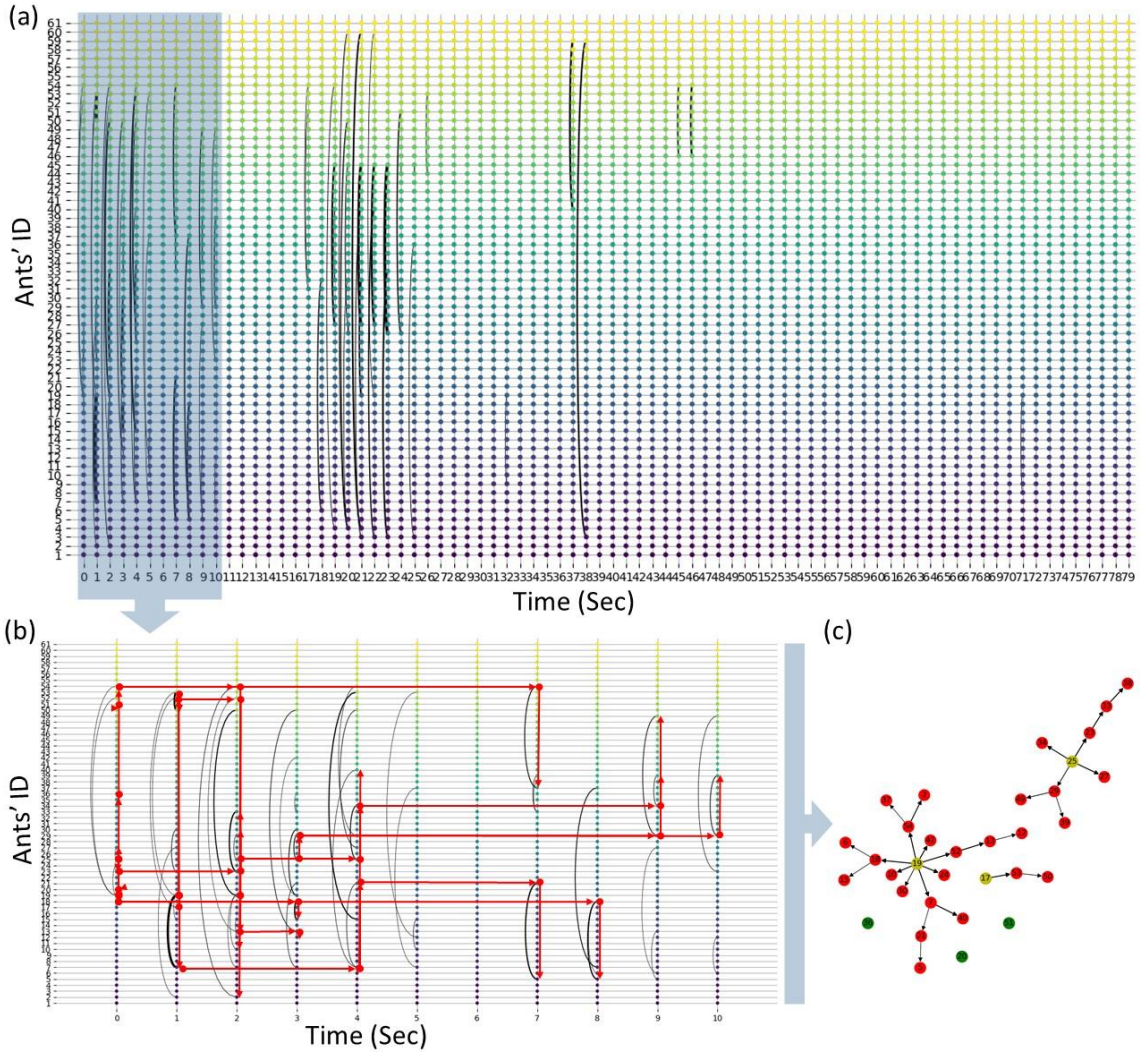
(a)
Ants' ID
Time (Sec)
(b)
Ants' ID
Time (Sec)
(c)